INTERFACIAL PROPERTIES OF MICROEMULSIONS IN RELATION TO
ENHANCED OIL RECOVERY SYSTEMS

By

YUSUF PITHAPURWALA

A DISSERTATION PRESENTED TO THE GRADUATE SCHOOL OF
THE UNIVERSITY OF FLORIDA
IN PARTIAL FULFILLMENT OF THE REQUIREMENTS FOR THE
DEGREE OF DOCTOR OF PHILOSOPHY

UNIVERSITY OF FLORIDA

1984

To

My father and my Mohammedmama

ACKNOWLEDGEMENTS

TABLE OF CONTENTS

iv

INTERFACIAL PROPERTIES OF MICROEMULSIONS IN RELATION TO
ENHANCED OIL RECOVERY PROCESS

By

YUSUF PITHAPURWALA

August, 1984

Chairman: Professor Dinesh O. Shah
Major Department: Chemical Engineering

The interfacial properties of microemulsions, such as solubili-
zation, interfacial tension and interfacial composition which are of
interest in enhanced oil recovery by surfactant-polymer flooding,
have been investigated. Studies were done on systems with pure and
commercial surfactants (sodium stearate, sodium dodecyl sulfate, TRS
10-80 and TRS 10-410). Both pure alkanes and a crude oil system were
employed in this investigation.

For oil-external microemulsions prepared using sodium stearate
or petroleum sulfonate with different oils and alcohols, there was a
critical electrolyte concentration where these microemulsions solu-
bilized the highest amount of brine. A chain length compatibility

was observed for microemulsions, i.e. there was a maximum brine solubilization when $l_a + l_o = l_s$, where l_a, l_o and l_s are the length of alcohol, oil and surfactant molecules respectively. The interfacial composition of sodium stearate-containing microemulsions was determined in terms of moles of alcohol per mole of surfactant present at the interface using a modified three compartment Schulman-Bowcott model.

The petroleum sulfonate-containing microemulsions also showed highest brine solubilization at optimal salinity. Moreover, the fluorescence intensity was found to be maximum at optimal salinity. The solubilization behavior is explained in terms of the solubility of alcohols in various phases of microemulsions. The fluorescence behavior is explained by higher surface charge density around the microemulsion droplet at optimal salinity.

Oil displacement tests were carried out in sandpacks and in Berea core at 80 ℃ using the surfactant system containing petroleum sulfonate and phosphated ester but with different cosolvents. The tertiary oil recovery was 92% when 0.2 PV of TAA-containing surfactant slug was injected while the tertiary oil recovery was poor in systems containing other alcohols. It is concluded that for these systems, the enhanced oil recovery, surfactant recovery and surfactant breakthrough are interrelated. Based on these observations, it is proposed that the mass transfer of TAA from the aqueous surfactant slug to the oil phase promotes the oil displacement presumably due to the ultra-low IFT associated with the transfer of cosolvent across the interface.

CHAPTER I
INTRODUCTION

1.1 Introduction

A reservoir bearing oil and gas may be defined as a body of porous and permeable rock containing oil and gas, through which fluid moves towards a production site under the pressure existing or that may be applied. Attaining maximum economic recovery of oil from the reservoir is a very complex matter. Each reservoir is unique, and the production process must utilize the appropriate combination of natural pressures and supplemental energy to optimize production rate and ultimate recovery. Among the key factors to consider in developing a production strategy are estimates of the reservoir rock containing the petroleum, the amount of petroleum contained in the pores of the rock, the amount of water contained in the rock, and the nature and magnitude of the natural drive mechanism present.

Almost all oil produced in the world today is recovered by primary and secondary methods. These methods make use of both naturally occurring, or primary, reservoir energy and injected gas or water as a secondary source of energy.

Primary Oil Recovery. Natural pressure within a petroleum reservoir causes oil to flow through the porous rock into wells and, if the pressure is strong enough, up to the surface. However, if natural forces are initially low or diminish with production, pumps or other means are used to lift the oil. The most common types of primary mechanisms are

        1. Solution gas drive

        2. Gas cap expansion drive

        3. Water drive

Table 1.1 gives the relative efficiency of primary and secondary methods.

Secondary Oil Recovery. Because primary recovery methods leave so much oil behind, secondary methods such as water flooding or gas injection into the reservoir are used to displace additional oil into the producing wells. Water flooding is found to be a more efficient method than gas injection (see Table 1.1).

When water is injected into an oil bearing zone, it moves away from the injection wells in all directions and pushes oil through the pores of the rock toward producing wells. The gas-injection method is limited to those reservoirs which have a gas cap and in which gas cap expansion is expected to be an efficient natural drive mechanism. Injected gas helps to maintain reservoir pressure and improves total oil recovery.

Even when skillfully applied, primary and secondary recovery operations leave a great deal of oil in the ground. The poor efficiency of these methods can be explained on the basis of two major factors. One is the difficulty of distributing the injected fluid throughout a reservoir and the other is the extent to which the oil can be displaced from those portions of the reservoir which are invaded by the injected fluid. On the average, only about 35 percent of the oil originally contained in a reservoir is recoverable by these methods. According to one report shown in Table 1.2, about 600-900 billion barrels will be left behind after primary and secondary methods.

1.2 Enhanced Oil Recovery

As the discovery of new oil fields has become increasingly difficult and more costly, the stimulus to increase recovery of oil from known fields has steadily become stronger. The extent to which the enhanced oil recovery (EOR) methods can increase the recovery of oil, that would otherwise be left behind remains to be seen. But something in the range of 100 to 200 billion barrels seems likely at this time according to an Exxon report on Improved Oil Recovery (1982). The potential for EOR has become very meaningful in the U.S., where most reservoirs have been water-flooded. All EOR methods increase the oil production by improving the sweep efficiency and by reducing the amount of oil left behind in the swept zone. EOR methods are usually divided into three broad groups as follows

Table 1.1 Relative Efficiency of Primary and Secondary
Recovery Methods+

Dominant Producing Method	Typical Recovery Range (Percent of Original Oil in Place)
Primary	
Solution Gas Drive	5-20
Gas Cap Expansion Drive	20-45
Water Drive	25-55
Secondary	
Waterflood	30-60
Gas Injection	20-45

+ from Improved Oil Recovery (1982)

Table 1.2 Enhanced Oil Recovery Potential From Already
Discovered Fields in Billions of Barrels+

	World	U.S.
Original Oil In Place	3000-4000	500-600
Recoverable by Primary and Secondary Methods	1100-1400	180-225
Already Produced	500	150
Remaining after Primary and Secondary Methods	600-900	30-75
Enhanced Oil Recovery Potential	100-200	20-30

+ from Improved Oil Recovery (1982)

1. Thermal methods such as steam flooding, cyclic steam injection, in-situ combustion etc.

2. Miscible flooding such as CO_2, N_2 and hydrocarbon flooding

3. Chemical flooding such as caustic, polymer, surfactant and surfactant-polymer flooding.

Figure 1.1 summarizes the basic tools for various EOR methods. Out of these methods, thermal methods are the most advanced in terms of field tests and have the least uncertainty in estimating the performance in the field. The chemical methods in general and the surfactant-polymer method in particular are the most complex and have the highest degree of uncertainty at present. Yet, if this process can be properly designed and controlled, it has the potential of achieving maximum oil recovery.

1.3 Surfactant-Polymer Flooding

The residual oil, after water flooding, is trapped in the pores as blobs or ganglia due to viscous and capillary forces. Capillary forces are determined mainly by the interfacial tension between reservoir oil and brine whereas the viscous forces are limited by the viscosity of phases and the flood rate of the process. The dimensionless ratio of the magnitude of viscous forces to capillary forces was defined as the capillary number (Foster, 1973).

$$N_{ca} = \frac{\mu v}{\sigma \phi} \tag{1.1}$$

Enhanced Oil Recovery Processes
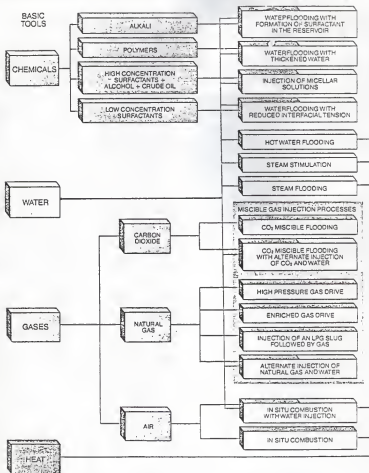
Figure 1.1 Basic Tools for Enhanced Oil Recovery Processes.

where μ : viscosity of the displacing fluid (gm/cm-sec)

w : flow velocity (cm/sec)

σ : oil/water interfacial tension (dynes/cm)

ϕ : porosity of the rock

For example, the capillary number for a flood velocity of 1 ft/day, oil viscosity of 10 centipoise, interfacial tension between oil and water of 30 dynes/cm and rock porosity of 0.2 is 5.8×10^{-6}. For a conventional water flooding process, the capillary number is about 10^{-6}. It is well known that this capillary number should be increased to 10^{-3} to 10^{-2} in order to achieve a high oil displacement efficiency (Melrose and Brandner, 1974; Foster 1973). Since the viscous forces cannot be increased to an extent that the capillary number is 10^{-3} or 10^{-2}, the capillary forces entrapping the oil ganglia can be decreased by lowering the interfacial tension to the ultra-low values in the range of 10^{-3} dynes/cm. It has been reported (Hill et al. 1973) that ultra-low values of interfacial tension can be obtained by using surfactant solutions. These solutions have been shown, both in the laboratory as well as in the field, to reduce the oil saturation far below the values obtained with a waterflood.

Polymer solutions are injected following the surfactant slug to propagate the micellar system efficiently through the reservoir. The polymer solution provides mobility control in the reservoir. A schematic representation of surfactant/polymer flooding is given in Figure 1.2. Considerable research has been directed towards developing the technology of surfactant flooding (Shah, 1981a, b; Shah and
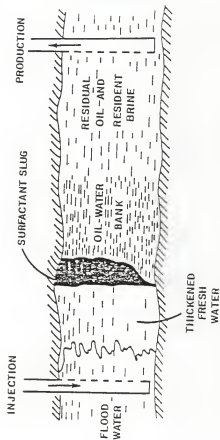
Figure 1.2. Schematic Representation of Surfactant-Polymer Flooding Process for Enhanced Oil Recovery(Shah,1981b)

Schechter, 1977; Holm, 1971; Hill et al., 1973; Bae et al., 1974; Reed and Healy, 1977).

Since the first use of surfactants to improve oil production in 1927 (Atkinson, 1927), essentially two concepts have been developed for surfactant-polymer flooding (Gogarty, 1976, 1978, 1983). One concept involves the use of several pore volumes of a dilute surfactant solution with a surfactant concentration of less than about 1%, which is generally called the low-tension waterflood process. The other concept involves the use of a small slug with 3 to 20% pore volumes of a high-concentration (5 to 20%) surfactant formulation. Depending on composition, the surfactant formulations are classified as microemulsions, micellar solutions or soluble oils. Evidence from both laboratory and field studies indicates, in general, that the low-tension waterflood process is unfavorable due to the excessive surfactant adsorption loss and the lack of mobility control (Gogarty, 1978; Goldberg; 1977; Widmayer et al., 1977). Sacrificial agents such as sodium carbonate and sodium tripolyphosphate have been used to reduce adsorption of surfactant. Thus, by injecting a preflush slug before surfactant slug, the ionic nature of the rock surface can be altered and thus the adsorption loses can be minimized.

The high-concentration surfactant-polymer flooding process is a much more complicated process. The performance of this process depends on the composition, structure, and wettability of rock as well as on the phase behavior, interfacial tensions and viscosity of the microemulsions produced in situ. The main factors affecting surfactant/ polymer flooding performance are (Gogerty, 1983)

1. Fluid system design; phase behavior, rock structure

2. Choice of surfactants and additives

3. Choice of cosurfactants and additives

4. Vertical conformance

5. choice of mobility control polymers

6. polymer preflush

7. Pattern type and spacing of injection and production wells

In order to have an in-depth understanding of the surfactant-polymer flooding process and to provide the guidelines for the design of surfactant formulations, it is necessary to elucidate the structure, interfacial compositions, phase equilibrium, solubilization capacity, viscosity and other colloidal aspects of surfactant stabilized microstructures.

1.4 Surfactants in Aqueous Media

Surface active molecules or surfactants are very unique molecules because they contain two distinct and different parts in the same molecule, namely the polar head group and the nonpolar tail. The polar portion may be either an ionic group, such as $-SO_3^-$, $-SO_4^-$, and $-NH_3^+$, or a nonionic group, $-OH$. The hydrocarbon tail may be straight or branched and saturated or unsaturated. Because of their unique structure, surfactants tend to accumulate at interfaces (e.g. air/water and oil/water) and have a specific orientation at the interface when dissolved in aqueous solutions. The Hydrophilic-Lipophilic Balance (HLB) is a measure of the relative strength of the polar and nonpolar parts of the surfactant molecules. The range of

the HLB value is between 1 and 40. The HLB value reflects the solu-
bility of the surfactant in a polar or nonpolar medium. Surfactants
with a strong polar soluble head group and a short hydrocarbon tail
are water soluble and those with long hydrocarbon tails are water
insoluble.

When the surfactant molecules are dissolved in water, they
remain as monomers up to a certain surfactant concentration. How-
ever, above this concentration, they form micelles (i.e. aggregates
of surfactant molecules). This specific concentration is known as
the critical micelle concentration or cmc is an important parameter
that characterizes the aqueous solutions of surfactants. The IUPAC
Manual of Symbols and Terminology (1972) defines the cmc as "the
relatively small range of concentrations separating the limit below
which virtually no micelles are detected and above which virtually
all additional surfactants form micelles." A micelle is an aggregate
of surfactant molecules in an aqueous solution, oriented such that
the nonpolar tails of the surfactant molecules are shielded from the
surrounding aqueous solution and their polar head groups at the sur-
face of the micelle, in contact with the surrounding aqueous solu-
tion.

The simplest type of micelle is the original Hartley spherical
micelle (Hartley, 1936), with the polar heads on the surface of the
sphere and the nonpolar tails in the interior of the sphere. These
simple micelles form at surfactant concentrations just above the cmc.
With increasing surfactant concentration, the other structures such
as cylindrical rods, ellipsoids, disks and lamellae have been

reported in literature (Winsor, 1968; Friberg, 1971; Shah, 1977). The number of monomers that make up the micelle is known as aggregation number. This number is typically around 80 to 100 for simple micelles. The polar heads will ionize in an aqueous solution and some of the ionized groups will have a counterion associated with them. These counterions can come from either the surfactant itself, or from added electrolyte in the solution. The degree of ionization is defined as the fraction of the polar groups that are ionized and is typically in the order of 0.2 to 0.8. Because of the ionization of the polar head groups, ionic micelles will have a net surface charge. This surface charge leads to a diffuse ionic layer of counterions associated with the micelle. The thickness of this double layer is largely a function of the ionic strength of the solution. Moreover, the surface pH of the micelle is different than the bulk pH due to the net charge at the micellar surface.

The driving force for micellization process is the "Hydrophobic Effect" which arises form the cohesiveness of the water molecules (Kauzman, 1959; Nemethy, 1967; Tanford, 1973; Franks, 1975). The surrounding water, while accepting the polar surfactant head, squeezes out the nonpolar surfactant tail. This effect, together with the repulsion between the head groups in ionic micellea, determines the formation and structure of the micelles.

1.5 Microemulsions

In general, oil and water do not mix with each other. A macroemulsion can be obtained upon addition of an appropriate

surfactant to the mixture of oil and water. Macroemulsions are thermodynamically unstable systems and they separate out into oil and water upon standing. If a suitable short chain alcohol is added to such systems, a clear transparent or translucent dispersions as microemulsions may be obtained. Microemulsions can be thermodynamically stable. They contain microdomains of oil and/or water stabilized by a mixed film of surfactant and cosurfactant. Microemulsions are four or five component systems containing oil, water, surfactant, cosurfactant, and in some cases electrolytes. Microemulsions have been studied extensively, theoretically as well as experimentally. Schulman and his co-workers used X-ray diffraction (Schulman and Riley, 1948), electron microscopy (Stockenius et al., 1969), light scattering (Schulman and Friend, 1949), ultracentrifugation (Bowcott and Schulman, 1955), and viscosity (Cook and Schulman, 1965) to show that the single phase microemulsions consisted of spherical droplets with a diameter ranging from 100 - 800 A. Microemulsions can be either water external (oil dispersed in water, O/W) or oil external (water dispersed in oil, W/O). The microemulsions can be formed by titrating turbid surfactant-oil- water emulsion with cosurfactant, usually short chain alcohols, to a transparent state (Bowcott and Schulman, 1955). Since the formation of microemulsions does not require extensive energy input, the role of alcohol in the formation of microemulsion is to provide a metastable negative surface free energy to break up the interface and produce the micro-droplets (Cook and Schulman, 1965). From the alcohol titration curves, interfacial composition of the microemulsions can be obtained (Pithapurvala and Shah, 1984a). It is possible to induce a phase separation from one

type of microemulsion to the other by adding increasing amounts of dispersed phase. Beginning with the mixed film theory of Bowcott and Schulman (1955), there have been several theories (Friberg, 1977; Ruckenstein, 1976; Eicke, 1979) to account for the existence and thermodynamic stability of microemulsions. However, there is yet no completely satisfactory theory to explain the formation and stability of microemulsions in terms of structure and concentrations of components needed to form such systems.

Microemulsions are capable of dissolving large quantities of dispersed phase. They also exhibit a very low interfacial tension between the dispersed and continuous phases (Ahmad et al., 1974). All surfactants are not capable of forming microemulsions. They do so under certain physicochemical conditions only. The nature and concentration of all components are very important in determining the formation of microemulsions. It has been reported in literature (Bansal et al., 1980) that the maximum solubilization capacity of a microemulsion exhibits a chain length compatibility effect; the maximum water solubilization capacity of a W/O microemulsion occurred when the chain length of the alcohol plus that of oil were equal to the chain length of the surfactant. They (Bansal et al., 1980) also illustrated the sensitivity of microemulsions to small variations in the chain length of the components. Microemulsions and swollen micellar solutions have many similarities, and the distinction between them is not clear. It is known that all micellar solutions cannot be swollen to the extent of microemulsions unless the specific structural requirements and conditions are satisfied. It has been

proposed, based on investigations using various physical techniques (Shah et al., 1977), that isotropic, clear and stable dispersions can be classified among three types; swollen micellar solutions, microemulsions or co-solubilized systems. The co-solubilized systems (Shah and Hamlin, 1971; Chan, 1978) resemble molecular solutions of all four components. However, the possibility of the presence of very small aggregates of water or emulsifiers is not ruled out. The co-solubilized systems exhibit very low electrical resistance even when relatively small amounts of water are added to the system (Shah et al., 1977).

Fluorescence technique has been used by various investigators to probe the interior of microemulsions (Eicke and Zinsli, 1978; Kumar and Balasubramanian 1980; Mackay et al., 1980). Eicke and Zinsli (1978) studied the effect of varying amounts of water and Aerosol OT on possible structural changes in W/O microemulsions using nanosecond fluorescence spectroscopy. They concluded, from observed rotational correlational times, that one could get the information regarding the binding of the fluorescent probe to the surfactant layer and its tendency to diffuse into the interface. Kumar and Balasubramanian (1980) investigated the microemulsion system of Triton-hexanol-cyclohexane-water. They concluded, from the emission spectra and quantum yields of 8- anilinonaphthalene sulfonic acid, that water in water pools of microemulsion is not significantly different from bulk water in its features. Mackay et al. (1980) have shown that the interphase region of the microdroplet in which the indicator is located has an effective dielectric constant of about 20.

1.5.1 Phase Diagrams

Systems of surfactant, oil and brine exhibit phase behavior that can be represented by one of the three phase-diagrams (Winsor, 1948, 1950, 1968) as shown in Figure 1.3. Type I is where the microemulsion along the binodal curve is in equilibrium with excess oil (Figure 1.3a); i.e. lower phase microemulsion in equilibrium with excess oil.

Type II is where the microemulsion is in equilibrium with excess brine (Figure 1.3b); i.e. upper phase microemulsion in equilibrium with excess brine.

Type III is where the microemulsion is in equilibrium with excess oil as well as excess brine. Figure 1.3c shows that the compositions in the right hand side lobe would form Type I microemulsion. And compositions in the upper left lobe would form Type II behavior whereas the region marked by 3-phase exhibits Type III behavior i.e. a middle phase microemulsion in equilibrium with excess oil and brine. In oil recovery literature, Type I, II and III behavior are also known as l (lower phase), u (upper phase) and m (middle phase) microemulsion respectively. Some of the variables that influence the l—> m —> u transitions are

1. salinity of the system

2. molecular weight, concentration and structure of surfactant

3. concentration and structure of cosurfactant

4. structure of oil
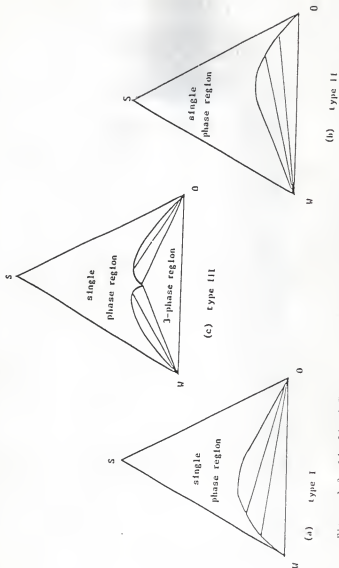
Figure 1.3 Idealized Ternary Diagram Representing Type I, II and III Systems.

5. temperature

6. the addition of polymers

7. water/oil ratio

8. pressure

All of these parameters change the relative affinity of the surfactant for the oil and water, and therefore tend to influence the system type. The transition from I —> II —> III has been shown to be very sensitive to the salinity. Temperature, on the other hand, does not strongly influence surfactant partitioning in general.

1.5.2 Structure of Middle Phase Microemulsions

Middle phase microemulsions or the Winsor Type II systems are of special interest to tertiary oil recovery for several reasons: First, they provide superior oil recovery; second, they exhibit ultra-low interfacial tension in the range of millidyne/cm with the excess oil and excess brine phases third, their microstructure must be of a remarkable nature; and fourth, their existence is a useful indicator of a hydrophilic-lipophilic balance (HLB) (Huh, 1979).

The Type I system, where the lower phase microemulsion co-exists with excess oil, is known to consist of a dispersion of oil in brine or water external microemulsions. In the Type II system where the upper phase microemulsion co-exists with excess brine, the microemulsion is oil external or dispersion of brine in oil. An intriguing question, then, is what is the structure of the Type III system or middle phase microemulsion that co-exists with oil and brine?

Since the importance of the middle phase formation in enhanced oil recovery using surfactant flooding has been realized, the elucidation of the structure of the middle phase is a very hotly pursued objective of the research in the field of tertiary oil recovery. Scriven (1976, 1977) proposed that the middle phase may have a bicontinuous structure of oil and water with continuous intervening surfactant layers. This surfactant layer divides the volume into two multiply connected, interpenetrating sub-volumes, each of them is physically continuous. Hatfield et al. (1978) reported that the structure of middle phase depends on the chain length of oil. The microemulsion with higher molecular weight alkane exhibits gradient structures. Friberg et al. (1976) and Huh (1979) proposed a structure for the middle phase, as a mixture of spherical aggregates and planar surfactant layers. Miller et al.(1977) proposed that the middle phase microemulsions may be formed by phase separation from either an oil-in-water or water-in-oil microemulsion into a continuous phase and another microemulsion phase richer in the droplets of the dispersed phase. However, they did not rule out the possibility that the middle phase may be oil or water external microemulsions at salinities other than optimal salinity.

Hsieh and Shah (1977) have suggested that the structure of the middle phase is that of a water-external microemulsions with monodispersed oil droplets suspended in a continuous aqueous phase. This conclusion was based on various observations. At low salinity (Type I system), the aqueous phase contains surfactant micelles with solubilized oil. As the salinity increases, the size of micelles

increases due to the increase in the amount of solubilized oil, presumably because of the increased size of micelles. Moreover, at higher salinity, the surfactant and oil present in the lower phase exhibit a greater tendency to come out of the aqueous phase due to "salting out." Also, the electrical repulsion between the swollen micelles decreases due to the neutralization of the surface charges and the compression of the electrical double layer around the micelles. Therefore, the microemulsion droplets can approach each other more closely through the Van der Waals attractive forces between them. And the buoyancy force on the swollen micelles increases with an increase in salinity because of larger size of micelles. The combination of above mentioned factors drives the swollen micelles out of the bulk brine phase. And consequently, a new phase containing swollen micelles is formed and separated from the brine phase, often referred to as the coacervate phase.

1.6 Oil Displacement Efficiency by Surfactant/Polymer Flooding

The process of surfactant/polymer flooding, if properly designed and controlled, has the potential for achieving maximum oil recovery from a water-flooded petroleum reservoir. Laboratory and field studies on oil displacement efficiency by surfactant-polymer flooding have been reported by a number of investigators (Hirasaki, et al., 1980; Nelson, 1980; Nelson and pope, 1978; Hill and Lake, 1978; Larson, 1979; Larson and Hirasaki; 1978; Kremsec and Treiber, 1978; Abrams, 1975; Gogarty et al., 1970; Gogarty and Tosch, 1968; Healy and Reed, 1974, 1976; Healy et al., 1975; Holm, 1971; Holm and Josendal, 1972; Bernard, 1975; Hill et al., 1973; Stegemeir, 1977; Bae and

Petrick, 1977; Trushenski, et al., 1977; Gupta and Trushenski, 1979; Glover et al., 1979; Paul and Froning, 1973; Rathmel et al., 1978; Boneau and Clampitt, 1977; Foster, 1973). In general, the process is such that after being conditioned by field brine or preflush, a sandstone core or a sand pack is oil-saturated to the irreducible water content. It is then water-flooded to the residual oil level. Finally, a slug of surfactant solution followed by a mobility buffer polymer is injected. The slug of surfactant solution can be either aqueous or oleic with a surfactant plus alcohol concentration of 5 — 15 %. Surfactant formulations consisting of petroleum sulfonate, alcohol, and electrolytes have been studied extensively for their ability to achieve ultra-low interfacial tension and their effectiveness in oil displacement (Shah and Schechter, 1977; Shah, 1981b). After a surfactant slug is injected into a water-flooded reservoir, the oil ganglia are released from the capillaries upon contact with the surfactant slug, and together with the formation water, they are pushed toward the production well. If the displacing fluid is less mobile than the displaced fluid, a plug flow pattern occurs. The displacing fluid produces "fingers" following the path of the least resistance if it exhibits significantly lower viscosity than that of the displaced fluid if it exhibits significantly lower viscosity than that of the displaced oil. Thus, for a more mobile displacing fluid, it will preferentially move ahead by bypassing the more resisting oil slow moving oil phase. Therefore, in the surfactant/polymer flooding process, not only the ultralow interfacial tension between oil/water interface is necessary, but also the mobility of each injected slug has to be properly adjusted. In other words, the mobility of the

polymer slug must be equal to or less than the mobility of the surfactant slug. The effectiveness of polymers as mobility buffer agents depends upon various physiochemical parameters such as salt concentration, temperature, shear degradation, adsorption, gel formation and polymer concentration. The main criteria for a successful oil recovery process (Glover et al., 1979; Bae et al., 1974) are

1. Ultra-low IFT between the chemical bank and residual oil and between the chemical bank and drive fluid

2. Brine compatibility (i.e. no surfactant precipitation etc.) and thermal stability of surfactant formulation

3. Mobility control of injected slugs

4. Small surfactant and polymer losses to reservoir rocks

5. Economic feasibility of the process

The success of the surfactant/polymer flooding depends significantly upon the surfactant loss in porous media due to adsorption, precipitation and other factors as described in the next section.

1.7 Surfactant Loss in Porous Media

A surfactant slug, upon injection into an oil reservoir undergoes complex changes as it traverses the reservoir. Dilution of surfactant slug occurs by mixing with the reservoir oil and brine. This places stringent requirements on the design of the surfactant flood. The magnitude of loss of chemicals is an important parameter determining the economic feasibility of the surfactant-polymer flooding process. Initially, the micellar fluid is miscible with the crude oil and reservoir brine. However, due to the surfactant loss mechanisms listed below, the flood can degenerate to an immiscible

displacement process. There are six major processes by which surfac-
tant is lost from the slug:

1. Adsorption of surfactant on reservoir minerals and
   rock

2. Precipitation of the surfactant due the multi-valent
   cations present in connate or formation water

3. Phase-entrapment of the surfactant-rich phase

4. Partitioning of surfactants in oil

5. Mixing of the surfactant slug with the polymer bank in
   porous media due to the inaccessible pore volume
   effect of polymer slug

6. Dead-end pores of the rock

Adsorption of Surfactants. It is well known that surfactants
tend to concentrate at interfaces. When the surfactant slug comes in
contact with the reservoir minerals and rock, surfactant would adsorb
at the solid-liquid interface. The adsorption loss of surfactant has
to be considered for the selection of an optimum surfactant size and
its ability to lower the oil-water interfacial tension. Adsorption
of various petroleum sulfonates on reservoir cores has been studied
by various investigators (Hill et al., 1973; Gale and Sandvik, 1973;
Hurd, 1976; Bae and Petrick, 1976, 1977; Trushenski, 1977; Malmberg
and Smith, 1977; Hanna and Somasundaran, 1977). The factors that are
important in determining the adsorption loss of petroleum sulfonates
are

1. Specific surface area and electrochemical characteris-
   tics of reservoir solids (i.e. rocks, sand and
   minerals)

2. Temperature of reservoirs

3. Equivalent weight of the surfactant

4. pH of the reservoir brine and slug

5. Microstructure of surfactant formulations

6. Composition and concentration of electrolytes in reservoir brine.

It has been found that the use of sacrificial agents such as sodium tripolyphosphate and sodium bicarbonate would effectively reduce the adsorption of petroleum sulfonate on the rock (Foster, 1973; Hill et al., 1973). It has been observed by Boneau and Clampitt (1977) that the extent of adsorption of sulfonate is greater in oil-wet cores than in water-wet cores. In case of commercial sulfonates with broad equivalent weight distribution, the adsorption and concentration of surfactant at which the maxima occurs are also dependent on the flow rates (Bae and Petrick, 1976).

Surfactant Precipitation. Petroleum reservoirs contain connate waters with a range of total dissolved solids. The salinity and divalent ion content may range from fresh water to as high as 250,000 ppm. During surfactant flooding, the surfactant bank comes in contact with both the connate and the waterflood water. Due to the gradient of electrolyte concentration, the oil-surfactant solution interfacial tension depends on the local conditions. Moreover, in many cases high salinities and high divalent ion concentration may precipitate the surfactant. The presence of ethoxylated alcohols (Dauben and Froning, 1971), phosphated esters (Sharma et al., 1983) and ethoxylated sulfonates (Maddox et al., 1975; Gale et al., 1976; Bansal and Shah, 1978a) can significantly increase the salt-tolerance of surfactant formulations.

Partitioning of Surfactant in the Residual Oil Phase. The sur-
factant slug, upon injection in the petroleum reservoir, comes in
contact with the residual oil. A successfully designed surfactant
formulation produces ultra-low interfacial tension between the resi-
dual oil and surfactant solution. Chan and Shah (1980) have proposed
a mechanism for the effectiveness of surfactant formulation in pro-
ducing low interfacial tension. They proposed that the equal parti-
tioning of surfactant in the oil and brine phase is responsible in
obtaining very low values of IFT. The partitioning of surfactant
with the oil phase has also been reported by Baviere (1976). The
extent of partitioning in the oil phase is dependent on residual oil
characteristics (e.g. equivalent alkane carbon number, aromaticity,
and the amount of oil in the reservoir), surfactant molecular weight,
salinity of brine phase as well as on temperature and presaure.

Mixing of Surfactant Slug with Polymer Solution.   Surfactant
interaction with the polymer in the mobility buffer bank may result
in surfactant phase separation and macroemulsion formation. It has
been shown that under certain conditions, a mixed solution of surfac-
tant and polymer may separate into two phases, an upper phase rich in
surfactant and a lower phase rich in polymer (Desai, 1983). The
extent of surfactant-polymer mixing is enhanced by "polymer inacces-
sible pore volume" of porous media (Dawson and Lantz, 1972; Desai,
1983). This arises from the fact that due to their size and greater
molecular volume, polymer molecules are excluded from the small pores
and can propagate through only the larger pores in porous media as
compared to surfactant molecules. In contrast, water and surfactant

molecules can travel through both the large and small pores. The pore volume available to the polymer molecule is, hence, less than that available to the water or surfactant. This leads to polymer molecules moving much faster than the carrier water. As a result, the polymer molecules invade the surfactant slug, which in turn leads to the surfactant-polymer mixing in the surfactant slug. It has been observed (Trushenski et al., 1974) that such a mixing causes a separation of the surfactant formulation into two phases. The surfactant-rich phase is trapped in the porous media due to high viscosity. The surfactant-polymer interaction can be reduced if the salinity of the polymer slug is lower than the salinity of the surfactant formulation (Chou and Shah, 1980). Addition of appropriate cosolvents or cosurfactants to the mobility buffer can also eliminate the phase separation (Trushenski, 1977).

1.8 Scope of the Dissertation

The main objective of the dissertation is to determine the interfacial composition of microemulsions and their fluorescence intensity. The understanding of these aspects of microemulsions is then used to establish some selection criteria for formulation of a surfactant slug for a reservoir crude oil under reservoir conditions of temperature and salinity. The attempt is made in this dissertation to answer several important questions pertaining to the ionic and interfacial properties of microemulsions and the oil displacement efficiency in porous media by surfactant/polymer flooding. A few of these questions are as follows:

1. Can microemulsions be modeled such that the determination of interfacial composition of such microemulsions is possible?

2. Is there a chain length compatibility effect in microemulsions?

3. Is the alcohol to surfactant ratio at interface maximum at optimal salinity?

4. Is there a correlation between solubilization capacity and fluorescence behavior of microemulsions?

5. What is the definition of optimal salinity in terms of molecular phenomena?

6. Can fluorescence measurements determine surface potential of micelles?

7. Is the concept of equivalent alkane carbon number (EACN) valid in modeling a reservoir crude?

8. Can the salt-tolerance and effectiveness of the surfactant slug be enhanced by the use of phosphated esters?

9. Can the partitioning of alcohols in equilibrated systems provide useful information for the mechanism of oil displacement process?

10. Is there a correlation between the oil displacement efficiency and surfactant retention, surfactant breakthrough and alcohol partitioning in the equilibrated phases?

Chapter II contains a detailed description of all the experimental techniques used in these studies, as well as a list of all chemicals used. A modified Schulman-Bowcott model for microemulsions is presented in Chapter III which can determine the alcohol to surfactant ratio (n_a^i/n_s) at the interface. The effect of salinity on the interfacial composition is studied. This chapter also deals with elucidation of chain length compatibility observed in microemulsions.

Chapter IV describes the fluorescence behavior of micelles and microemulsions. The fluorescence technique is a very useful tool in exploring the microenvironment of surfactant containing systems. Surface potentials of sodium dodecyl sulfate micelles and the effect of added electrolytes on the surface potential of micelles using Gouy-Chapman theory are calculated. This chapter also contains the effect of oil and alcohol chain lengths on fluorescence and solubilization behavior of petroleum sulfonate containing microemulsions. A correlation between fluorescence behavior and solubilization capacity of microemulsions is presented. Finally, a definition of optimal salinity is given in terms of interfacial composition of microemulsions.

Chapter V contains results of phase behavior and equilibrium properties of surfactant-alcohol-oil-brine systems. The effect of sacrificial agents such as sodium tripolyphosphate and sodium carbonate on solubilization parameters of three phase systems and optimal salinity is shown. The equivalent carbon number of Ankleshwar crude oil is modeled using the phase behavior of surfactant formulations. This chapter also includes viscosity measurements of

surfactant-rich phases. Finally, the alcohol partitioning in the equilibrated phases is also investigated.

Chapter VI describes the transport and chromatographic separation of surfactant slug constituents in porous media. The effect of salinity and nature of alcohol on oil displacement efficiency is shown. This chapter also includes the studies on surfactant retention and surfactant breakthrough in porous media. Finally, based on these observations, a mechanism for oil displacement efficiency is proposed.

Chapter VII summarizes the conclusions from the previous chapters and offers some suggestions for future research in this area.

CHAPTER II
MATERIALS AND METHODS

2.1 Introduction

Commonly used surfactants in tertiary oil recovery are manufactured by the process of sulfonation of a refinery stream. The historical development of sulfonates for EOR is given in Table 2.1. The resulting petroleum sulfonates have a straight hydrocarbon chain (nonpolar tail) attached to a benzene sulfonate (polar head). Such surfactants have the advantages from economic and supply points of views. However, the major drawbacks associated with the use of these surfactants are the presence of organic and inorganic impurities in the surfactants and a broad variety of surfactant species, and differences in the polar and nonpolar portions of the surfactant molecules. Since the aim of this dissertation was twofold: to elucidate the ionic and interfacial properties of microemulsions, as well as their structure and modeling, and to examine the effects of such properties on enhanced oil recovery process by microemulsion flooding. Hence, it was essential that the surfactant employed in these studies be a representative of those that are widely used in EOR processes, such as petroleum sulfonates. The results obtained using petroleum sulfonates are compared with those obtained using well

characterized and isomerically pure surfactants such as sodium stearate and sodium dodecyl sulfate for accurate interpretation.

2.2 Materials

The following surfactants, cosurfactants and oils are used in this dissertation.

Commercial Surfactants. Petroleum sulfonates TRS 10-410 and TRS 10-80 were obtained from Witco Chemical Company and they were used as received. The manufacturer specifications for these two surfactants are given in Table 2.2. A phosphated ester, KF AA-270 was obtained from BASF Wyandotte Company and was used as received.

Pure Surfactants. Two pure surfactants were used in delineating the structure and model of microemulsions and micelles. Sodium stearate, a fatty acid soap and sodium dodecyl sulfate were purchased from Matheson, Coleman and Bell Inc. and Fisher Scientific Company respectively and were used as received.

Oils. All the hydrocarbon oils used in this study were of at least 99% purity and were obtained either from Chemical Samples Company or from Phillips Petroleum Company. These oils were all saturated, straight chain alkanes of the homologous series C_nH_{2n+2}. They are listed in Table 2.3 together with some of their physical properties. It should be noted that the chain length of the oils is denoted by C_n, where n is the number of carbon atoms in the chain.

Crude oil from Ankleshwar oil field located in the western part of India was obtained from the Institute of Reservoir Studies, India.

Table 2.1 Historical Developments of Sulfonates for
Enhanced Oil Recovery+

Feedstock	Sulfonating Agent	Extraction Step	Comments
Gas-Oil Fractions	H_2SO_4	Generally yes, Either Feed or Product	Sludge Disposal Problem
Gas-Oil Fractions	SO_3	Generally yes, Either Feed or Product	Expensive
Crude Oil	SO_3	No	Inexpensive but Contain Impurities
Synthetics	SO_3	No	Possible Way of Future

+ from Gogarty (1983)

Table 2.2 Compositional Assay of TRS 10-80 and TRS 10-410
Petroleum Sulfonates (supplied by the manufacturer)

	TRS 10-80	TRS 10-410
Percent Active Sulfonate......	80	62
Free Oil (%)	7-8	33
Water (%)	10-12	4-5
Inorganic Salt (%)	1.0	0.1
Average Molecular Weight......	420	418

Table 2.3 Specifications of Oils Used in This Research

Chemical Name	Chemical Composition	Molecular Weight	Density (g/cc)+
n-Hexane	C_6H_{14}	86	0.660
n-Heptane	C_7H_{16}	100	0.684
n-Octane	C_8H_{18}	114	0.702
n-Nonane	C_9H_{20}	128	0.718
n-Decane	$C_{10}H_{22}$	142	0.730
n-Dodecane	$C_{12}H_{26}$	170	0.749
n-Tetradecane	$C_{14}H_{30}$	198	0.763
n-Hexadecane	$C_{16}H_{34}$	226	0.773

+ from Dean (1973).

It was used as received. The characteristics of this crude oil is shown in Table 2.4.

Alcohols. The alcohols used in this study were at least 99% pure and were obtained either from Chemical Samples Company or from Phillips Petroleum Company. These alcohols were either straight chain or branched chain and were fully saturated. They are listed in Table 2.5 together with some of their physical properties.

Miscellaneous Chemicals. For fluorescence measurements, a surfactant type of fluorescent dye was synthesized in our laboratory. The chemical structure of this dye, 4-heptadecyl umbelliferone, is shown in Figure 2.1.

The sodium chloride and sodium tripolyphosphate used were of reagent grade and were purchased from Fisher Scientific Company. Sodium carbonate was obtained from Mallinckrodt company. For oil displacement studies, the polymer Pusher^{TM} -1000 was used and was obtained from Dow Chemical Company. The water was deionized and distilled from an all glass still.

2.3 Methods

Fluorescence Measurements. A majority of analytical methods are based on the interaction of radiant energy with the matter. In a typical molecule, the first few energy levels may be shown as in Figure 2.2. Here, the molecule has a singlet ground state designated as S_0 which represents its normal unexcited condition. Upon absorption of radiant energy, two series of excited states exist, the singlet

Table 2.4   Characteristics of the Ankleshwar Crude Oil

API Gravity	....	43-51
Density at 15 C, gm/cc	....	0.77-0.81
Kinematic Viscosity at 80 ℃, centistokes		1.4-2.3
Pour Point, ℃	....	15-24
Sulfur (%)	....	0.01-0.04
Wax (%)	....	6.8-14.5
Asphaltenes (%)	....	0.08-0.24
Resins (%)	....	0.57-4.1
Gasoline, 100-150 ℃ (%)	....	18.6-42.2
Kerosene, 150-200 ℃ (%)	....	22.9-31.4
Gas-Oil, 250-350 ℃ (%)	....	15.0-26.1
Residue After 350 ℃ (%)	....	16.5-28.0

Table 2.5 Specifications of Alcohols Used in This Research

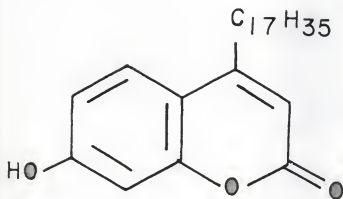| Chemical Name	Chemical Composition	Molecular Weight	Density $(g/cc)+$	Solubility in Water (parts per 100)+
Isopropanol	C_3H_7OH	60	0.785	
n-Butanol	C_4H_9OH	74	0.810	9.0
sec-Butanol	C_4H_9OH	74	0.808	12.5
Isobutanol	C_4H_9OH	74	0.779	10.0
n-Pentanol	$C_5H_{11}OH$	88	0.818	2.7
tert-Pentanol	$C_5H_{11}OH$	88	0.809	
n-Hexanol	$C_6H_{13}OH$	102	0.822	0.60
n-Heptanol	$C_7H_{15}OH$	116	0.824	0.054

+ from Dean (1973)

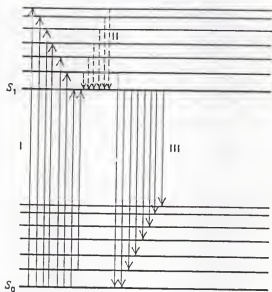Figure 2.1 Chemical Structure of 4-Heptadecyl Umbelliferone

Figure 2.2 Transitions Involved in Molecular Fluorescence.

series S and the triplet series T. Each electronic level (S or T) has associated with it a series of vibrational sublevel, corresponding to the energy required to excite various modes of vibration within the molecule. The closely spaced lines related to each vibrational sublevels correspond to the energy of rotation within the molecule.

The energy gained by a molecule by absorption of a photon does not remain in that molecule but is lost by any of several mechanisms. Of considerable importance in solution chemistry is the case in which part of energy is converted to heat, lowering the net energy of the molecule to the lowest vibrational and rotational level within the same electronic (singlet) level. The remainder of the energy is then radiated, returning the molecule to its ground state. This is the phenomenon of fluorescence as shown in Figure 2.2 by processes I, II and III. The emitted radiation has less energy per photon than exciting radiation because of loss of energy due to vibrational relaxation and hence the emitted radiation has a longer wavelength. Many organic and some inorganic compounds, when irradiated with ultraviolet light, fluoresce in the visible region. In studies of fluorescence, one is generally concerned with three types of spectra namely, the absorption spectrum, the excitation spectrum and the emission spectrum. The excitation spectrum and absorption spectrum are nearly identical and are mirror images of each other.

Since fluorescent radiation originates in the sample, it is emitted equally in all directions, and so in principle, it can be observed from any angle. In practice, three different geometries are

used. An angle of 90 degrees from the incident beam is the most con-
venient angle from the design point of view. Observation at a small
angle is advantageous if the solution is so concentrated that most of
the absorption, and hence, most of the fluorescence generation take
place close to the irradiated surface. This configuration is also
desirable if the solution absorbs appreciably at the wavelengths of
fluorescence, because the emitted radiation need travel only a
minimal thickness of solution.

Since the fluorescence depends on pumping energy into a molecule
at one wavelength and emission of light by the molecule at some
longer wavelength, one must have a primary high energy source (e.g. a
Xenon lamp), a monochromator to provide selective excitation light to
the sample (excitation monochromator), a monochromator to provide
selective emission from the sample (emission monochromator), a detec-
tor and a recorder.

The fluorescence work reported in this dissertation was carried
out using a Perkin-Elmer fluorescent spectrophotometer, model MPF-44B
with differential correction unit DCSU-2. The optical diagram of
this model is shown in Figure 2.3. This fluorescent spectrophotome-
ter has two grating monochromators with continuously variable
bandpass selection from 0.2 to 20 nm. The excitation monochromator
isolates wavelengths from the Xenon source lamp and irradiates the
sample with monochromatic light in the range of 200 nm to 1200 nm.
The emission monochromator views the emitted light from the sample
and permits selective measurement of its intensity in the 200-1200 nm
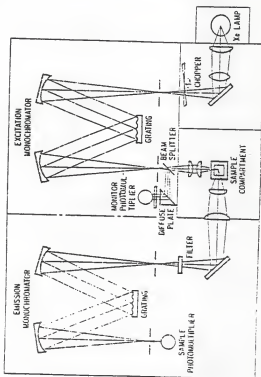wavelength range. The light from the emission monochromator is

Figure 2.3 Optical Diagram of Fluorescence Spectrophotometer

measured by a photomultiplier detector with a broad spectral response. A block diagram of this instrument is shown in Figure 2.4.

The mathematical treatment of fluorescence is much more complicated than the mathematics of simple absorption leading to Beer's law. For one thing, the amount of primary radiation absorbed varies exponentially throughout the body of the solutions, in accordance with the absorption law. For another, the fluorescent light is always subject to at least slight absorption in the solution, and thickness of solution through which it passes is not constant, because the radiation does not originate at a single point(Ewing, 1975).

Analysis of Surfactant. The concentration of the surfactants was determined by the two-phase dye titration method. The two-phase titration method is applicable only for determination of concentration of anionic surfactants. The indicator used in this method is a mixture of Dimidium Bromide (cationic) and Disulfine Blue VN (anionic) dyes. The sample containing unknown amount of surfactant is mixed with chloroform, water and the indicator and titrated against a standard solution of the cationic surfactant Hyamine-1622 (p-ter octylphenoxyethoxyethyl dimethyl benzyl ammonium chloride). The mixed indicator and the Hyamine-1622 were both obtained from BDH Chemicals Ltd., Poole, England. The two phases employed in the titration are an aqueous phase and a chloroform phase. The chloroform was A.R. grade from Mallinckrodt Inc. Surfactant concentrations were calculated using the following expression.
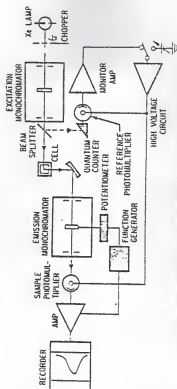
THE UNITS MARKED AS ☐ ARE COMPONENTS OF THE CORRECTED SPECTRA UNIT.

Figure 2.4 Block Diagram of Fluorescence Spectrophotometer

$$C_s = \frac{M_1}{10} \cdot C_H \cdot \frac{V_1}{V_2}$$ (2.1)

where C_s : surfactant concentration in wt %,

M_1 : molecular weight of the anionic surfactant,

C_H : the molarity of the Hyamine-1622,

V_1 : the titre value of Hyamine-1622,

V_2 : the volume of the sample

It has been reported (Noronha, 1980) that the presence of oil, alcohol or electrolytes does not affect the determination of surfactant concentration by this method. The accuracy of the surfactant concentrationa determined by this method is 2% of the mean value for concentrations above 0.1% (w/v).

Analysis of Alcohol. The concentration of various alcohols was determined using Perkin Elmer 900 gas chromatograph with SE column having 3% chromosorb support. Flame ionization detector was used for all gas chromatograph work under isothermal conditions. Calibration curves were prepared using known concentrations of alcohol in water as well as oils. Samples containing unknown amounts of alcohol were injected in the gas chromatograph using the calibration curves. Alcohol concentrations thus obtained in oil as well as in water were reproducible within 0.5% of the mean value.

Electrical Conductivity. Electrical conductivity measurements can be used to determine the continuous phase of microemulsions or cmc of various ionic surfactants. Electrical conductivities were measured using a Beckman model RC 16 B2 conductivity bridge. The

cell used in these measurement had a cell constant of 1.0 cm^{-1}. The readings were taken at room temperature (23 ℃).

Viscosity. Viscometric measurements of surfactant containing phases were carried out using Brookfield viscometer having the shear rate from 1.15 to 230 sec^{-1}. All the readings were obtained at 80 ℃ by circulating hot water in the jacket surrounding the viscometer plate. A small amount of the sample was introduced into the viscometer plate and readings were taken after two minutes of shearing, when the pointer was stable. Readings were taken for ascending as well as descending shear rates.

Interfacial Tension. Spinning drop interfacial tensiometer was used to measure interfacial tensions between phases. This technique, developed by Cayias et al.(1976) consists of filling a capillary tube with the denser liquid and then introducing a drop of lighter liquid into it. The tube containing the sample is rotated about its major axis which results into the deformation of the drop to an elliptical shape. The apparatus uses a hysteresis synchronous motor whose speed can be controlled by varying the frequency from a frequency generator. To measure the dimensions of the drop, a Gaertner microscope with a filar eyepiece was used.

When the shape of the drop is such that the ratio of the major axis to minor axis is greater than 4.0, the drop can be treated as a cylinder with hemispherical ends. For such shape , the interfacial tension can be calculated using the following equation:

$$\gamma = 1.234 \times 10^6 \times \frac{\Delta \rho\ d^3}{P^2}$$

where γ : the interfacial tension in dynes/cm

                 $\Delta\rho$: the density difference between the two phases, gm/cc

                 d   : the diameter of the drop in cm

                 P   : the speed of rotation in msec/rev.

All the readings were taken at room temperature. The accuracy and reproducibility of interfacial tensions measured by this method depends upon the system under investigation, the order of mixing, the time of equilibrium of the samples and the duration of measurement of the interfacial tension (Noronha, 1980). The measurements were made after a thorough equilibrium of oil and surfactant formulation on a rotor for 24 hours and allowing additional two weeks for the phase separation. Interfacial tension values reported are for the equili- brated phases.

The methodology used in porous media study is incorporated in Chapter VI.

3.1 Introduction

Mixtures of oil and water are naturally unstable but can be sta-
bilized by the addition of appropriate surfactants and cosurfac-
tants. In contrast to regular macroemulsions which are unstable,
microemulsions are thermodynamically stable. They are clear or
translucent systems containing microdomains of oil and/or water sta-
bilized by a mixed film of surfactant and cosurfactant (Shah et al.
1972; Gerbacia and Rosano, 1973). Microemulsions have been studied
extensively theoretically as well as experimentally by various inves-
tigators (Schulman and Riley, 1948; Shah and Hamlin, 1971; Shah et
al. 1972; Clausse et al. 1976; Prince, 1977; Eicke and Shephard 1977;
Shinoda and Friberg 1975; Shinoda and Kuneida, 1973 Sharma et al.
1983; Friberg and Buraszenka 1978). The formation and various phy-
sicochemical properties of the microemulsions are influenced by the
alkyl chain length of surfactant, cosurfactant as well as hydrocar-
bons. For example the interfacial composition and distribution of
alcohol in the oil and aqueous phases are influenced by the alkyl
chain length of alcohol and oil (Bansal et al., 1979, 1980).

Phase diagram studies (Gilberg et al., Ekwall et al., 1972; Shi-
noda, 1967b; Ahmad et al., 1974; Friberg et al., 1976; Rance and Fri-
berg, 1977) have shown that water-external microemulsions are a

continuation of aqueous micellar solutions whereas oil-external microemulsions are a continuation of the inverted micellar solution. Recently, it was reported (Siano, 1983) that the transition from the swollen micelles to microemulsions of nonionic surfactants takes place at a certain oil content of the system. Above this concentration, the particles behave as nonassociating hard spheres, while below this concentration, the particles are anisotropic in shape and are probably undergoing some type of association and they are similar in their properties to the surfactant micelle. It was further reported that the kinetics of solubilization of oil is much slower for the microemulsions than the swollen micelles when the system is initially dilute.

From the view point of phase equilibria, it appears that the difference between micellar solutions and microemulsions is only a matter of sementics. However, the energetics involved in the formation of micelles or microemulsions may be different (Chou, 1980). The formation of micelles is largely determined by the hydrophobic and electrostatic interaction between surfactant molecules (or ions) in the case of normal micelles (Debye, 1949; Tanford, 1977; Shinoda 1967a, Mukerjee, 1976) or by the ion-dipole interactions in the case of inverted micelles in non-polar media (Eicke, 1975; Kitahara et al., 1969; Eicke, 1977; Eicke and Rehak, 1976). For microemulsions, it has been shown theoretically that the specific interfacial free energy or the interfacial tension has a decisive effect on the stability of microemulsions. Other important factors influencing the formation and stability of microemulsions are energy of formation of

electrical double layer, double layer repulsion and van der Waals attraction between dispersed particles, and entropy of dispersion (Prince, 1967, 1969; Reiss, 1975; Ruckenstein and Chi, 1975; Overbeek, 1978; Adamson, 1969; Levine and Robinson, 1972). Winsor (1948, 1950; 1954; 1968; 1974) developed a theory of intermicellar equilibrium between molecules and different micellar species. Using phase diagrams of surfactant systems, he formulated the R-theory of solubilization to characterize the microstructure of solutions. He defined the parameter R, as follows:

$$R = \frac{A_{co}}{A_{cw}} \tag{3.1}$$

where A_{co} : the affinity between surfactant

and hydrocarbon phases

A_{cw} : the affinity between surfactant

and aqueous phases

The orientation of surfactant molecules and the intermolecular forces between the polar heads determine the curvature of the interfacial film and correspondingly determine the type of dispersion (i.e. W/O or O/W).

Thermodynamic treatment of surfactant containing systems have been reported in literature and general reviews on micelles and microemulsions are available (Eicke, 1980; Forest and Reeves, 1981; Lindman and Wennerstrom, 1980; Motomura and Baret, 1983; O'Connell and Brugman, 1977; Wennerstrom and Lindman, 1979). These studies have addressed various aspects such as the mechanism of surfactant

aggregation process, the role of intermolecular forces and the stability of the dispersions. Rehbinder (1957) recognized that the interfacial tension need not be negative for spontaneous emulsification to occur. However, the interfacial tension should be very low to allow for a very large increase in interfacial area in microemulsion systems. Ruckenstein and coworkers (Ruckenstein and Krishnan, 1979, 1980; Ruckenstein and Chi 1975; Ruckenstein 1976; Ruckenstein and Nagarajan, 1975, 1976; Nagarajan and Ruckenstein, 1977) have discussed the origin of the thermodynamic stability of microemulsions from the point of view of dispersion entropy and free energy of formation of microemulsions. They also have been successful in modeling the formation of microemulsions based on thermodynamics. In one of their models (Ruckenstein and Krishnan, 1979), they assumed that the solubilized phase was dispersed as globules in the continuous phase with the droplets surrounded by adsorbed surfactant. They concluded that the single nonionic surfactants possessing the usual range of heats of adsorption and with the head group area less than 100 angstrom per surfactant molecule are not likely to generate microemulsions. In a subsequent paper (Ruckenstein and Krishnan, 1980), they described the domain of existence of microemulsions using phase diagram approach.

The structural models of microemulsions include hard water and oil globules (Lagues et al. 1978), a lamellar structure (Shinoda and Saito, 1968; Saito and Shinoda, 1970), cosolubilized system (Shah et al. 1976), randomly arranged polyhedra (Talmon and Prager, 1978), bicontinuous structure (Scriven, 1976; 1977) and random curvature

droplets (Friberg et al. 1976). Adamson (1969) proposed a model
whereby microemulsions were treated as system of swollen micelles in
which Laplace and Osmotic pressures are balanced. Geometric aspects
of microemulsions such as droplet radius, packing factor etc. can be
determined by a pseudophase model (Biais et al. 1981) using two par-
tition coefficients for alcohol and oil. A test for such pseudophase
model was provided by Damaszewski and Mackay (1984) for microemul-
sions containing different types of surfactants. The ionic surfac-
tants were found to fit the model over most of the compositions of
microemulsion range of existence, while the nonionic surfactants did
not fit the model.

One of the earliest models for microemulsions was that by
Bowcott and Schulman (Bowcott and Schulman, 1955). They attributed
the formation of microemulsions to the molecular interactions taking
place at the interface. The interface was seen as a third phase in
equilibrium with the oil and the aqueous phases. Using the model
involving the distribution of alcohol in various phases and assuming
that the solubility of alcohol was negligible in water and that all
the surfactant molecules partitioned in the interphase, the alcohol
to surfactant ratio at the interface was determined (Bowcott and
Schulman, 1955).

The assumption that all surfactant is present at the interface
may be satisfactory in the case of oil-external microemulsions if
high volume fraction of the dispersed phase (water) is present in the
system. However, the assumption that the alcohol does not partition
in the aqueous phase may be questionable particularly in the case of

butanol and pentanol. In this chapter the Schulman-Bowcott treatment is modified to predict the ratio of alcohol to surfactant at the interface taking into account the solubility of alcohol in either aqueous phase or the oil phase for sodium stearate system. The aqueous phase used was brine and the oils used were straight chain hydrocarbons. The brine solubilization capacity and optimal salinity of these microemulsions were determined experimentally. Dilution of these microemulsions with brine as well as oil provided necessary information to determine the molecular ratio of alcohol to surfactant at the interface.

3.2 Experimental

Sodium stearate of 99% purity from Matheson, Coleman and Bell, Inc. was used for preparing microemulsions. Pentanol and oils were purchased from Chemical Samples Company and were of 99% purity or greater. Double-distilled water was used in making all the microemulsions.

Brine Solubilization Limit.   The microemulsions were prepared by mixing surfactant (1 gm), alcohol (4 ml), oil (10 ml) and brine of different concentrations to get a clear solution. The brine solubilization limit was determined by mixing additional brine slowly from a graduated 1-ml pipette to the microemulsion, until turbidity was observed and two-phase formation occurred. In all cases, the end point was sharp (within 0.1 ml of added brine). At the endpoint the systems were initially turbid, but after a few minutes of standing two clear phases formed.

Electrical Conductivity. The electrical resistivity of the sodium stearate containing microemulsions was measured using a Beckman model RC16B2 resistivity bridge at 50 Hz. at room temperature. The cell used in these measurements had a cell constant of 1 cm^{-1}.

3.3 Optimal Salinity and Brine Solubilization Capacity of Microemulsions

The brine solubilization capacity of sodium stearate microemulsions as a function of brine concentration for different oils is shown in Figure 3.1. As the electrolyte concentration is increased, the solubilization limit increases, passes through a maximum and then decreases. Upon addition of brine, a new microemulsion phase forms whose structure has to be determined by the phase behavior and other physicochemical measurements. Up to a certain extent, the alcohol from the oil phase can partition into the interface to stabilize the additional interfacial area. However, as the alcohol in the oil phase is depleted further growth of water droplets would increase the interfacial tension at the oil/water interface due to an increase in the area per molecule and thus destabilize the microemulsion, and hence prevent further solubilization of brine.

The solubilization of brine is maximum at a specific NaCl concentration for each oil. It has been shown (Chou, 1980; Pithapurwala and Shah, 1984b) that the salinity at which the highest amount of brine is solubilized in oil corresponds to the optimal salinity of the microemulsions as determined by phase behavior and interfacial measurements (Reed and Healy, 1977). The optimal salinity at which
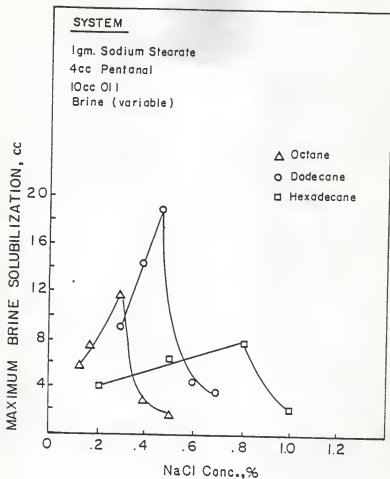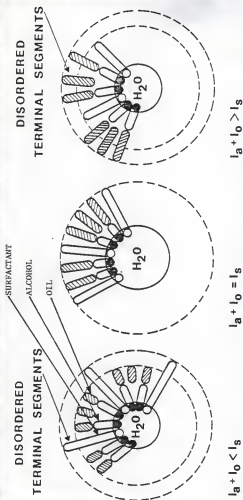
Figure 3.1 Brine Solubilization Capacity of Sodium Stearate-
Pentanol Microemulsions in Presence of Different
Oils.

middle phase microemulsion solubilizes equal volume of oil and brine
(Chan and Shah, 1979). It is seen that as the alkyl chain length of
oil increases, the optimal salinity also increases as shown in Figure
3.1. This observation is in agreement with the study carried out
using petroleum sulfonates (Hsieh and Shah, 1977; Pithapurwala and
Shah, 1984b). The concept of optimal salinity and solubilization
capacity of microemulsions is very important in enhanced oil recovery
processes by surfactant flooding (Shah and Schechter, 1977; Shah,
1981; Chou and Shah, 1981).

There is a preferred chain length of oil at which the highest
amount of brine is solubilized (dodecane as shown in Figure 3.1).
This can be explained on the basis of chain length compatibility
effect observed in microemulsions (Bansal et al., 1980; Clausse et
al., 1982) as well as in other systems (Schick and Fowkes, 1957;
Fort, 1962; Cameron and Crouch, 1963). When $l_a + l_o = l_s$, where l_a
is chain length of alcohol, l_o, chain length of oil and l_s, chain
length of surfactant, there will not be a region of disordered hydro-
carbon chains near methyl groups around the droplet as shown in Fig-
ure 3.2. Using mixed monolayer we have shown that the thermal motion
of the terminal segment produces a disruptive effect on the packing
of surface active molecules and increases the area per molecule at
the interface (Shah and Shiao, 1975). It was further shown (Shiao,
1976) that this disruptive effect causes an increase of 0.05 angstrom
in the intermolecular distance between surfactant molecules at the
interface. When dodecane was used as an oil for making the microemul-
sion, the relation $l_a + l_o = l_s$ was satisfied (approximately, but

DISORDERED TERMINAL SEGMENTS

SURFACTANT

ALCOHOL

OIL

DISORDERED TERMINAL SEGMENTS

H_2O

H_2O

H_2O

$l_a + l_o < l_s$

$l_a + l_o = l_s$

$l_a + l_o > l_s$

l_a, l_o AND l_s ARE CHAIN LENGTH OF ALCOHOL, OIL AND SOAP MOLECULES

Figure 3.2 A Chain Length Compatibility Effect in Microemulsions

much better than either with octane or hexadecane), the amount of brine that the microemulsion could solubilize was the highest due to maximum cohesive interaction between hydrocarbon chains, or in other words, due to a minimum disruptive effect in the interfacial region under these conditions.

At optimal salinity not only the molecular packing is the highest but also the molecular ratio of alcohol to surfactant is maximum at the interface. The following section describes the determination of this ratio at the interface using extended Schulman- Bowcott model.

3.4 Schulman-Bowcott Model

Bowcott and Schulman (1955) attributed the formation of microemulsion to the molecular interactions taking place at the interface. The interface was seen as the third phase in equilibrium with the oil and the aqueous phase as shown in Figure 3.3. They assumed that all surfactant was present in the interphase. This assumption holds good if there is a high volume fraction of water to provide a large area for the soap to be at the interface for oil-external microemulsions. When the system is diluted with oil, it is necessary to have a critical alcohol to oil ratio in the continuous phase to maintain the interfacial conditions necessary for the formation of microemulsions, i.e.

$$n_a^o/n_o = K_1 \tag{3.2}$$

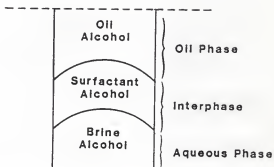where n_a^o is the number of moles of alcohol in the oil phase and n_o is

Figure 3.3 A Three Compartment Model of Microemulsion.

the moles of oil. If n_a^i is the moles of alcohol present in the interphase and n_a^{aq} is the moles of alcohol in the aqueous phase, the total alcohol n_a in the microemulsion can be represented as

$$n_a = n_a^o + n_a^i + n_a^{aq} \tag{3.3}$$

Substituting equation (3.3) in (3.2) and dividing the whole expression by the number of surfactant moles, n_s, present in the system

$$\frac{n_a}{n_s} = \frac{K_1 n_o}{n_s} + \frac{n_a^i}{n_s} + \frac{n_a^{aq}}{n_s} \tag{3.4}$$

The dilution of microemulsion by oil makes the system eventually turbid. This turbid emulsion is titrated with alcohol until it becomes clear. By plotting this molar ratio of alcohol to surfactant vs. the ratio of oil to surfactant, a straight line may be obtained if the formation of the microemulsion obeys Schulman-Bowcott model. The slope of the line gives the value of K_1 and the intercept of this line on y-axis gives $\frac{n_a^i}{n_s} + \frac{n_a^{aq}}{n_s}$ from equation (3.4). For a long chain alcohol such as hexanol, the solubility of alcohol in aqueous phase is negligible and hence the intercept of the line gives the alcohol to surfactant ratio at the interface i.e. $\frac{n_a^i}{n_s}$.

3.4.1 Modified Schulman Bowcott Model

The precise calculation of interfacial alcohol concentration is not possible using the Schulman-Bowcott model especially when a short

chain alcohol which partitions in oil, water and interphase, is used for the preparation of microemulsions. However, using similar arguments as Schulman Bowcott model , the molar ratio of alcohol to surfactant can be determined accurately by extending this model further. For a microemulsion (say w/o) if the volume fraction of dispersed phase is increased, it is necessary to maintain a critical ratio of alcohol to water in the aqueous phase for the formation of microemulsion and hence,

$$n_a^{aq}/n_{aq} = K_2 \qquad (3.5)$$

where n_a^{aq} is the number of alcohol moles in the aqueous phase and n_{aq} is the moles of brine in the microemulsion. Substituting equation (3.5) in (3.3) and dividing by the moles of surfactant, n_s,

$$\frac{n_a}{n_s} = \frac{n_a^o}{n_a} + \frac{n_a^i}{n_s} + \frac{K_2 n_{aq}}{n_s} \qquad (3.6)$$

Combining equations (3.2) and (3.6) yields,

$$\frac{n_a}{n_s} = \frac{n_a^i}{n_s} + \frac{K_1 n_o}{n_s} + \frac{K_2 n_{aq}}{n_s} \qquad (3.7)$$

As described earlier, the dilution of microemulsion with oil can give the value of K_1 and the intercept which includes n_a^i/n_s . If the microemulsion is concentrated with the dispersed phase (increasing the amount of brine in the system) the system becomes turbid . This turbid emulsion is titrated with alcohol until it becomes clear. This

method is repeated and the data are plotted as n_a/n_s vs. n_{ac}/n_s and if the formation of microemulsion obeys the extended Schulman -Bowcott method, a straight line may be obtained according to equation (3.7) with a slope K_2 and a y-intercept $n_a^i/n_s + K_1 n_o/n_s$ for a fixed value of n_o/n_s. The value of K_1 is known from the oil dilution experiment and hence the value of molar alcohol to surfactant ratio at the interface can be obtained from this intercept. A check of this value could also be provided if the oil dilution results are expressed in the form of equation (3.7).

3.4.2 Experimental Verification of Modified Schulman Bowcott Model

Following approach was taken to check the validity of this modified model. Microemulsions were prepared using sodium stearate, pentanol, various straight chain hydrocarbons and brine as an aqueous phase. The clear microemulsion was diluted with oil or concentrated with brine until it became turbid. The turbid macroemulsion was then titrated with pentanol until it became clear. For brine dilution experiments, the initial microemulsion contained surfactant (1 gm), oil (10 ml), and a small amount of brine. This mixture was titrated with pentanol until it became clear. For oil dilution experiments, the initial microemulsion contained surfactant (1 gm), brine (amount selected based on solubilization limit at high salinity for each oil), and a small amount of oil. This mixture was titrated with pentanol until it became clear. The dilution data were plotted in the form of equation (3.7) for all the systems. Figure 3.4 shows the variation of total alcohol in the system per mole of surfactant as a function of moles of octane present in the microemulsion per mole
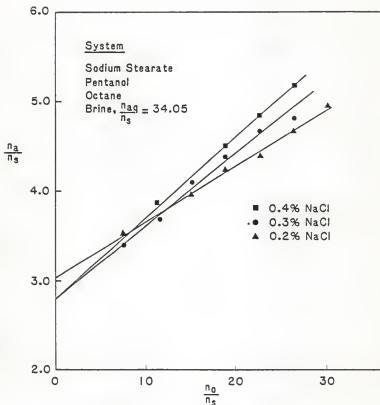
Figure 3.4 Effect of Brine Concentration on Octane/Alcohol
Titration Plots of Microemulsions

of surfactant at fixed brine to surfactant ratio The brine concentrations were below, at, and above the optimal salinity for each oil. As mentioned before, the n_{aq}/n_s molar ratio was fixed for each oil. The specific value of naq/n_s was based on solubilization limit at high salinities. Whereas Figure 3.5 shows the moles of alcohol per mole of surfactant as a function of the moles of brine per mole of surfactant at fixed octane to surfactant ratio for different concentrations of brine. It is seen that the dilution data are well represented by a straight line for all brine salinities. The intercept of these lines according to equation (3.7) gives two values of n_a^i/n_s. These values agree within 20%. The dilution data for dodecane containing microemulsions are shown in Figures 3.6 and 3.7. It is seen that these data lie on a straight line for oil dilution (Figure 3.6). However, when the microemulsion was diluted with other than optimal salinity brine, some deviation was observed for high values of n_{aq}/n_s (Figure 3.7). This deviation was positive when the dilution was done with the lower than optimal salinity brine while negative deviation was found for higher than optimal salinity brine. The values of molar alcohol to surfactant ratio at the interface was obtained using the straight line portion of the brine dilution data. These values agree within 20%. Figures 3.8 and 3.9 represent the results of microemulsions prepared using hexadecane. For all three salinities the data lie on a straight line. The values of $\dfrac{n_a^i}{n_s}$ calculated from equation (3.7) agree within 10%.

The average values of the molar alcohol to surfactant ratio at the interface is shown in Figure 3.10 as a function of brine
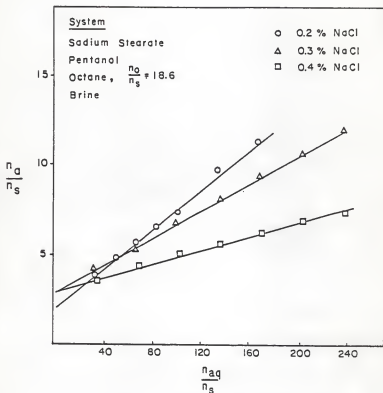
Figure 3.5 Effect of Brine Concentration on Brine/Alcohol
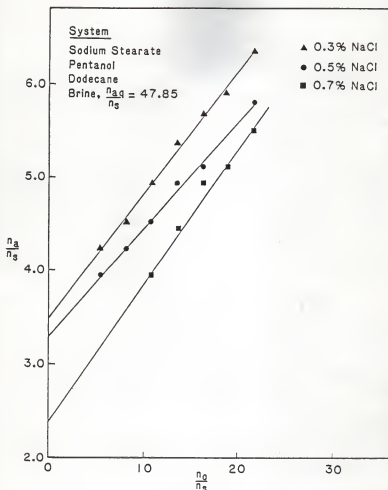Titration Plots of Microemulsions.

Figure 3.6 Effect of Brine Concentration on Dodecane/Alcohol
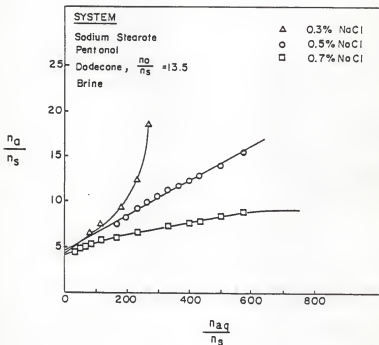Titration Plots of Microemulsions.

Figure 3.7 Effect of Brine Concentration on Brine/Alcohol
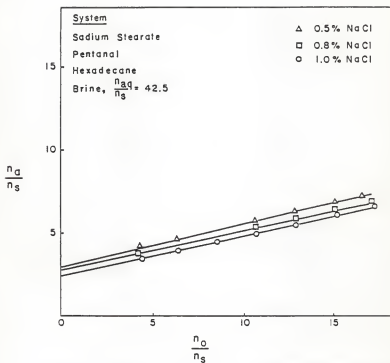Titration Plots of Microemulsions.

Figure 3.8 Effect of Brine Concentration on Hexadecane/Alcohol
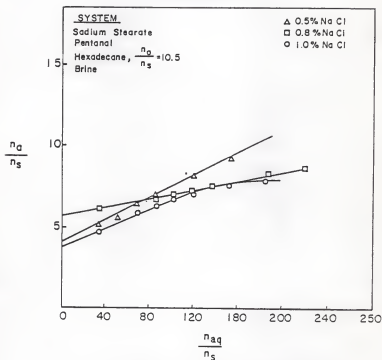Titration Plots of Microemulsions.

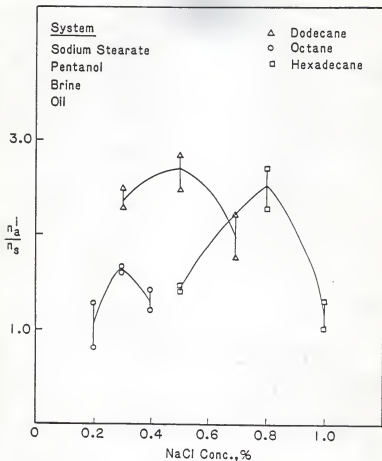Figure 3.9 Effect of Brine Concentration on Brine/Alcohol Titration Plots of Microemulsions.

Figure 3.10 Effect of Oil Chain Length on the Molar Ratio of Alcohol to Surfactant at the Interface (n_a^i/n_s) at Various Salinities.

concentration for octane, dodecane and hexadecane containing microemulsions. It is seen that at a particular salinity this ratio is maximum for each oil and this brine concentration corresponds to the optimal salinity of the system. Further, the dodecane containing microemulsion has the highest alcohol to surfactant ratio at the interface. This is a supporting evidence for the highest brine solubilization capacity of the dodecane containing microemulsion at its optimal salinity.

3.5 Electrical Resistivity of Microemulsions

The electrical resistance behavior of the sodium stearate and pentanol containing microemulsions is shown in Figure 3.11 as a function of water oil ratio for.different alkyl chain length of oil at respective optimal salinity of microemulsions. The electrical resistance values are normalized with the resistance of respective optimal salinity brines. It is seen that as the microemulsion is diluted with brine, the electrical resistance of the microemulsions decreased. The hexadecane containing microemulsions showed a much steeper decrease in electrical resistance than either octane or dodecane containing microemulsions. A similar behavior was also observed by Bansal et al.(1980) for microemulsions containing sodium stearate. This can be explained on the basis of surface resistance model (O'Conski, 1968) for polyelectrolyte systems. This model considers the effective volume resistivity as the sum of two parts, namely, parallel bulk resistivity and the surface resistivity. The surface resistivity is a function of the size of the dispersed phase and the mobility of the ions in the ionic environment of the water droplets.
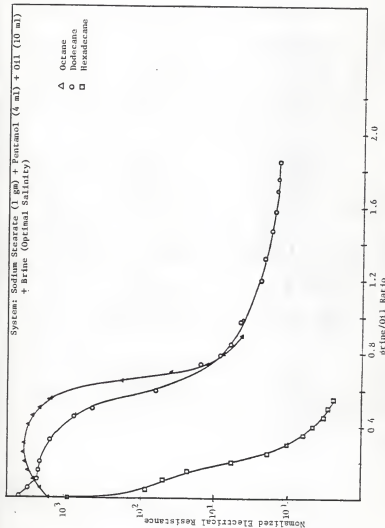
Figure 3.11 Effect of Brine/Oil Ratio on Normalized Electrical Resistance of Microemulsions.

At a given brine to oil ratio in the microemulsions, there is an increase (Figure 3.11) in the normalized electrical resistance with a decrease in the alkyl chain length of oil used in preparing these microemulsions. This suggests that the total effective volume resistivity decreases due to a smaller contribution of surface resistivity when the oil chain length is increased. The decrease in hexadecane-containing microemulsions is more pronounced because a significant amount of surfactant and alcohol may dissolve in the bulk oil decreasing the bulk resistance. Bansal et al. (1980) have attributed this to the lower degree of ionization of the sodium stearate molecules at the interface resulting into a thinning of ionic atmosphere at the interface based on their dielectric measurements of these microemulsions.

3.6 Summary

The following conclusions can be drawn from this chapter:

1. Optimal salinity increases as chain length of oil increases for sodium stearate/pentanol/oil/brine system.

2. There is a preferred chain length of oil (dodecane) where the microemulsion can solubilize maximum amount of brine. This can be explained on the basis of chain length compatibility in microemulsions.

3. The molar ratio of alcohol to surfactant can be accurately determined using the extended Schulman-Bowcott model.

4. At optimal salinity, the alcohol to surfactant ratio (molar) is maximum for the systems studied.

5. The electrical resistance of microemulsions at a given brine to oil ratio decreases as the alkyl chain length of the oil increases.

CHAPTER IV
SOLUBILIZATION AND FLUORESCENCE
BEHAVIOR OF SURFACTANT CONTAINING SYSTEMS

4.1 Introduction

The polar-nonpolar nature of surfactant molecule causes the formation of organized association structures. A schematic illustration of the formation of various structures in solution upon increasing the concentration of surfactant (Bansal and Shah, 1977) is shown in Figure 4.1. The aggregation of monomers arises not only from attractive forces between non-polar tails, but also is due to the cohesiveness of water molecules. In other words, the surrounding water, while accepting the polar head of the surfactant molecule, squeezes out the non-polar tail. This effect together with the repulsion between surfactant headgroups appears to determine the formation, structure and stability of the micelles (McBain, 1940; Alexander, 1950; Winsor 1954, 1968; Hartley, 1955; Zettlemoyer, 1958; Ekwall, 1964; Muller and Platko, 1971; Muller, 1973; Tanford, 1973; Krechek, 1974; Mukherjee et al., 1977; Hartley, 1977).

Apart from aqueous solutions, molecular association can also occur in nonpolar solvents, in which case the aggregates are called inverted micelles. The process of formation of inverted micelles is different than that of normal micelles (Mukerjee, 1969; Ekwall, 1969; Ray, 1969; Lindblom et al., 1970; Saito and Shinoda, 1970; Kon-No and

STRUCTURE FORMATION IN SURFACTANT SOLUTION

MONOMERS

SURFACTANT CRYSTAL

MICELLE

CYLINDRICAL MICELLE (RANDOMLY ORIENTED)

HEXAGONAL PACKING OF CYLINDERS

LAMELLAR MICELLE

10-35 Å WATER

10-35 Å

10-35 Å

HEXAGONAL PACKING OF WATER CYLINDER

H_2O

MICROEMULSION
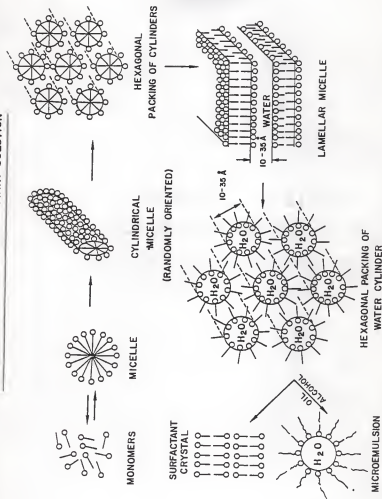
OIL

ALCOHOL

H_2O

Figure 4.1 A Schematic Illustration of Structures in Surfactant Solution (Bansal and Shah, 1977)

Kitahara, 1971 a,b,c; Fendler et al., 1973; Eicke and Christen, 1974; Eicke, 1977, 1979; Kitahara et al., 1979). Compared to the volume of work that has been reported in literature, there are much fewer investigations on inverted micelles.

The static and dynamic properties of solutions containing surfactant structures have been investigated by a variety of methods, namely, x-ray scattering (Reiss-Husson and Luzzati, 1970), light scattering (Anacker, 1958; Debye and Anacker, 1951; Emerson and Hotzer, 1967), Rayleigh scattering (Bellocq and Fourche, 1980), electrophoresis (Stigter and Mysells, 1955), temperature jump (Bennion and Eyring,1970; Lang and Eyring, 1972), NMR (Erickson and Gilberg, 1966; Fendler and Day, 1972; Muller, 1973), relaxation studies (Clifford and Pethica, 1965; Williams et al., 1973; Levy et al., 1973), ESR spin labelling (Dorich et al., 1972,; Oakes, 1973; Atherston and Strack, 1972; Waggoner et al., 1967), vapor pressure (Damaszewski et al., 1984) and positron annihilation (Boussaha and Ache, 1980). Information regarding the size, shape, and the mobility of hydrocarbon chains in the surfactant aggregates have been obtained using these techniques.

4.2 Fluorescence Probes for Surfactant Systems

The first studies of surfactant systems by fluorescence techniques were directed towards measurements of basic parameters such as cmc and the size of micelles. In this technique, a small amount of fluorescent dye is added to the micellar system. Two important factors to be considered here are; namely the concentration of the dye

should be very small so that it does not disturb the system and secondly, the fluorescent dye must display a selective affinity for a given region of an aggregate and reflect the nature of its environment in its emission properties (Gratzel and Thomas, 1976).

The fluorescent probes generally used in micellar studies are rhodamine G (Corrin and Harkins, 1947; Klein and Haar, 1978), and rhodamine B (Arkin and Singleterry, 1948; Singleterry and Weinberger, 1951). The behavior of arylaminonaphthalene sulfonates (ANS) has been explored in detail owing to their extensive use as fluorescent probe in biological systems (Weber and Laurence, 1954; Turner and Brand, 1968; Teisse, 1979). The fluorescence behavior of this dye and its derivatives have also been studied in aqueous micellar solutions (Rubalcava et al., 1969; Herman and Schelly, 1979; Birdi et al., 1978; Horowitz, 1977, Mast and Haynes, 1975). Other fluorescent probes extensively used in micellar solutions are pyrene (Thomas, 1977; Almgren et al., 1979; Sinitzky et al., 1971, Infelta, 1979, Infelta and Gratzel, 1979) and naphthalene (Bockstade 1978). These probes have the advantage over ANS in that their ground state and excited states have much smaller dipole moments and hence they are much less likely to perturb the environment they explore. According to Gratzel and Thomas (1977) these probes penetrate to the interior of surfactant micelles due to their distinct lipophilicity.

A promising development in the field of fluorescence studies with the micellar system is the design of surfactant analog probes labeled with a fluorophore at a specific site of the hydrocarbon

chain. The emission properties of such probes reveal the nature of different transverse region of the micelle.

Three principal types of fluorescence measurements are used to investigate the microenvironment of surfactant containing systems (Edelman and McClure, 1968; Radda, 1971, Brand and Gohlke, 1972). They are

1. The nature of the spectrum of the fluorescence

2. The degree of polarization of fluorescence

3. The time dependence of the fluorescence

The parameters which provide information regarding the structure of such systems are quantum yields and decay times. Rehfeld (1970 a,b) studied the surfactant system containing sodium phenylundecanoate by measuring the changes in absorption and fluorescence spectra and concluded that the micelle has a liquid hydrocarbon core of a phenyl group. The same system was investigated by Almgren (1972) using naphthalene as a fluorescent probe who concluded that both naphthalene and phenyl group of the surfactant are in micelle interior. Micellar solutions containing sodium dodecyl sulfate (SDS) have been investigated extensively (Kubota et al., 1973; Hauser and Klein, 1972; Gratzel and Thomas, 1973; Wallace and Thomas, 1973; Birdi et al., 1979; Horowitz, 1977; Kim et al., 1981) by fluorescence emission spectra, time dependence fluorescence, and polarization method to estimate the micellar size and the cmc and also to investigate the effect of salt and short chain alcohol on the size of the micelles. Birdi et al. (1979) concluded that if the aggregation number of the micelle is known, the free energy of interaction ΔG^{o},

between the probe and the micelle can be calculated. From the variation of ΔG^o with temperature and the enthalpy of interaction ΔH^o, the entropy of interaction ΔS^o can be determined. They also concluded that the interaction between the probe and micelle was hydrophobic. The addition of salt increased the association constant between the micelle and the fluorescent probe. The fluorescent polarization of 2 methyl anthracene was explored in sodium taurocholate n-dodecyl betain system (Chen et al., 1974). It was concluded that the interior of the micelle was more rigid and ionic headgroups were more widely spaced than for SDS micelles. Using the same fluorescent probe and polarization technique, Shinitzky and coworkers (Shinitzky et al., 1971) concluded that the interior of dodecyl, tetradecyl, hexadecyl, and octadecyl trimethyl ammonium bromide micelles resemble aliphatic hydrocarbon solvents.

Depolarization of fluorescent probes has also been used profitably to gain information on the microviscosity of the environment of the probe (Weber, 1953; Weber and Shinitzky, 1970; Shinitzky et al., 1971). The microviscosity of various micellar systems of alkyl-trimethyl ammonium bromide with alkyl chainlength from C_{12} to C_{16} was found to be in the range of 17-50 centipoise (Shinitzky et al., 1971). Aoudia and Rodgers (1979) also carried out investigation on microviscosity of alkyl benzene sulfonate isomers. Investigations (Keh and Valeur, 1981) on the size and internal fluidity of AOT containing inverted micelles have suggested that the micellar size is independent of surfactant concentration below 0.3M.

The knowledge of the distribution of the fluorescent probe in micellar phase and aqueous phase is important in analysing the experimental results of steady-state and time dependent fluorescence.

Infelta (1979) and Infelta and Gratzel (1979) proposed a statistical model describing the distribution of the fluorescent probe on the basis of their kinetic interaction with the host micelles. The assumptions involved in their model were: the micelle-hydrophobic probe has reached the equilibrium, the probe molecules migrates from micelle to micelle via the aqueous phase, at equilibrium the concentration of micelles remains constant and hence the distribution of the probe molecules remains unaltered, and all the micelles have identical properties, and the possible properties due to size distribution around the mean aggregate number is neglected. Thus the distribution obtained corresponded to a Poisson law governing the occupancies of individual micelle by fluorescent probes. This model was tested on cetyl trioxyethylene sulfate micelles with pyrene as a fluorophore. The data obtained experimentally by the steady-state and time-resolved fluorescence techniques, were in excellent agreement with the prediction of the model.

The structural aspects of microemulsions using fluorescence techniques have been reported in literature (Eicke and Zinsli, 1978; Kumar and Balasubramaniun, 1980; Mackay et al., 1980). Eicke and Zinsli (1978) have studied the effect of varying amounts of water and AOT on possible structural changes in microemulsions containing iso-octane using nanosecond fluorescence spectroscopy. From the observed rotational correlation times, information regarding the binding of

fluorescent probe to the surfactant layer and its tendency to diffuse
into the interface was obtained from the observed rotational correla-
tion times. Kumar and Balasubramanium (1980) have investigated Tri-
ton X-100/ hexanol/cyclohexane/water microemulsions. From the
fluorescence measurements (emission spectra and quantum yields), it
was shown that the water present as dispersed phase in microemulsions
was not different from the bulk water in its features. The surface
potentials of cationic, anionic and nonionic surfactants stabilized
by short to medium chain length alcohols (C_4 to C_6) in hexadecane or
mineral oil was determined (Mackay et al., 1980) using chromophores
such as chlorophenol red and methyl red. The values reported for
cationic surfactant (CTAB) microemulsions were in the range of 30-50
mv depending upon the concentration of the aqueous phase. They
further concluded that the interphase region of the microdroplet in
which the indicator is located had an effective dielectric constant
of about 20.

In this chapter, a quantitative study on the determination of
the surface potential of sodium dodecyl sulfate micelles and the
effect of addition of salt on surface potential of such micelles is
presented. A qualitative treatment on the fluorescence and solubili-
zation behavior of petroleum sulfonate-containing microemulsion is
given The effect of alcohol as well as oil chain length on the solu-
bilization and fluorescence behavior is also investigated. A corre-
lation between the fluorescence behavior with the brine solubiliza-
tion limit of microemulsions is established.

4.3 Experimental

Micellar solution of 24 mM SDS was prepared in distilled water This surfactant concentration is above the cmc of SDS. The pH of the solution was varied by adding a small amount of NaOH or HCl of different normality. The pH of the solutions was measured using a glass electrode by a pH meter (Orion Research Model 701A). A petroleum sulfonate TRS 10-410 (Witco Chemical Co.) was used aa received for preparing microemulsions. This surfactant has an average molecular weight of 418. All the alcohols and oils were of 99% purity or greater.

Brine Solubilization Limit. The microemulsions were prepared by mixing 1 gm TRS 10-410, 0.8 gm alcohol and 8 gms of oil. The brine solubilization limit was determined by mixing the brine slowly from a graduated 1 ml pipette to the microemulsions, until turbidity was observed and two phases formed. In all cases, the end point was sharp (within 0.1 ml of brine). At the end point the systems were initially turbid, but after a few minutes of standing, two clear phases formed.

Fluorescence Measurements. The fluorescence behavior of micellar solutions and microemulsions was studied using Perkin Elmer, MPF-44B fluorescence spectrophotometer with the differential correction unit (DCSU -2). The surfactant type fluorescent dye used in this study was 4-heptadecyl umbelliferone which was synthesized in our laboratory. The dye was dissolved in isopropanol. The structure of the dye was shown in Figure 2.1. The dye was added to each sample

in such amounts as to make its concentration the same (10^{-4} M/liter) for all samples. The samples were excited at 366 nm and emission spectra were obtained. The maximum emission was found to be at 486 nm. Samples were also run without the addition of the dye for microemulsion samples and it was found that TRS 10-410 has its own fluorescence characteristics and when excited at 366 nm, the maximum in emission occurred around 480 nm.

4.4 Surface Potential of SDS Micelles

At an electrically charged interface in contact with an electrolyte solution, an electrical potential is built up by the electrical double layer. This surface or interfacial properties affect the concentration of ions at the interface. Accordingly, the pH at the charged surface is quite different from the pH of the bulk. Consequently, a fluorescent probe located at the interface, is sensitive to the microenvironment and to the surface potential. In micellar solutions, it is known that the charged head groups and relatively small counterions of the ionic micelles are located in a contact region, known as the Stern layer, which extends from the core to within a few angstroms of the shear surface of the micelle. The compactness of the Stern layer is responsible for the reduction of the net charge on the micelle. Most of the counterions are, however, located outside the shear surface in the Gouy-Chapman electrical double layer where they are completely dissociated from the charged aggregates and are able to exchange with the ions in the bulk solution (Fendler and Fendler, 1975).

In 1910, Guoy put forward his theory of diffuae double layer (Davies and Rideal, 1963) and solved Boltzman equations for the distribution of cations and anions in terms of potential ψ_o near the surfacer relative to the bulk of the liquid. The basic assumptions are that the charged surface is impenetrable, that the charge is uniformly apread over it and that the counter iona behave as point charges. The Boltzman equations for 1-1 electrolyte are

and

$$_s C_- = \exp(+e\psi_o/kT) \tag{4.1}$$

$$_s C_+ = \exp(-e\psi_o/kT) \tag{4.2}$$

where ψ_o : surface potential

$_s C$: ionic concentration at the surface

C : ionic concentration in bulk

e : electronic charge

k : Boltzman constant

T : abaolute temperature

The above equations in conjunction with Laplace equation and the basic assumptiona lead to an expresaion which allows the calculation of ψ_o, aa followa

$$\psi_o = '(2kT/e) \, \text{Sinh}^- \left\{ \frac{\sigma \, (500\pi/DRT)^{0.5}}{C_i^{0.5}} \right\} \tag{4.3}$$

where σ : surface charge denaity

D : dielectric conatant

R : universal gas constant

The effect of ψ_o is to alter the pH at the surface (Goddard, 1974), pH_s, which differs from that in the bulk, pH_b as given by the Boltzman equation for proton concentration

$$pH_s = pH_b + e\psi_o/kT \qquad (4.4)$$

Only when the surface potential is zero, the surface and the bulk pH values are equal. If ψ_o is negative, the surface pH is less than the bulk pH because the charge attracts hydrogen ions into the viscinity of the surface. The potential may arise from ionization of polar groups or adsorbed ions at the surface.

Mackay et al. (1980) and Mukerjee and Banerjee (1964) used various chromophores to determine the surface potential of micelles and microemulsions from the shift in the dissociation constant, pK, of these dyes between the surface and the bulk from the equation

$$pK_a = pK_s - e\psi_o/2.3 \ kT \qquad (4.5)$$

At 25^oC, the shift in the pK value is

$$\Delta pK = - \frac{\psi_o}{59.16} \qquad (4.6)$$

To determine the surface potential of SDS micelle, a surfactant-type fluorescent dye was synthesized in our laboratory. The structure of the dye 4-heptadecyl umbelliferone was shown in Figure 2.1. The dye was found to be insoluble in water as well as straight chain hydrocarbon oils. However, it was soluble in a

micellar solution of SDS. To accurately determine the surface potential of SDS micelle, it was necessary to establish the orientation of the fluorescent dye at the interface. Figure 4.2 shows the effect of dye concentration in 24mM SDS micellar solution on the fluorescence intensity. It is seen that as the dye concentration was increased, the fluorescence intensity increased linearly. By the extrapolation of the straight line, it was found that at zero dye concentration, the fluorescence intensity was zero. A positive x-axis intercept would mean that a fraction of the dye was partitioning in the bulk or in the interior of the micelles. However, the zero intercept suggests that the dye indeed oriented at the interface as shown in Figure 4.3.

The effect of pH on fluorescence intensity of SDS micellar solution containing various concentration of NaCl is shown in Figure 4.4. As the pH of the solution was increased, the degree of dissociation of the dye increased. At a lower pH, the dye is not dissociated as reflected by the zero fluorescence intensity. However, as the pH was increased the fluorescence intensity increased rapidly and at very high values of pH, the fluorescence intensity leveled off indicating complete dissociation of the dye. The data shown in Figure 4.4 for the variation of fluorescence intensity as a function of pH in water was taken from Montal and Gitler (1973) who used a water soluble form of umbeliferrone (without the long nonpolar chain). The pK value of the dye is defined as the value of pH at which 50% of it is dissociated. A positive pK shift was found when the dye was added in 24 mM SDS micellar solution. However, when various amounts of
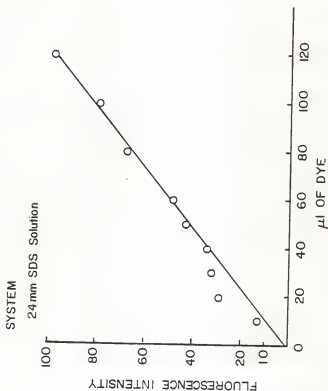
Figure 4.2 Effect of Dye Concentration on Fluorescence Intensity for SDS Micelles

The Orientation of the Dye Molecule at the Interface of Microemulsion Droplets
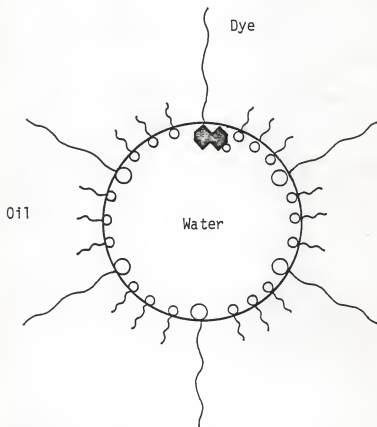

Figure 4.3 A Schematic Representation of the Orientation of the Fluorescent Dye at the Interface
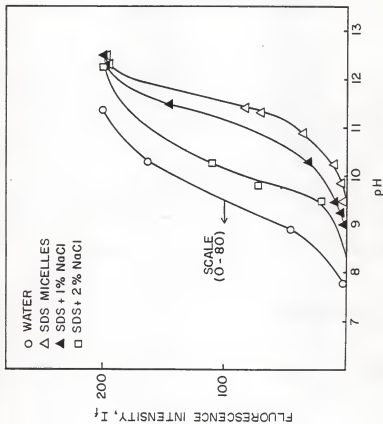
Figure 4.4 Effect of Salt on pK Shift of SDS Micelles

salt was added in the micellar solution, the shift in the pK value of the dye decreased. The values of surface potential was calculated from the shift in pK value using Eq. 4.6. These surface potential values are listed in Table 4.1.

It is known that the addition of salt compresses the electrical double layer. The slope of the surface potential as a function of electrolyte concentration at constant surface charge density predicted by Gouy-Chapman theory is 58 mv for a ten-fold change in salt concentration. In the present case, the addition of salt decreased the surface potential of SDS micelles (shown in Table 4.1). However, the lowering of the surface potential did not obey the Gouy-Chapman theory. The discrepancy between theoretical values and the values obtained using fluorescence technique for surface potential could be due to the assumptions made in the theory as described earlier which may not be true in the present system. The dielectric constant of water may be lower than 80 near the charged surface due to the electric field. Also, the theory does not take into account the polarization of water around each counter ion. Moreover, the non-zero size of the counterions decrease (Davies and Rideal, 1963) the ionic concentration near the surface.

The surface potential of -121.3 mv of SDS micelles found here agrees with value of -134 mv for the same micelles by Fernadez and Fromhertz (1977). Montal and Gitler (1973) reported the surface potential of 24 mM SDS micelles to be -86 mv. Funasaki and coworkers (1977 a, b, c) have also investigated the surface potential of mixed micelles from the dissociation constant of the chromophores.

Table 4.1 Surface Potential of SDS Micelles in Presence of Salt Using Fluorescence

System	pK	Shift in pK	Surface Potential+ mv
Water-Soluble hydroxycoumarin	9.5	—	—
24 mM SDS	11.55	2.05	-121.3
24 mM SDS + 1 % NaCl	11.20	1.70	-100.5
24 mM SDS + 2% NaCl	10.15	0.65	-38.4

+ at 25 ℃

4.5 Solubilization and Fluorescence Behavior of Microemulsions

The brine solubilization capacity of TRS 10-410-containing microemulsions as a function of brine concentration is shown in Figure 4.5 for oils ranging from hexane to hexadecane. For every oil, as the electrolyte concentration is increased the solubilization limit increases, passes through a maximum, and then decreases which can be explained as follows. Upon addition of brine, the size of the droplet is expected to increase, resulting in a concomitant increase in interfacial area. Up to a certain extent, the alcohol from the oil phase can partition into the interface to stabilize the additional interfacial area. However, as the alcohol in the oil phase is depleted, further growth of water droplets would increase the interfacial tension at the oil/water interface due to an increase in area per molecule and thus, destabilize the microemulsion, and prevent further solubilization of brine. The electrolyte concentration at which the largest amount of brine is solubilized is a function of the extent of the partitioning of alcohol in the oil phase, interphase and brine phase. The critical electrolyte concentration depends on the oil chain length. A similar observation is reported in enhanced oil recovery literature for surfactant/oil/alcohol/brine systems. Here, upon increasing the salinity, there is a transition from the lower phase, to the middle phase, to the upper phase microemulsion. The salinity, at which there is an equal solubilization of oil and brine in the middle phase, is defined as the optimal salinity of the system. It has been shown (Chou, 1980) that the critical electrolyte concentration, at which the most brine is solubilized in a single
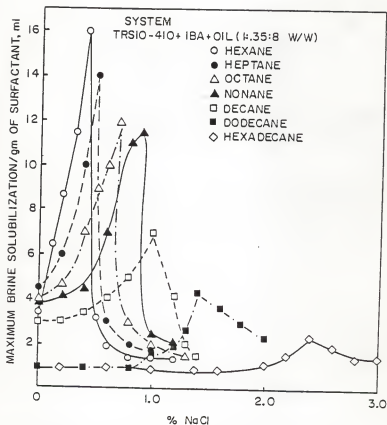
Figure 4.5 Effect of Salinity on Brine Solubilization Capacity of Microemulsions Containing Different Oils

phase microemulsion corresponds to the optimal salinity of the formu-
lation, hence this critical electrolyte concentration will be
referred to as the optimal salinity hereafter. When brine is added
beyond the maximum brine solubilization limit, the system becomes
turbid and upon standing excess oil phase remains in equilibrium with
the lower phase microemulsion for all salinities below optimal salin-
ity. Above optimal salinity, excess brine remains in equilibrium with
the upper phase microemulsion.

The proposed molecular mechanism for the effect of salt concen-
tration as reported by Chan and Shah (1979), is shown in Figure 4.6.
At low salt concentration, most of the surfactant remains in the
aqueous phase, and hence very little of it partitions into the inter-
phase or the oil phase. As the salt concentration increases, the
surfactant preferentially dissolves in the oil phase. At optimal
salinity, the surfactant concentration is approximately the same both
in oil and brine phases. Thus, the partition coefficient is near
unity at optimal salinity. Noronha (1980) also showed that at or
near optimal salinity, surfactant starts migrating from aqueous to
oil phase. This presumably results in the highest interfacial con-
centration of surfactant, and hence the lowest interfacial tension.
The surface tension of equilibrated brine phase was also found to be
lowest at this salt concentration (Chan and Shah, 1979).

4.5.1 Effect of Oil Chain Length

Solubilization Behavior. The brine solubilization data for
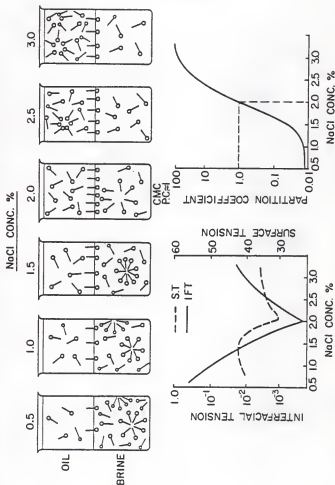petroleum sulfonate containing system shown in Figure 4.5 indicated

Figure 4.6 A Proposed Mechanism on the Effect of Salt on Interfacial and Surface Tensions (Chan and Shah, 1979).

that increasing oil chain length increased the optimal salinity of microemulsions. The increase in the optimal salinity for higher chain length oil can be explained in terms of the stronger van der Waals forces between the chains for longer chain hydrocarbons. Higher salt concentration is required to drive the surfactant molecules into the oil phase. These data are consistent with reported results (Hsieh and Shah, 1977) for petroleum sulfonate containing systems where the optimal salinity was determined either as the salinity at which equal volume of oil and brine was solubilized in the middle phase in three phase regions or as the salinity at which interfacial tension at the middle phase microemulsion/excess oil and excess brine/middle phase microemulsion was found to be equal.

The decrease in solubilization capacity for increasing oil chain length can be explained in terms of of the partitioning of water-soluble isobutanol in the microemulsion. As the oil chain length is increased, the partitioning of isobutanol in the oil phase will be less. Since the amount of alcohol used for each system was the same, a concomitant increase in the alcohol concentration in the aqueous phase and at the interface will occur upon increasing the oil chain length. The aqueous phase, which contains isobutanol, will solubilize surfactant molecules from the interface and result in a decreased concentration of surfactant molecules at the interface. There will be less crowding of surfactant molecules at the interface. This will decrease the interfacial area of the oil/brine interface, and hence decrease the solubilization capacity of microemulsions.

Fluorescence Behavior of Microemulsions The maximum emission
intensity of different microemulsion samples at 486 nm is shown as a
function of sodium chloride concentration with corresponding maximum
brine solubilization in Figure 4.7 for various oils. As the salinity
is increased, the fluorescence intensity increases, passes through a
maximum, and then decreases for all the oils studied. The maximum in
the fluorescence intensity was found to be at the optimal salinity
for every oil. The similarity in Figures 4.5 and 4.7 suggest a
correlation between the brine solubilization and fluorescence inten-
sity of the microemulsions. The increase in the fluorescence inten-
sity could be due to higher surface charge density or higher concen-
tration of surfactant at the interface or in the aqueous phase,
and/or increased ionization around the water droplet in the oil
external microemulsions.

Chiang et al. (1978) have reported an interesting correlation
between interfacial tension and electrophoretic mobility for TRS 10-
80/1% NaCl/octane system as shown in Figure 4.8. This system exhi-
bited a minimum in interfacial tension at 0.005% surfactant concen-
tration. It was observed that at the same concentration, there was a
maximum in electrophoretic mobility. It was concluded that the elec-
trophoretic mobility, which is an indirect measure of surface charge
density, has a definite correlation with the interfacial tension for
oil/surfactant solution system.

Similar results have been reported for caustic/crude oil system
(Bansal et al., 1977) for three different crude oils. It was shown
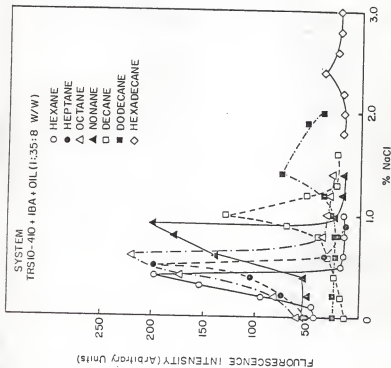that at a specific NaOH concentration, there was a minimum in

Figure 4.7 Effect of Salinity on Fluorescence Behavior of Microemulsions Containing Different Oils.
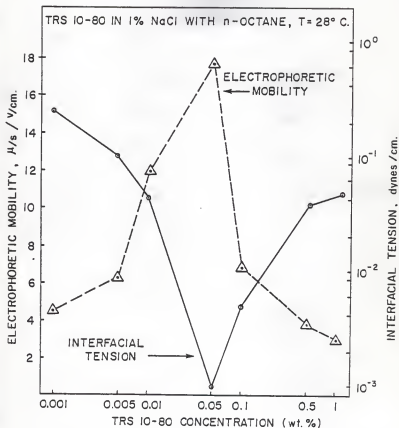
Figure 4.8 Effect of Surfactant Concentration on Interfacial Tension and Electrophoretic Mobility.

interfacial tension and a corresponding maximum in electrophoretic mobility. The explanation given for this behavior was based on the surface charge density at the crude oil/caustic interface. The natural surfactants present in crude oil contain carboxylic groups. These groups react with the caustic and increase the magnitude of the charge on crude oil/caustic interface. When the concentration of the caustic is low, the carboxylic groups present in the crude oil would be in the unionized (RCOOH) form and therefore, the interface would have less charges. This would result into smaller electrophoretic mobility. However, increasing the NaOH concentration would ionize the carboxylic group forming $(R-COO)^-$. This results in an increase in the charge at the interface increasing the electrophoretic mobility. At a much higher NaOH concentration, there would be a formation of carboxylic acid soap (RCOONa) which decreases the electrophoretic mobility. The maximum in electrophoretic mobility for crude oil/caustic system occurs when the interfacial tension is minimum, suggesting that the higher surface charge density is indeed an important factor influencing the interfacial tension.

The lowering of interfacial tension at oil/brine or crude oil/caustic interface is due to crowding of surfactant molecules at the interface. Similar crowding in high surfactant concentration systems leads to higher brine solubilization by microemulsions. The maximum fluorescence intensity at optimal salinity shown by these petroleum sulfonate-containing microemulsions may be an indication of higher surface charge density or higher surface concentration of surfactant at oil/brine interface.

Figure 4.9 summarizes the effect of oil chain length on optimal salinity, maximum brine solubilization, and fluorescence behavior of petroleum sulfonate/isobutanol microemulsions. The optimal salinity increased linearly with the chain length of oil while the brine solubilization limit and fluorescence intensity decreased for all oils higher than octane. For reasons not known, the fluorescence intensity did not change significantly when oils used were hexane, heptane, and octane. The decrease in the fluorescence intensity could be explained in terms of a lower degree of ionization of the sulfonate group or, decreased thickness of the electrical double layer upon increasing the oil chain length, or a decrease in interfacial concentration of surfactant.

4.5.2 Effect of Alcohol Chain Length

In this section, the effect of various alcohols (butanol, pentanol, hexanol and heptanol) on optimal salinity, maximum brine solubilization, and fluorescence behavior of petroleum sulfonate-containing microemulsions has been investigated. Figures 4.10 to 4.12 show the effect of NaCl concentration on maximum brine solubilization of microemulsions for various alcohols containing different oils namely, octane (Figure 4.10), dodecane (Figure 4.11), and hexadecane (Figure 4.12). It is seen that for every alcohol, as the electrolyte concentration is increased, the brine solubilization capacity increases, passes through a maximum, and then decreases. The optimal salinity and brine solubilization capacity were determined from these data. The fluorescence intensity was measured at optimal salinity for microemulsions containing maximum brine.
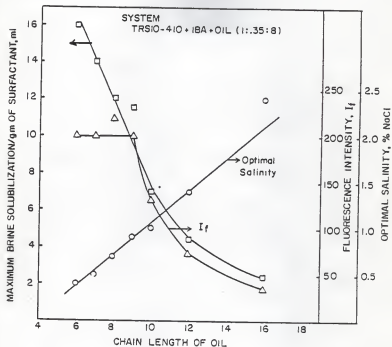
Figure 4.9 Effect of Oil Chain Length on Solubilization and
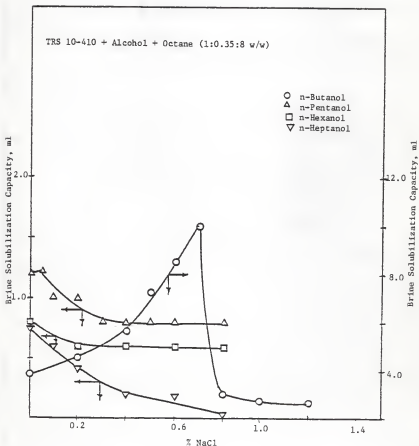Fluorescence Behavior of Microemulsions.

Figure 4.10 Effect of Salinity on Brine Solubilization of Microemulsions for Different Alcohols.

Figure 4.11 Effect of Salinity on Brine Solubilization Capacity of Microemulsions for Different Alcohols.
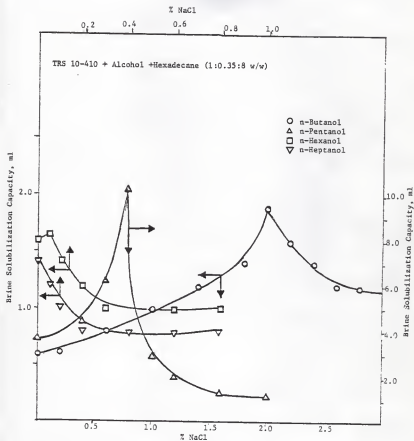
Figure 4.12 Effect of Salinity on Brine Solubilization Capacity of Microemulsions for Different Alcohols.

Figure 4.13 shows the effect of alcohol chain length on solubil-
ization and fluorescence parameters of microemulsions containing
octane. Upon increasing the chain length of alcohol, optimal salin-
ity decreased. This is in agreement with results reported in oil
recovery systems (Hsieh, 1977). Water-soluble alcohols such as n-
butanol and isobutanol are found to increase the optimal salinity,
whereas water-insoluble alcohols such as hexanol and heptanol
decrease the optimal salinity, the reason being that higher concen-
tration of salt is required to migrate the surfactant molecules from
the pool of alcohol-containing aqueous phase to the oil phase. Since
the solubility of hexanol and heptanol is negligible in water, the
surfactant migration from aqueous phase to oil phase occurs at a very
low salt concentration. Optimal salinities are below 0.1% NaCl when
hexanol and heptanol are used for making microemulsions.

The maximum brine solubilization capacity of microemulsions
decreased (Figure 4.13) upon increasing the chain length of alcohol.
This is again related to the negligible solubility of longer chain
length alcohol in the aqueous phase and higher partitioning of sur-
factant molecules in oil. This results into significantly less
interfacial area for solubilization of brine in microemulsions.

The fluorescence intensity at optimal salinity of microemulsions
containing maximum brine also decreased as the alcohol chain length
increased. This is related to much lower brine solubilization at
higher chain length of alcohol and presumably to lower surface charge
density at the microemulsion droplet. Bansal et al. (1979) investi-
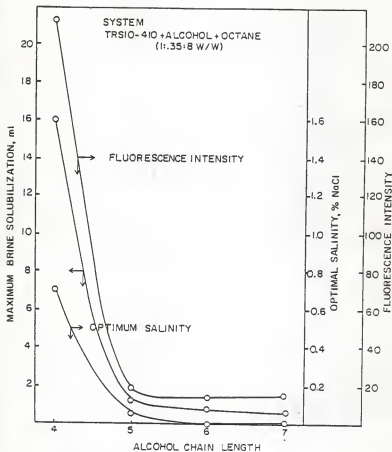gated the effect of alcohol chain length on solubilization and

Figure 4.13 Effect of Alcohol Chain Length on Brine Solubilization Capacity, Optimal Salinity, and Fluorescence Intensity for TRS 10-410/Octane Microemulsions.

dielectric properties of sodium stearate-containing microemulsions and concluded that the molecular motion, interfacial composition, the thickness of the electrical double layer, and the degree of ionization were different in the presence of different alcohols.

Similar behavior was observed for optimal salinity, brine solubilization capacity, and fluorescence intensity for microemulsions prepared using dodecane as shown in Figure 4.14 and alcohols from n-butanol to n-heptanol. However, the hexadecane-containing microemulsions showed a different trend in brine solubilization and fluorescence behavior as shown in Figure 4.15. It is seen that there is a preferred alcohol chain length where the microemulsions solubilized highest volume of brine as well as there was a maximum in fluorescence intensity when this alcohol was used for making microemulsions. These maxima were observed for pentanol-containing microemulsions. This can be explained in terms of the partitioning of various components in different phases of the microemulsion. n-Butanol being considerably more soluble in water than higher alcohols, it partitions between aqueous phase, interface, and the oil phase. The aqueous phase with butanol has the ability to solubilize surfactant molecules from the interface, and hence creats higher oil/water interfacial tension while decreasing interfacial area. The latter decreases the solubilization parameter. However, in the case of pentanol-containing microemulsions, the partitioning of alcohol is much less into the aqueous phase than with butanol. The partitioning of pentanol into oil phase is much less than hexanol and heptanol. Thus, more pentanol molecules will be present at the interface than
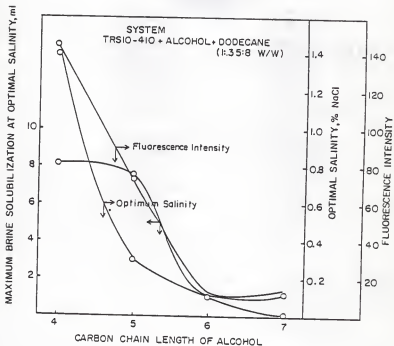
Figure 4.14   Effect of Alcohol Chain Length on Brine
Solubilization Capacity, Optimal Salinity and
Fluorescence Intensity of TRS 10-410/Dodecane
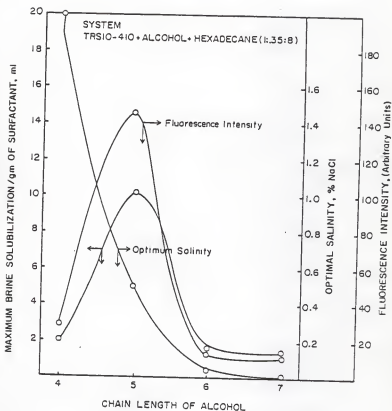Microemulsions.

Figure 4.15 Effect of Alcohol Chain Length on Brine
Solubilization Capacity, Optimal Salinity, and
Fluorescence Intensity of TRS 10-410/Hexadecane
Microemulsions

any other alcohol, which is in agreement with results in literature (Bansal et al., 1980). And since the aqueous phase containing a small amount of pentanol can not significantly solubilize surfactant molecules from the interface, there is a highest concentrations of surfactant and alcohol at the interface. The quantitative determination of the amount of surfactant alcohol is described in section 4.8. Owing to the highest concentrations of surfactant and alcohol at the interface, a maximum interfacial area is available for brine solubilization in TRS 10-410/pentanol/hexadecane system. This preferred chain length of alcohol (pentanol) was only observed in the hexadecane system. In-dodecane containing system (Figure 4.14), butanol, and pentanol microemulsions were found to be equally capable of solubilizing brine whereas in the octane-containing system (Figure 4.13), the brine solubilization limit was drastically lowered when pentanol or higher alcohols were used in place of butanol.

Figures 4.16 and 4.17 show the optimal salinity and brine solubilization as a function of oil chain length of oil for various alcohols respectively. Optimal salinity increased approximately linearly with the oil chain length for all alcohols. (Fig. 4.16). Water-soluble alcohols (butanol and iso-butanol) gave high values of optimal salinities, whereas in microemulsions containing water-insoluble alcohols, low values of optimal salinities were found. The brine solubilization limit decreased with increasing oil chain length for butanol and iso-butanol, (Fig. 4.17) whereas it increased for pentanol and did not change significantly for hexanol- and heptanol-containing microemulsions.
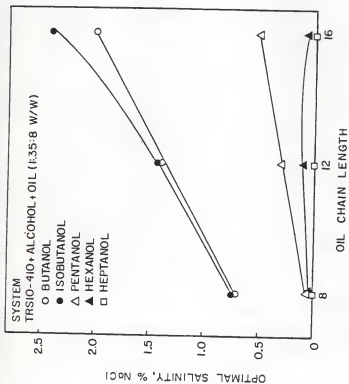
Figure 4.16 Effect of Oil Chain Length on Optimal Salinity of TRS 10-410 Microemulsions.
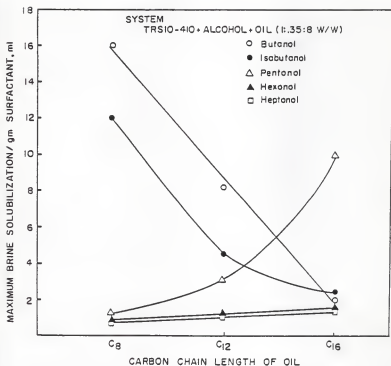
Figure 4.17 Effect of Oil Chain Length on Brine Solubilization
Capacity of Capacity of TRS 10-410 Microemulsions.

4.6 A Correlation Between Solubilization and Fluorescence
Behavior of microemulsions

A simple correlation was found between the fluorescence inten-
sity and the brine solubilization limit of petroleum sulfonate-
containing microemulsions. This correlation is independent of the
type or carbon chain length of alcohol or oil used in preparing the
microemulsions. Figure 4.18 shows the fluorescence intensity of
microemulsions as a function of maximum brine solubilization of
microemulsions at optimal salinity. A linear relationship exists
between these two parameters as follows:

$$I = 15 \ S_b \tag{4.7}$$

where I : fluorescence intensity of microemulsion samples

S_b : brine solubilization capacity at optimal salinity

Figure 4.19 shows the fluorescence intensity of microemulsions
containing TRS 10-410/IBA/brine and oils ranging from hexane to hexa-
decane as a function of brine solubilization limit at salinities
below, above and at optimal values. A linear relationship was again
found between these two parameters as below:

$$I = 15.7S_b - 5.0 \tag{4.8}$$

The correlation coefficient for the linear fit was found to be 0.93.
Equations 4.7 and 4.8 suggest that there is a simple correlation

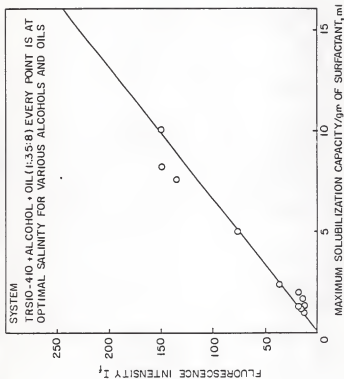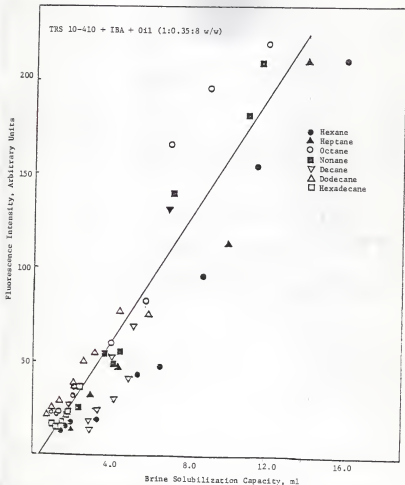Figure 4.18 A Simple Correlation Between Fluorescence Intensity and and Brine Solubilization Capacity of TRS 10-410 Microemulsions

Figure 4.19 A Simple Correlation Between Fluorescence Intensity and Solubilization Capacity of TRS 10-410 Microemulsions.

between solubilization and fluorescence behavior of microemulsions and it is independent of salinity as well as chain length of alcohol and oil. However, it should be pointed out that the fluorescent intensity is expressed in arbitrary units. The value of fluorescent intensity depends upon the setting of the fluorescent spectrophotometer such as slit width and signal gain. For the same spectrophotometer settings, a linear relationship between fluorescent intensity and brine solubilization of microemulsions is expected.

4.7 Molecular Composition at the Interface at Optimal Salinity

The concept of optimal salinity is very important for enhanced oil recovery by surfactant-polymer flooding (Shah, 1981; Shah and Schechter, 1977). The optimal salinity can be determined by phase behavior or interfacial tension behavior of the microemulsions. A detailed description of optimal salinity is provided in section 5.3. The importance of optimal salinity is evident from the various interfacial phenomena (Noronha and Shah, 1982) occurring at optimal salinity as shown in Figure 4.20. At this salinity, not only the tertiary oil recovery is maximum, but the coalescence time of emulsion is minimum, which indicates that under these conditions, it is easiest to mobilize and propagate an oil bank. Therefore, a better understanding of optimal salinity in molecular terms, would significantly improve the present understanding of the phenomena occurring at optimal salinity. In this section a quantitative determination of surfactant and alcohol concentration at different salinities, including the optimal salinity of TRS 10-410/pentanol/hexadecane microemulsions is attempted.

Various Phenomena Occurring at the Optimal Salinity
in Relation to Enhanced Oil Recovery by Surfactant
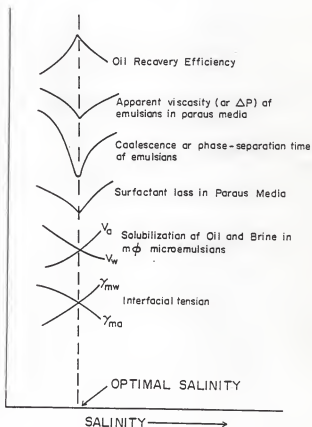Flooding

Figure 4.20   Various Phenomena Occurring at Optimal Salinity

As discussed in section 4.5, there is a preferred chain length of alcohol namely, pentanol, for TRS 10-410/hexadecane microemulsions in terms of the brine solubilization capacity at optimal salinity. From the partitioning behavior of pentanol and petroleum sulfonate, it was shown that more alcohol and surfactant were present at the interface at optimal salinity than microemulsions containing other alcohols. The molar ratio of alcohol to surfactant can be calculated using Schulman-Bowcott model which is described in detail in section 3. It was shown that the number of moles of alcohol at the interface n_a^i is related to the total moles of alcohol, n_a present in the microemulsion by the following equation

$$\frac{n_a}{n_s} = \frac{n_a^i}{n_s} + \frac{n_a^{aq}}{n_s} + K_1 \frac{n_o}{n_s} \qquad . \quad (4.9)$$

where n_s : total moles of surfactant

n_a^{aq} : moles of alcohol in the aqueous phase

n_o : total moles of oil

K_1 : a constant representing the critical ratio
of alcohol to oil for microemulsion formation

Neglecting the solubility of pentanol in water, Eq. 4.9 can be written as

$$\frac{n_a}{n_s} = \frac{n_a^i}{n_s} + K_1 \frac{n_o}{n_s} \qquad (4.10)$$

The dilution of the microemulsions by oil makes the system turbid. This macroemulsion is titrated with pentanol until a clear microemulsion is obtained. By plotting these dilution data in the form of $\frac{n_a}{n_s}$ vs. $\frac{n_o}{n_s}$, a straight line may be obtained if the formation of microemulsion obeys the Schulman-Bowcott model. The y-intercept of this line gives the molar alcohol to surfactant ratio at the interface.

The above approach is taken to determine $\frac{n_a^i}{n_s}$ below, at, and above the optimal salinity for the petroleum sulfonate-pentanol-hexadecane-brine microemulsions containing maximum amount of brine at corresponding salinities. Figure 4.21 shows the plot of $\frac{n_a}{n_s}$ vs. $\frac{n_o}{n_s}$ for this system. It is seen that the data fall on straight lines obeying the Schulman-Bowcott model. The molar ratio of alcohol to surfactant can be obtained from the y-intercept of these lines. This ratio was found to be highest at optimal salinity. A schematic representation of $\frac{n_a^i}{n_s}$ at different salinities is shown in Figure 4.22.

The of maximum brine solubilization depends upon the extent of crowding by alcohol as well as surfactant at the interface. The Schulman-Bowcott method only provides the ratio of alcohol to surfactant at the interface. In order to determine the absolute amount of alcohol and surfactant, information regarding partitioning of surfactant is necessary. Figure 4.23 shows the effect of surfactant concentration on solubilization of brine by microemulsions at different
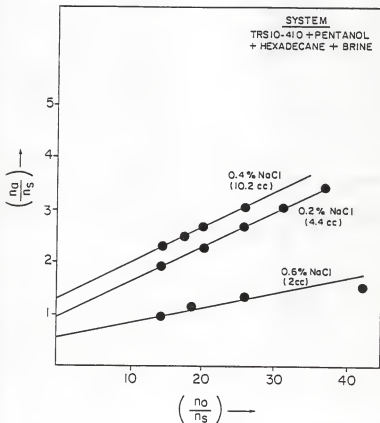
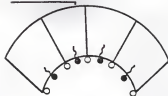Figure 4.21 Alcohol/Oil Titration Plots at Various Salinities for TRS 10-410/Pentanol/Hexadecane Systems.

BELOW OPTIMAL SALINITY

$$\frac{n_a^i}{n_s} = 0.95$$

AT OPTIMAL SALINITY

$$\frac{n_a^i}{n_s} = 1.30$$

ABOVE OPTIMAL SALINITY

$$\frac{n_a^i}{n_s} = 0.53$$

Figure 4.22 A Schematic Representation of Alcohol to Surfactant Ratio at the Interface for TRS 10-410/Pentanol/Hexadecane System.
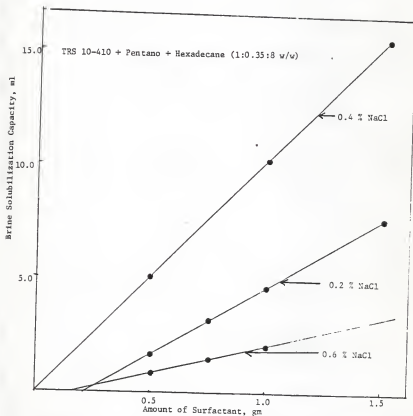
Figure 4.23 Effect of Surfactant Concentration on Brine Solubilization Capacity of TRS 10-410/Pentanol/Hexadecane Microemulsions.

salinities. The microemulsions contained a fixed amount of alcohol
and oil at all salinities. As the surfactant concentration was
increased, the brine solubilization capacity increased linearly at
all salinities due to an increase in the interfacial area. However,
the rate of increase of brine solubilizing capacity with the added
surfactant was much slower at salinities other than the optimal
salinity. The x-intercept of these lines would suggest the amount of
surfactant not at the interface since any amount of surfactant, how-
ever small, partitioning at the interface would generate some inter-
facial area and solubilize brine. At the optimal salinity, the x-
intercept of the line is zero (Figure 4.23), indicating that all the
surfactant molecules are at the interface. However, at other salini-
ties, there was a positive intercept and hence all the surfactant was
not at the interface.

The values of alcohol to surfactant ratio at the interface
obtained by using Schulman-Bowcott model (Figure 4.21) and the parti-
tioning of surfactant at the interface (Figure 4.23) makes it possi-
ble to determine the amount of alcohol as well as surfactant at the
interface. Figure 4.24 shows the fraction of alcohol and surfactant
at the interface as a function of salinity. More than 70% of the
total alcohol present in the microemulsion partitioned at the inter-
face at optimal salinity. The fraction of the alcohol partitioning
at the interface at other salinities was much lower. Above optimal
salinity, only 7% of the total alcohol was present at the interface.
At this salinity, most of the alcohol probably partitioned in the oil
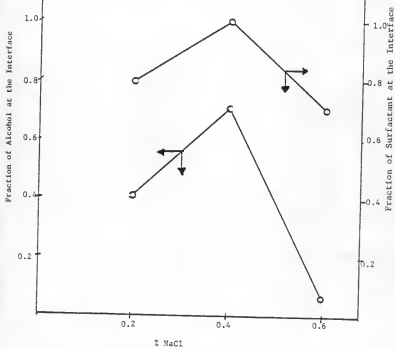phase. All the surfactant was found to be at the interface at

Figure 4.24 Amount of Alcohol and Surfactant at the Interface at Various Salinities.

optimal salinity whereas at other salinities more than 30% surfactant partitioned, either in the aqueous or the oil phase. These results are substantiated by the highest brine solubilization at optimal salinity and the lowest brine solubilization above the optimal salinity. It is to be noted that the amount of alcohol as well as surfactant at the interface was lowest for the above optimal salinity case.

Thus, the optimal salinity of microemulsions can be defined on molecular basis. It is the salinity at which the interface is crowded by a maximum molecules of surfactant and alcohol. At this salinity the surfactant to alcohol ratio is also maximum. The rate of solubilization of brine per mole of surfactant is also the highest at this salinity. This results into the highest interfacial area available for brine solubilization.

4.8 Summary

The following conclusions can be made from this chapter:

1. The surface potential of SDS micelle can be determined using fluorescence technique. The surface potential of SDS micelle was found to be -121.3 mv.

2. The addition of salt decreased the surface potential of micelles due to the compression of the electrical double layer.

3. For oil external microemulsions, there is a critical electrolyte concentration at which maximum brine can be solubilized. This critical salinity corresponds to the optimal salinity of the formulation.

4. As the chain length of oil is increased, the optimal salinity increased for all the alcohols studied. However, the increase in optimal salinity was much greater for water soluble alcohols than for pentanol, hexanol or heptanol.

5. The brine solubilization limit decreased as the oil chain length was increased for n-butanol-and iso-butanol-containing microemulsions. This is explained in terms of partitioning of alcohols in the various phases of microemulsions and the inter-facial area available for solubilization.

6. There is a preferred chain length of alcohol (n-pentanol) for TRS 10-410/brine/hexadecane microemulsions for maximum brine solubilization.

7. There exists a simple correlation between the fluorescence and solubilization behavior of petroleum sulfonate-containing microemulsions.

8. At optimal salinity, the amount of alcohol as well as surfactant at the interface was maximum.

CHAPTER V
PHASE BEHAVIOR AND EQUILIBRIUM PROPERTIES OF
SURFACTANT/COSURFACTANT/OIL/BRINE SYSTEMS

5.1 Introduction

The phase behavior of the surfactant system is one of the most important aspects of enhanced oil recovery process. For a successful surfactant slug design, such knowledge about phase behavior, solubilization of oil and brine in surfactant-rich phase, viscosity, interfacial tension and alcohol partitioning in equilibrated phases is necessary for the application of laboratory data to field tests and understanding of the displacement mechanism. The surfactant slugs are designed to be at least partially miscible with the formation fluids in the reservoir, namely brine and oil. However, when the slug traverses the reservoir, it gets diluted with oil and water. Moreover, the slug gets depleted of some of the chemicals due to adsorption, phase entrapment, precipitation, partitioning etc. Thus, a process that may have been designed to be in the miscible or single phase region may be shifted into the immiscible or multiphase region (Healy et al, 1975). Healy and Reed (1974) showed that phase behavior is related to physical properties and solution microstructure. Since then the phase behavior of several commercial surfactant systems has extensively studied, particularly using the concepts

of pseudocomponents and pseudoternary diagrams (Fleming and Vina-
tieri, 1977; Vinatieri and Fleming, 1979) to develop interrelation-
ship for physical properties.

The phase behavior of a surfactant containing system used in
microemulsion flooding is near the Winsor's III region (Winsor,
1948, 1950) In this multiphase region, three phases coexist in
equilibrium as discussed in Chapter I. The formation of the
surfactant-rich middle phase is considered responsible for the
ultralow interfacial tension, a necessary condition for maximum oil
recovery. Recognition of this phenomena led to considerable interest
in the phase behavior of surfactant-alcohol-oil-brine systems and its
correlation with interfacial tension between phases (Hsieh and Shah,
1977; Wade et al., 1978; Chan, 1978). Although most of these studies
were carried out using commercial sulfonates, such multiphase
behavior was also found in non-ionic systems by Shinoda and coworkers
(Shinoda, 1967b; Saito and Shinoda, 1970; Shinoda and Kuneida,
1973).

The transition from lower phase to middle phase to upper phase
microemulsion can be brought about by many variables, most impor-
tantly by change in salinity of the system. The transition can be
characterized by changes in the solubilization parameters and inter-
facial tension of the microemulsion or surfactant phase.

The main objective of this chapter is to formulate a surfactant
system for reservoirs at high temperature, $80^{\circ}C$ and having a salinity
in the range of 20-30 gms/liter. Both, the reservoir crude oil and

the equivalent simulated pure hydrocarbons are used for phase behavior studies studies. Effect of inorganic salts such as sodium tripolyphosphate and sodium carbonate on solubilization parameters and optimal salinity is investigated. Isopropyl alcohol, isobutyl alcohol, secondary butyl alcohol and tertiary amyl alcohol are employed as cosolvents in this study. To increase the salt-tolerance of surfactant system, a phosphated ester is blended with petroleum sulfonate system. Finally, the viscosity and the partitioning of alcohol in equilibrated phases is reported.

5.2 Experimental

The surfactant used in this study was TRS 10-80 (Witco Chemical Company). KF AA-270 (BASF Wyandotte Company), a phosphated ester was used as a cosurfactant to increase the salt-tolerance of the mixed surfactant system. Oils used were pure hydrocarbons and a crude oil from Ankleshwar reservoir located in western India. Sodium tripolyphosphate and sodium carbonate were used as sacrificial agents.

For the phase volume behavior studies, the petroleum sulfonate and cosurfactant blend were mixed with equal volumes of brine of desired salinity and oil. Surfactant and cosurfactants were added in oil, while the inorganic salts, in brine. The solutions were vigorously shaken and equilibrated until no further change in respective phase volumes was observed. The equilibration time for this study was about two weeks to a month. Alcohol concentration was measured using the Perkin Elmer 900 gas chromatograph and viscosity of surfactant-rich phase was measured by the Brookfield viscometer.

5.3 Optimal Salinity and EACN Concept

When a high concentration (5-15%) surfactant formulation consisting of petroleum sulfonate and alcohol is equilibrated with oil, a surfactant-rich middle phase is formed within a particular salinity range. This middle phase microemulsion contains solubilized oil, brine, alcohol and nearly all the surfactant. If the volume of the solubilized oil in the middle phase is V_o, the volume of the solubilized water V_w, and the volume of surfactant V_s, the solubilization parameters $\frac{V_w}{V_s}$ and $\frac{V_o}{V_s}$ indicate the solubilized volume of water and oil per unit volume of surfactant in the microemulsion phase. As the salinity of the aqueous phase is increased, the volume of the oil solubilized in microemulsion phase increases and hence $\frac{V_o}{V_s}$ increases. Whereas, upon increasing salinity, the brine solubilization in the middle phase decreases and hence $\frac{V_w}{V_s}$ decreases. If these solubilization parameters are plotted as a function of salinity, the intersection point of $\frac{V_o}{V_s}$ and $\frac{V_w}{V_s}$ is defined as optimal salinity for phase behavior. In other words, optimal salinity is the salinity at which equal volume of oil and brine is solubilized in the middle phase microemulsion. It was also found that (Healy and Reed, 1974, 1976) interfacial tension between middle phase microemulsion and oil (γ_{mo}) decrease as the salinity increases, while brine-microemulsion phase interfacial tension (γ_{mw}) increases with increasing salinity. If these interfacial tensions are plotted as a function of salinity, the

intersection point between γ_{mo} and γ_{mw} was defined as optimal salinity for interfacial tension behavior. In other words, at optimal salinity, the interfacial tension between the microemulsion and oil, and between the brine and microemulsion phase is equal. Healy and Reed (1974, 1975) also defined optimal salinity on the basis of the height of the multiphase region in the ternary diagram. Here, the optimal salinity is the salinity that requires the minimum surfactant concentration to produce a single phase of 50/50 water-oil mixtures. The value of optimal salinity obtained by the above three methods for a specific formulation was found to be nearly equal.

The optimal salinity, solubilization parameters and interfacial tension at optimal salinity depend upon several variables. Among them, the structure of surfactant, temperature, cosurfactant, nature and chain length of the oil are important. It has been found (Reed and Healy) that by increasing the non-polar chain length of surfactant, the optimal salinity decreases by a factor of more than 20 and the interfacial tension at optimal salinity decreases by about an order of magnitude. The effect of increasing temperature is to reduce interfacial tension between the middle phase and brine whereas to increase interfacial tension between the middle phase and oil. Increasing the aromatic content of the oil also decreases the optimal salinity and interfacial tension (Reed and Healy, 1977).

EACN Determination. The EACN concept, which allows the substitution of a crude oil by an alkane or an alkane mixture for phase volume or interfacial tension studies, has been generally accepted. This concept arises from the observation that the interfacial

properties of any oil with a surfactant can be modeled by the behavior of alkanes. In addition, the EACN of a mixture of hydrocarbons follows the simple mixing rule

$$(EACN)_{mixture} = \sum_i x_i (EACN)_i \qquad (5.1)$$

where x_i is the mole fraction of component i. Cayias et al.(1976) found that the EACN of an oil (crude, pseudocrude or hydrocarbons) is independent of the surfactant, cosurfactants used in the formulation and that this equivalence always holds. Crude oil being dark in color and usually quite viscous can make equilibrium attainment very slow and phase observation difficult. Replacing crude oil facilitates screening of surfactant formulation and therefore the EACN concept is a valuable one.

Glinsmann (1979) defined the EACN of a crude oil by comparing its optimal salinity based on the equality of the microemulsion-oil vs. the brine-microemulsion interfacial tensions with those of a pure n-paraffin. Tham and Lorenz (1981) used the same approach except that the optimal salinity was based on equal solubilization of brine and oil. Recently, Puerto and Reed (1982) used a three parameter representation to describe equivalent carbon number. The three parameters used were, the optimal salinity, solubilization parameter and oil molar volume. They concluded that this three parameter representation provided a more nearly unique description of microemulsion phase behavior than available in the past.

The characteristics of Ankleshwar light crude oil are shown in Table 2.3 The EACN of this crude oil was determined by comparing the optimal salinity based on equal brine and oil solubilization. Figure 5.1 shows the solubilization parameters as a function of salinity for TRS10-80/IBA/crude oil/brine formulation. The ratio of surfactant to alcohol used in this section was 1. The optimal salinity for this system was found to be 0.73% NaCl. The solubilization parameters of this surfactant formulation with pure alkanes such as nonane, decane, dodecane and tridecane are plotted in Figures 5.2 through 5.5. The intersection of the solubilization parameters $\frac{V_o}{V_s}$ and $\frac{V_w}{V_s}$ provided optimal salinity for each oil. These optimal salinities are plotted as a function of alkane carbon number (ACN) in Figure 5.6. It is seen that the optimal salinity increased linearly with the ACN. This is in agreement with earlier studies (Tham and Lorenz, 1981; Hsieh and Shah, 1977). It was observed that as the alkane carbon number increased, the solubilization of brine and oil in the middle phase decreased. By comparing the optimal salinity of the crude oil system with the pure hydrocarbons, the EACN of the crude was found to be 9.3. Since the optimal salinity with petroleum sulfonate and IBA was found to be (7.3 gms/liter) much lower than the salinity of the Ankleshwar reservoir brine (20 to 30 gms/liter), and the value of solubilization parameters was small, it was necessary to design a formulation with high salt tolerance and capacity to solubilize more oil and brine.
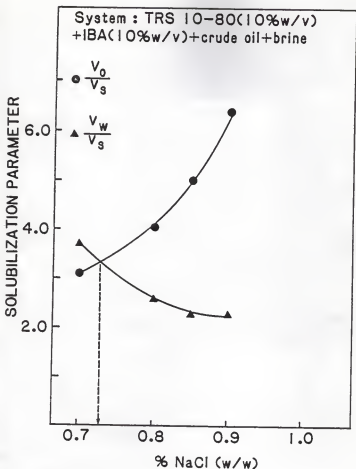
Figure 5.1 Effect of Salinity on Solubilization Parameter
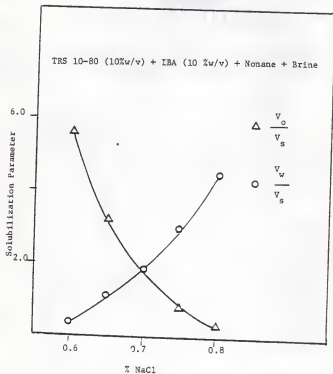of TRS 10-80/IBA/Ankleshwar Crude Oil/Brine System.

Figure 5.2 Effect of Salinity on Solubilization Parameter
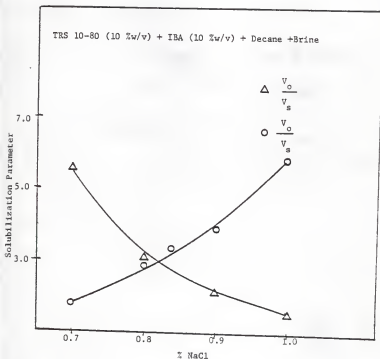of TRS 10-80/IBA/Nonane/Brine System.

Figure 5.3 Effect of Salinity on Solubilization Parameter of
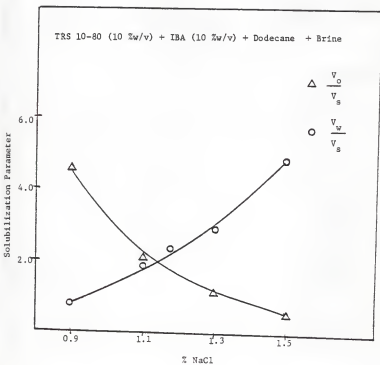TRS 10-80/IBA/Decane/Brine System.

Figure 5.4 Effect of Salinity on Solubilization Parameter of
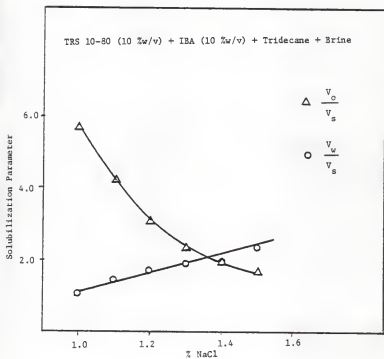TRS 10-80/IBA/Dodecane/IBA

Figure 5.5 Effect of Salinity on Solubilization Parameter of TRS 10-80/IBA/Tridecane System.
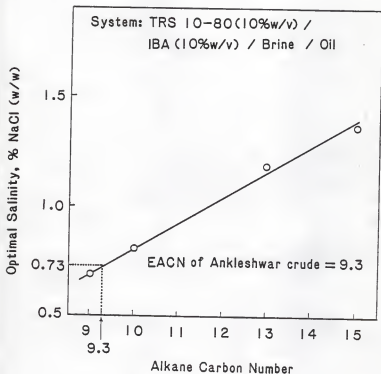
Figure 5.6 Effect of Alkane Carbon Number on Optimal Salinity of TRS 10-80/IBA/Brine System.

5.4 Salt-Tolerance of Mixed Surfactant Systems

Petroleum sulfonates have been found to exhibit low salinity tolerance. A variety of chemical compounds have been patented for use as cosurfactants with the goal of making petroleum sulfonates more compatible with reservoir fluids (Shankar et al., 1982). Nonionic surfactants tolerate higher level of hardness and salinity, although they have lower surface activity per unit weight and are more expensive than petroleum sulfonates. In this investigation, Klearfac AA-270, a phosphated ester was used as a cosurfactant in different weight ratios to increase the salt-tolerance of petroleum sulfonate. The total surfactant concentration (petroleum sulfonate, TRS10-410 and KF AA-270) used in this section was 0.2% (w/w). Surfactant to alcohol (IBA) ratio was kept at 5/3. For interfacial tension measurements, octane was used as oil (WOR=0.1). The equilibrated system was a two-phase system at various salt concentrations.

Interfacial tension was measured at room temperature (25°C). Figure 5.7 shows the effect of salinity on IFT for a mixed surfactant system. It is seen that when no Klearfac was present in the system, the salt tolerance of the system was only 2% NaCl and the minimum in IFT at 1% NaCl. Beyond this salinity, surfactant precipitated. As the concentration of Klearfac was increased, the salt tolerance of the mixed surfactant system increased to as high as 15% NaCl. It is interesting to note that besides increasing the salt tolerance, the addition of KF AA-270 decreased the IFT and broadened the IFT minimum. However, KF AA-270 alone (without blending it with petroleum sulfonate) did not reduce the IFT. Similar results have
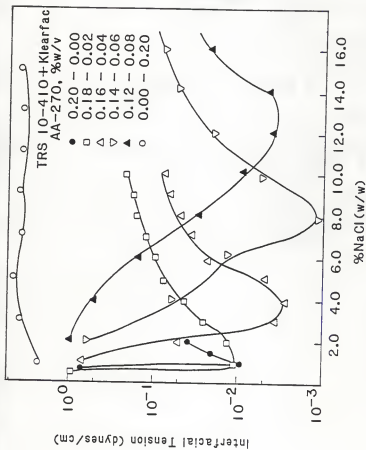
Figure 5.7 Effect of Addition of KF AA-270 on Salt Tolerance and Interfacial Tension of TRS 10-410/IBA/Octane/Brine System.

been reported by Hayes et al. (1979) for mixed surfactant system containing alkyl (C_{18}) xylene sulfonates and KF AA-270. One possible explanation of this synergistic behavior could be that upon adding the cosurfactant, mixed micelles are formed. The surface charge density in aqueous as well as at the interface is increased thus decreasing the IFT.

5.5 Phase Volume Behavior Studies

It has been shown in the literature (Salager et al., 1976, 1979; Healy and Reed, 1976) that the phase behavior of surfactant/brine/oil system is a key factor in interpreting the performance of oil recovery by microemulsion flooding. By systematically varying salinity, higher solubilization of brine as well as oil in the middle phase and ultra-low interfacial tensions can be achieved in or near the salinity ranges giving three phases. Optimal salinity concept has been developed as a tool for designing microemulsions. It is the salinity at which the solubilization of brine and oil in the middle phase is equal.

The phase-behavior of surfactant systems can be represented in pseudoternary diagrams. However, it can be plotted differently to highlight the properties of various phases formed and to monitor the transition from l--> m --> u type of microemulsion. It is then convenient to present the phase behavior on a phase-volume diagram as illustrated in Figure 5.8. Since a large number of data in this section will be plotted in this fashion, a brief explanation of these figures is necessary. These diagrams directly represent the relative
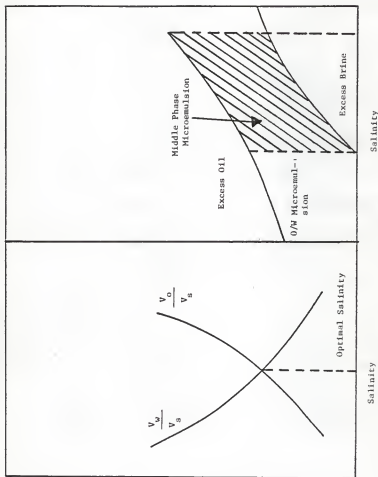
Figure 5.8 A Schematic Representation of Phase Volume Diagram for Surfactant Systems

position of the two interfaces and therefore, the relative volume of each phase. Figure 5.8 is a schematic representation of a phase-behavior diagram. It shows the phase volume behavior of a system containing surfactant, oil, alcohol and brine as a function of salinity. At low salinity as shown in Figure 5.8, only two phases exist in equilibrium with each other: a surfactant-rich phase and an excess oil phase. The surfactant-rich phase is called the lower phase (l) microemulsion. At moderate salinity, three phases are formed where the middle phase is the surfactant-rich phase which is in equilibrium with the excess oil phase and the excess brine phase. This has been referred to as the middle phase (m) microemulson. At very high salinity the system forms two phases: a surfactant-rich phase in equilibrium with the excess brine phase. This has been referred to as the upper phase (u) microemulsion.

As mentioned earlier, the optimal salinity of the formulation may be obtained by plotting solubilization parameter as a function of salinity as shown in the left portion of Figure 5.8. The intersection of $\frac{V_o}{V_s}$, the volume of oil solubilized in the surfactant-rich phase and $\frac{V_w}{V_s}$, the volume of brine solubilized in the surfactant-rich phase provides, the optimal salinity of the system. Thus, representation of phase volume behavior in this fashion not only gives the value of optimal salinity, but also provides the relative volumes of all phases formed and the salinity range over which the three phases exist. Efforts have been made (Puerto and Gale, 1977) to estimate the optimal salinity and solubilization parameters since this would

considerably assist in designing the screening procedure. They have demonstrated that the optimal salinity and solubilization parameters for any mixture of orthoxylene sulfonate can be estimated by the summation of mole-fraction weighted component properties. The concept they used was that a given property of a mixture of components could be related to the sum of products of mole fraction of components in the mixture (X_{ij}) and the "mixing value" of the property (Y_j) in question for the component (Y_j). In other words,

$$Y_i = X_{ij} Y_j \qquad (5.2)$$

The above equation permits prediction of optimal salinity within 3% for any mixtures of alkyl orthoxylene sulfonates. This method, however, is only valid for fixed over-all concentration of surfactant, cosurfactant, oil and brine.

Figures 5.9 through 5.12 show the effect of salinity on solubilization parameters and volume fractions of phases at $80^{\circ}C$ for TRS10-80 (5% w/v), KF AA-270 (2% w/v), alcohol (3% w/v) system for different alcohols, namely IPA, IBA, SBA and TAA. The solid lines in these figures refer to the phase behavior with pure alkanes (EACN=9.3) whereas the dotted lines refer to that with the Ankleshwar crude oil. Experiments were also carried out to determine the optimal salinity of this system in the absence of KF AA-270. Table 5.1 summarizes these results. The optimal salinity for all the alcohols investigated, was found to be less than 1.3% for formulations containing TRS10-80-oil-brine. The addition of KF AA-270
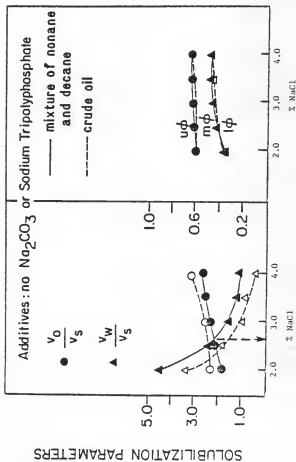
Figure 5.9 Effect of Salinity on Phase Behavior of TRS 10-80/IPA/Oil/ Brine Systems.

VOLUME FRACTION OF PHASES
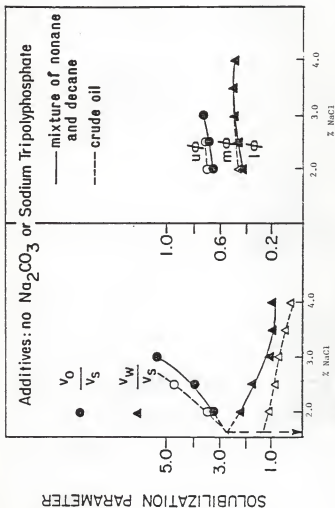
Figure 5.10 Effect of Salinity on Phase Behavior of THS 10-80/KF AA-270/Oil/Brine/IBA Systems.

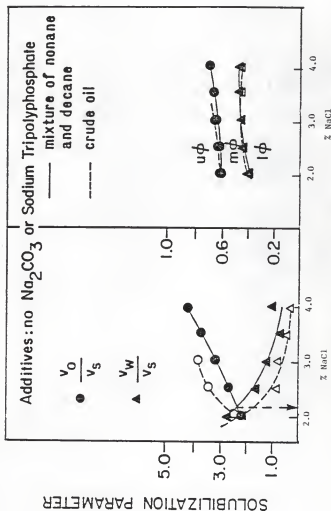
Figure 5.11 Effect of Salinity on Phase Behavior of TRS 10-80/SBA/KP AA-270/Oil/ Brine Systems.

150
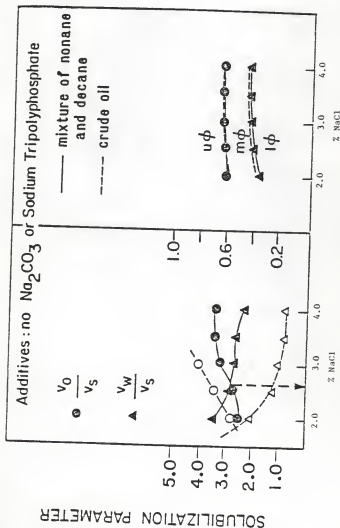
Figure 5.12 Effect of Salinity on Phase Behavior of TRS 10-80/KF AA-270/TAA/Oil/Brine Systems.

Table 5.1 Optimal Salinity and Solubilization Parameter at
Optimal Salinity for of Various Formulartions

Sysrtem: TRS 10-80 (5% w/v) + Alcohol (3.0%) + Brine + Oil

Temperature: 80 °C

Formulation		Type of Alcohol Used			
		IPA	IBA	SBA	TAA
(a)+ Without KF AA-270, sodium carbonate or tripolyphosphate	o.s.	1.3%	0.7%	<1.0%	<1.0%
	s.p.	4.0	3.8	4.0	4.0
(b)+ Without sodium carbonate or tripolyphosphate	o.s.	2.6%	1.8%	2.1%	2.5%
	s.p.	2.2	2.7	2.3	2.5
(c)+ With 1 % sodium carbonate and no tripolyphosphate	o.s.	3.0%	2.8%	3.3%	3.4%
	s.p.	4.4	4.4	4.0	4.4
(d)+ With 1% sodium carbonate and 0.3% tripolyphosphate	o.s.	2.8%	2.5%	3.1%	3.0%
	s.p.	4.2	4.0	3.6	4.5
(e)++ Same as part (b)	o.s.	2.3%	1.3%	1.9%	1.9%
	s.p.	2.4	1.4	2.3	2.6
(f)++ Same as part (d)	o.s.	3.2%	1.9%	2.4%	2.6%
	s.p.	3.6	4.2	3.8	4.2

+ A mixture of nonane and decane was used such that EACN = 9.3
++ Ankleshwar crude oil was used
o.s. = optimal salinity
s.p. = solubilization parameter at optimal salinity

increased the optimal salinity above 2% NaCl except for IBA formulation. However, the solubilization parameter decreased significantly. The effect of different alcohols on the optimal salinity and solubilization parameters was not significant for the systems investigated here. However, there are reports in the literature (Hsieh and Shah, 1977; Reed and Healy, 1977; Healy et al., 1975) on the investigation of alcohol effect on optimal salinity. Hsieh and Shah (1977) reported that as the chain length of normal alcohols increased, the optimal salinity decreased. In other words, water soluble alcohols increased the optimal salinity of the system, whereas oil soluble alcohol decreased the optimal salinity. They also found that the solubilized volume of oil and brine and interfacial tension at optimal salinity were not significantly different for different alcohols. One report (Reed and Healy 1977) has indicated that changing the alcohol from tertiary amyl alcohol to tertiary butyl alcohol increased both the optimal salinity and interfacial tension at optimal salinity.

The optimal salinity of KF AA-270 containing system was found to be slightly lower for crude oil than for a mixture of pure alkanes for all alcohols employed here as shown in Table 5.1. However, the solubilization parameter at optimal salinity remained about the same except for the system containing IBA. The slight difference in optimal salinity between the crude oil containing system and pure alkane containing system may be due to the aromatic content of the crude oil.

The petroleum sulfonates are known to be effective low tension
producers (Gale and Sandvik, 1973), but they are also easily adsorbed
on the reservoir rock. Cheap chemicals can be used as a preflush or
in the surfactant formulation to saturate the surface adsorption
sites. Sodium carbonate and sodium tripolyphosphate are used as sac-
rificial agents (Hurd, 1976; Bae and Petrick, 1976; Hill et al.,
1973). The effect of such chemicals on optimal salinity and solubil-
ization parameters of surfactant formulations containing a blend of
petroleum sulfonate and KF AA-270 have not been reported. The
results of such a study are presented below.

Figures 5.13 through 5.16 show the effect of salinity on solu-
bilization parameters and volume fraction of phases at $80^{\circ}C$ for TRS
10-80/KF AA-270/alcohol formulation containing 1% sodium carbonate
and 0.3% sodium tripolyphosphate for different alcohols, namely, IPA,
IBA, SBA and TAA. The solid lines in these figures refer to the
phase behavior with pure alkanes whereas the dotted lines refer to
that with the Ankleshwar crude oil. Table 5.1 summarizes the optimal
salinity and solubilization parameter at optimal salinity of these
formulations. When 1% Na_2CO_3 was added in brine, the optimal salin-
ity increased [case (c) in Table 5.1] and it was in the range of 25
to 35 gms/liter. Moreover, the solubilization parameter almost dou-
bled for all the alcohols used in the study. It is known that (Law-
son, 1978) the effect of sodium tripolyphosphate, a common detergent
builder, is to minimize adsorption loss of anionic surfactant to the
rock. The addition of 0.3% sodium tripolyphosphate reduced the
optimal salinity of the system slightly. Comparing case (d) and (f)

Figure 5.13 Effect of Salinity on Phase behavior of TRS 10-80/IPA/KF AA-270/Oil/Brine Systems in Presence of Additives.

Figure 5.14 Effect of Salinity on Phase Behavior of TRS 10-80/IBA/KF AA-270/Oil/Brine Systems in Presence of Additives.

Figure 5.15 Effect of Salinity on Phase Behavior of TRS 10-80/SBA/KF AA-270/Oil/Brine Systems in Presence of Additives

VOLUME FRACTION OF PHASES
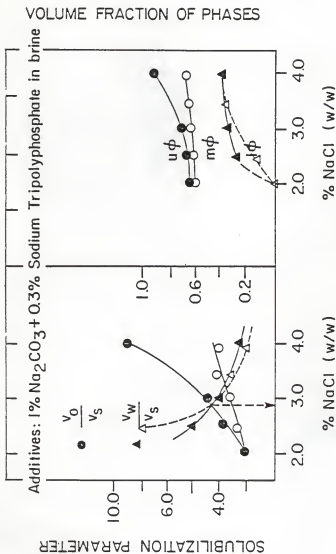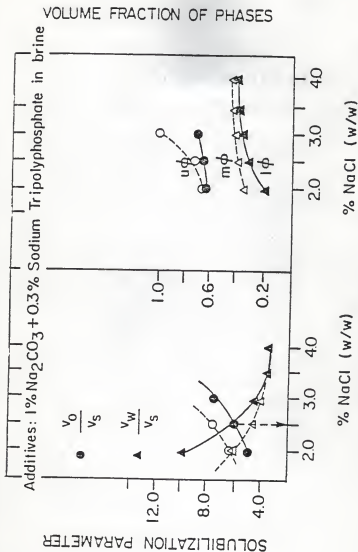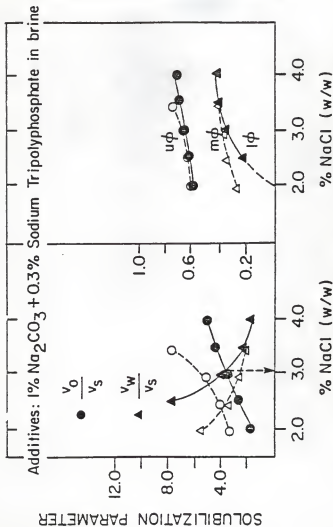
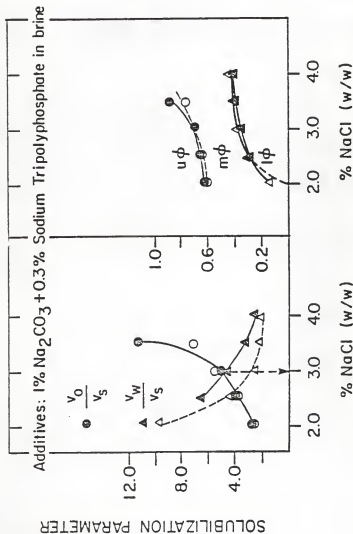Additives: 1% Na₂CO₃ + 0.3% Sodium Tripolyphosphate in brine

Figure 5.16 Effect of Salinity on Phase Behavior of TRS 10-80/IAA/KF AA-270/Oil/Brine Systems in Presence of Additives.

in Table 5.1, it is seen that in the presence of these additives, the optimal salinity of crude oil containing system was somewhat lower than that with pure alkanes having the same EACN. However, the phase volume behavior of crude oil was well represented by a mixture of pure alkanes.

The increase in the optimal salinity upon the addition of non-ionic surfactant, KF AA-270, does not seem to be due to the lowering of pH of the aqueous phase. The phase behavior of the system TRS10-80/IPA/brine/ alkanes with the pH of aqueous phase at 2, 7 and 11 was investigated. The pH was adjusted by adding appropriate amounts of H_2SO_4 or Na_2CO_3. Figure 5.17 shows the effect of pH on the phase behavior of this formulation at different salinities. It is seen that the optimal salinity as well as the solubilization parameter did not change considerably at pH=2 or pH=11. Same results were obtained at pH=7.

From this section, it can be concluded that the blending of petroleum sulfonate with phosphate ester allowed the optimal salinity in the range of 20-35 gms/liter. The addition of Na_2CO_3 increased the solubilization parameter which was not due to change in pH. Both these observations are true for all four alcohols employed in the phase behavior but the choice of proper alcohol was not possible from this study.

5.6 Alcohol Partitioning

The partitioning of chemicals into different phases has an important bearing on the transport of these chemicals in the
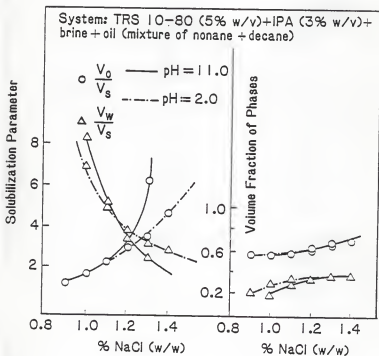
Figure 5.17   Effect of pH on Phase Behavior of TRS 10-80/IPA/Oil/Brine System

reservoir. In general, it is known that most of the surfactant par-
titions into microemulsion phase, regardless of whether it is lower,
middle or upper phase. The concentration of surfactant in excess
water generally tends to decrease and that in excess oil to increase
as the salinity increases (Bae and Petrick, 1981). The partitioning
of a petroleum sulfonate also depends on its average equivalent
weight, crude oil EACN, temperature, nature of alcohol, water-oil
ratio etc. The partitioning of alcohol, on the other hand, deter-
mines the optimal salinity of formulation to a certain extent. The
alcohol chain length, structure and its solubility in brine (Salter,
1977) affects the partitioning of alcohol in different phases. High
water soluble alcohols generally give higher optimal salinity formu-
lation. Alcohols used in oil recovery formulations are often
referred to as cosolvents or cosurfactants. They play an important
role in achieving desired stability of microemulsions. However, the
mechanism by which alcohols act to stabilize microemulsion is not yet
fully understood (Baviere et al., 1981).

The alcohol concentration in the equilibrated phases at $80^{\circ}C$ in
the three phase region is plotted as a function of salinity in Fig-
ures 5.18 through 20 for the system TRS 10-80 (5%)/KF AA-270 (3%)/
alcohol (2%)/alkanes. It is seen that IPA partitioned mainly in the
excess brine phase and in the middle phase whereas TAA partitioned in
the excess oil and in the middle phase. The alcohol concentration in
excess brine did not change appreciably as the salinity was increased
except for TAA which decreased slightly at a higher salinity. The
partitioning of alcohols in excess oil phase increased as the
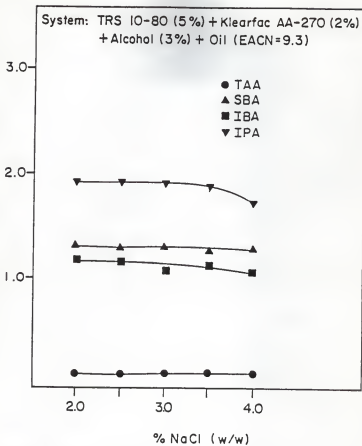
Figure 5.18 Effect of Salinity on Alcohol Partitioning in Excess
Brine Phase for Various Alcohols.
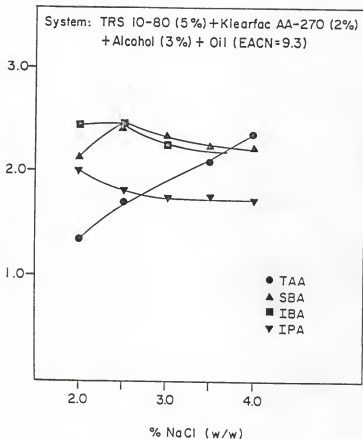
Figure 5.19 Effect of Salinity on Alcohol Partitioning in Middle Phase for Various Alcohols.
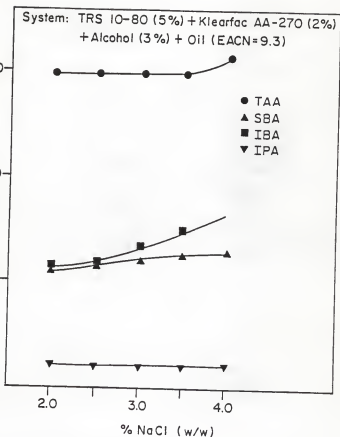
Figure 5.20 Effect of Salinity on Alcohol Partitioning in Excess Oil Phase for Various Alcohols.

salinity increased for all alcohols except for IPA which remained unchanged. In the middle phase, however, significant amount of each alcohol partitioned in the entire three phase region. TAA and IPA again showed opposite effect in terms of their partitioning dependence of salinity. TAA concentration increased while IPA concentration decreased in the middle phase upon increasing the salinity. This is expected because as the salinity was increased, brine solubilization in the middle phase decreased and oil solubilization increased. Now since IPA partitioned mainly in the excess brine phase, its concentration in the middle phase decreased upon increasing the salinity. However, TAA partitions mainly in oil. Upon increasing salinity, its concentration in the middle phase increases. Partitioning of various alcohols in the excess brine phase correlated with their solubility in water. IPA being infinitely soluble in water partitioned the most in the excess brine.

5.7 Viscosity of Equilibrated Surfactant-Rich Phases

When the injected surfactant forms a microemulsion in situ, one important property in relation to its transport is the viscosity of the microemulsion. Microemulsions are considered to have uniform droplet size and if the volume fraction of the dispersed phase is less than 0.35, they conform with the equation for homogeneous dispersion of solid spheres (Roscoe, 1952; Brinkman 1952):

$$\eta_{rel} = (1 - 1.1355\phi)^{-2.5} \tag{5.3}$$

where ϕ : volume fraction of the dispersed phase

η_{rel} : relative viscosity

However, if the volume fraction of the dispersed phase increases, a significant deviation is observed from Eq. 5.2. Matsumoto and Sherman (1969) proposed an equation for relative viscosity for higher volume fraction of the dispersed phase as:

$$\eta_{rel} = \exp\ (a\ (\phi - \phi_s)/(1 - k(\phi - \phi_s)))\ \ \ \ \ \ (5.4)$$

where ϕ_s : volume fraction of oil solubilized within the micelles

k : hydrodynamic interaction coefficient

When the particles are rigid, the value of k is 2.5. The viscosity behavior could also suggest possible structure of middle phase microemulsions (Thurston et al., 1979).

In this section, the viscosity of microemulsions containing pure alkanes and Ankleshwar crude oil is reported. In Figure 5.21, the viscosity at shear rate 23 sec^{-1} of the surfactant-rich phase is plotted as a function of salinity both for the formulations containing pure alkanes as well as the crude oil. The viscosity of the crude oil containing surfactant-rich phase at each salinity was found to be generally higher than that of alkane containing microemulsions. The viscosity of these microemulsions did not depend significantly on the shear rate or the salinity of the formulations. In the absence of 1% Na_2CO_3 and 0.3% sodium tripolyphosphate, the viscosities of the surfactant-rich phase were lower. The viscosity of the microemulsions with TAA showed a maximum with crude oil. This type of
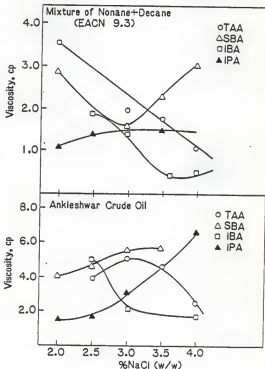
Figure 5.21 Viscosity of Surfactant-Rich Phase at Various Salinities.

behavior has been reported in the literature (Bae and Petrick, 1981). The increase in the viscosity could be attributed to the increase in surfactant partitioning in the middle phase. At higher salinities (above 3% NaCl), the viscosity of crude oil containing microemulsions varied in the same way as the alkane containing microemulsions.

5.8 Summary

In this chapter it was shown that a reservoir crude oil can be successfully modeled using the equivalent carbon number concept in describing the phase behavior of the surfactant formulations. The salt-tolerance of the petroleum sulfonate containing system can be enhanced by blending a phosphated ester in the formulation. The effect of sacrificial agents such as sodium tripolyphosphate and sodium carbonate is to increase the solubilization of brine and oil in the middle phase microemulsion. The following conclusions can be made from this chapter:

1. The EACN of Ankleshwar crude oil was found to be 9.3. A mixture of nonane and decane with EACN 9.3 represented similar phase behavior as the crude oil.

2. The addition of KF AA-270, a phosphated ester increased the salt tolerance of the petroleum sulfonate system and broadened the IFT minimum.

3. The addition of Na_2CO_3 and sodium tripolyphosphate increased the solubilization parameters as well as the optimal salinity.

4. From the partitioning of alcohols in the equilibrated phase, it can be concluded that IPA partitioned mainly in the middle phase as well as in the excess brine phase whereas TAA partitioned in the middle phase as well as in the excess oil phase.

CHAPTER VI
TRANSPORT OF SURFACTANT SLUG AND OIL
DISPLACEMENT EFFICIENCY IN POROUS MEDIA

6.1 Introduction

Flow of fluid in porous media is a complex phenomenon and it can not be described as explicitly as flow through pipes. This is because there are no clear-cut flow paths in porous media, making the measurement of flow very difficult. The analysis of fluid flow in porous media has evolved along two fronts - analytical and experimental. Physicists, engineers and hydrologists have examined experimentally the flow through porous media ranging from sand packs to fused Pyrex glass. On the basis of their analysis they have attempted to formulate laws and correlations which can then be utilized to make analytical predictions for similar systems.

In 1856, as a result of experimental studies on the flow of water through unconsolidated filter beds, Darcy formulated a law which is known as Darcy's law (Craft and Hawkins, 1959) and introduced a new concept i.e. permeability of the porous medium. According to Darcy's law, the rate of flow through a porous medium is proportional to the pressure gradient and inversely proportional to the viscosity of the fluid, i.e.

$$v = \frac{K}{\mu} \frac{dP}{ds} \qquad (6.1)$$

where v : apparent velocity

$\dfrac{dP}{ds}$: pressure gradient in the the direction of v

K : permeability of the porous medium

μ : viscosity of the fluid

The permeability, K, is usually expressed in darcy units. A rock of one darcy permeability is one in which a fluid of one centipoise viscosity moves at a velocity of one centimeter per second under a pressure gradient of one atmosphere per centimeter. By dimensional analysis, it can be shown that the unit of darcy in MLT system is L^2.

In the derivation of Darcy's law, there were certain assumptions involved as listed below:

1. The fluid is homogeneous.

2. No chemical reaction takes place between the fluid and the porous medium.

3. Permeability is independent of fluid, temperature, pressure, and location.

4. The flow is laminar.

5. There is no electrokinetic effect.

The permeability is a measure of the ability of the rock to transmit fluid. For a single phase flow, and for the case of the fluid saturating 100% pore space of the rock, permeability is a property of a rock and not that of a fluid theoretically. However, due

to fluid-solid interactions and for gases at low pressures, different values of permeability of the rock may be obtained by using different fluids. When there is more than one phase present in the porous media, both the number of channels and the cross sectional area available to flow for any one phase are reduced, and this results in a decreased permeability to that phase. This reduced permeability is called effective permeability, K_i, which is a function of phase i saturation and its distribution in pores. The ratio of the effective permeability to the absolute permeability is the relative permeability, K_{ri}, expressed in percent. It is known that the sum of all effective permeabilities is less than the absolute permeability because the flow paths become more tortuous and the cross sectional area decreases in multi-phase flow (Craft and Hawkins, 1959; Langnes et al., 1972). Therefore, the sum of all relative permeabilities is also less than unity.

Figure 6.1 shows a typical plot of oil and water relative permeability curves for a particular rock as a function of water saturation. It is seen that as the water saturation decreases from 100% to 85%, the relative permeability decreases sharply from 100% to 60% And at this saturation, the permeability to oil is zero. This value of oil saturation, 15% in this case, is called the residual oil saturation, the saturation at which oil will first begin to flow as the oil saturation increases. It is the value below which the saturation can not be reduced in an oil-water system. This is the primary reason for less than 100% oil recovery efficiency by water flooding process.
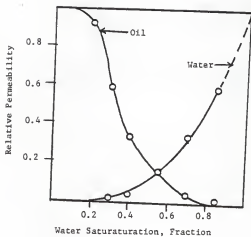
Figure 6.1 Water-Oil Relative Permeability Curves

6.2 Multi-Phase Multi-Component Transport in Porous Media

To understand the flow of multi-component multi-phase transport
in porous media, it is necessary to postulate a system of equations
which govern the behavior of these fluids. The basic equations can
be obtained by combining several physical principles, namely

1. Conservation of mass

2. Rate Equations- Darcy's law

3. phase equilibria and partitioning of components
   between fluid phases

4. Adsorption of chemical species on reservoir rocks

A number of studies have been reported in literature on the
theory of multi-phase, multicomponent displacement in porous media
(Hirasaki, 1981; Helfferich, 1981; Van Quy and Labrid, 1983; Todd et
al., 1978; Pope and Nelson, 1978; Ramirez and Riley, 1984; Friedman
and Ramirez, 1977; Lantz, 1971; Fayers and Perrine, 1959; Pope, 1980;
Lake and Helfferich, 1978; Perkins and Johnson, 1963; Coats and
Smith, 1964; Gupta and Greenkorn, 1973; Barakat and Clark, 1966).
The purposes of these studies were to aid in interpreting laboratory
experiments and to answer technical questions concerning the determi-
nation of the optimal size and composition of various chemical slugs
such as surfactant and polymer fluids in forecasting oil recovery.
The term multicomponent, multiphase displacement in porous media
means the induced flow of any number of simultaneous, not fully mis-
cible fluid phases containing any number of components. The com-
ponent may partition between the fluid phases. The partitioning of
components in various phases determine the physical properties of the
fluid phases.

Two different and independent approaches are known for solving equations of multi-phase, multicomponent displacement. The first of these is the theory of multicomponent chromatography, which allows for any number of components affecting the distribution behavior of one another but admits only one mobile and stationary phase (Helfferich and Klein, 1970). The second approach is the fluid dynamic theory of immiscible displacement in porous media which allows more than one mobile phase but does not allow partitioning of components.

Extension of the above theories to multi-phase, multi-component displacement in media to account for partitioning, phase behavior and flow properties of the phases (relative permeabilities), requires as input either empirical correlations of experimental data on phase equilibria, or theories which predict these correlations (Helfferich, 1981). Other major mass transfer mechanisms, namely, diffusion/dispersion, convection and partitioning of components between solid and fluid phases must also be considered in theory. Diffusion/dispersion is the mass transfer from high concentration to low concentration. While this may not be a major mechanism with regard to some additives where physical diffusion is masked by numerical dispersion (which only depends on time and space), there may be a considerable "apparent" dispersion even at low flow rates (low Peclet number) and in macroscopically homogeneous media (Van Quy and Labrid, 1983). This could be due to the fingering caused by inaccessible channels. Mass transfer by convection mechanism is due to the velocity of fluids in porous media. Therefore, gravity, relative permeability, interfacial tension, viscosity, and mobility ratios

govern this type of mass transfer. Component partitioning depends upon local conditions of composition, pressure, and temperature. This mechanism is a major mass transport phenomenon governing oil displacement efficiency. The phases do not flow at the same flow rates, and non-equilibrium compositions may be present in porous media. This results in a redistribution of components, which brings the multi-phase mixture toward a state equilibrium. The new compositions of the phases influence convection by modifying the interfacial properties and mobilities. They also change the dispersion coefficients and the adsorption levels. Therefore, it is necessary to deal with constituent partitioning among phases as accurately as possible. Besides the usual thermodynamic parameters (pressure and temperature), an increase in salinity may transform initially hydrophilic compounds into hydrophobic compounds as shown by the transition of Winsor Type I to Type II systems while passing through Type III.

The partitioning of components between fluid and solid phases is controlled by ion exchange as well as adsorption and desorption. The last two mechanisms depend on parameters such as the concentration level of the surfactant in solutions as well as on the chemical nature and specific surface area of the porous media. While dispersion causes mixing and dissipation of a surfactant slug, adsorption can result in a real chemical loss of surfactant to the reservoir; the ultimate success of a chemical recovery process is controlled by the nature and magnitude of the loss. The mathematical treatment of the chromatographic separation of slug constituents due to selective adsorption is reported by Harwell et al. (1982).

The classical dispersion equation can be extended in order to take into account the adsorption of a chemical solution flowing through (Satter et al., 1980) a porous medium as follows:

$$D \frac{\partial^2 C}{\partial x^2} - D \frac{\partial C}{\partial x} = \frac{\partial C}{\partial t} + \frac{(1-\phi)}{\phi} \rho_r \frac{\partial C_r}{\partial t} \qquad (6.2)$$

where D : dispersion coefficient which can be expressed as

$$D = \lambda \frac{q}{A} \qquad (6.3)$$

    λ : dispersion parameter

    q : flow rate

    A : cross sectional area

    ρ_r: density of the rock

    C : surfactant concentration in the aqueous phase

    C_r: chemical adsorption on the solid phase

    ϕ : porosity of the rock

The assumptions made in deriving the above mass balance equation (Eq. 6.2) are

1. The porous medium is homogeneous.

2. Fluid flows at a constant rate under isothermal conditions.

3. Dispersion occurs only in the longitudinal direction.

4. Molecular diffusion is negligible and the dispersion coefficient is independent of the chemical concentration.

5. Chemical reaction between the injected solution and the in-place fluid or rock is negligible.

6. Fluid and rock compressibilities are negligible.

Lapidus and Amundson (1952) considered a fluid flow through a semi-infinite medium and linear equilibrium adsorption such that

$$C_r = a\, C \tag{6.4}$$

where a is the equilibrium constant. The general boundary and initial conditions for a finite length porous medium are

$$C\,(x,0) = 0 \qquad\qquad 0 < x < L \tag{6.5}$$

$$C_r\,(x,0) = 0 \qquad\qquad 0 < x < L \tag{6.6}$$

$$(C - \lambda\frac{\partial C}{\partial x})|_{x=0} = C_0 \qquad 0 < t < t_1 \tag{6.7}$$

$$(C - \lambda\frac{\partial C}{\partial x})|_{x=0} = 0 \qquad t > t_1 \tag{6.8}$$

$$\frac{\partial C}{\partial x}\Big|_{x=L} = 0 \qquad t > 0 \tag{6.9}$$

The analytical solution of Eq. 6.2 for a semiinfinite medium under the above initial and boundary conditions was worked out by

Lapidus and Amundson (1952). The effluent concentration of the chemical species is given by

$$\frac{C}{C_o} = \frac{1}{2} \text{ erfc } ((1-I/\theta)/(2(I\lambda/\theta L)^{0.5}))$$

$$- (\frac{I\lambda}{\pi \theta L})^{0.5} \frac{\exp((-\theta L/4I\lambda(1-I/\theta)^2)}{(1+I/\theta))}$$

$$(1 - \frac{6I/\theta}{1+I/\theta} - \frac{2(I/\theta)^2}{(1+I/\theta)^2}) \qquad (6.10)$$

where

$$\theta = 1 + \frac{\rho_r(1-\phi)}{\phi} a$$

I is the pore volumes of the fluid injected.

Eq. 6.10 is not very precise in determining the effluent concentration of surfactant in a displacement study because the assumption that equilibrium adsorption is linear with the concentration of the surfactant is not accurate. However, adsorption of dilute surfactant and polymer solutions on porous rocks can be described by the Langmuir isotherm model (Langmuir, 1915) which is described by the following equation

$$\frac{\partial C_r}{\partial t} = K_1 (1 - \frac{C_r}{C_r^*}) C - K_2 \frac{C_r}{C_r^*} \qquad (6.11)$$

where K_1 : kinetic rate constant for adsorption

K_2 : kinetic rate constant for desorption

C_r^* : maximum equilibrium adsorption on the rock

The solution of Eq. 6.11 for a constant C, with the condition $C_r = 0$ at t= 0 is given by

$$C_r = \frac{K_1 C_r^* ((1 - \exp (-(C K_1 + K_2) t/C_r^*)) C}{(C K_1 + K_2)} \qquad (6.12)$$

As t= ∞, Eq 6.12 reduces to Langmuir equilibrium isotherm:

$$C_r = a C /(1 + b C) \qquad (6.13)$$

with $a = (K_1/K_2) C_r^*$ and $b = K_1/K_2$.

To calculate chemical concentrations in the aqueous and the solid phase for equilibrium adsorption, Eq. 6.2 and 6.13 must be solved simultaneously with the initial and boundary conditions given in Eq. 6.5 through 6.9. Analytical solution of this set of equations is not possible. However, Gupta and Greenkorn (1973) presented numerical solutions to the dispersion/adsorption equations using the Clark-Nicholson method. In their solution the porous medium was assumed to be semi infinite and a step change of chemical concentration was imposed at the inlet end. Satter et al. (1980) reported the numerical solution of these equations using the Barakat-Clark (Barakat and Clark, 1966) finite difference method for a finite length porous medium. The parametric study was also carried out using this model to investigate the effect of various dimensionless groups such as dispersion, $\frac{\lambda}{L}$, adsorptive capacity, $\frac{(1-\phi)C_r^*}{\phi C_0}$, flow rate, $\frac{C_0 K_1 v_p}{q C_r^*}$, and kinetic rate, $\frac{K_2}{K_1 C_0}$ on chemical transport

behavior in terms of the effluent concentration and chemical adsorption histories for various cases (Satter et al., 1980).

In the present chapter, the effluent concentrations of surfactant and alcohol for oil displacement studies have been determined experimentally. Two types of porous media, namely sandpacks and Berea sandstones, have been used in the experimental work. The effect of salinity and cosolvent structures on the effluent surfactant concentration and oil displacement efficiency is studied. Finally, a mechanism of oil displacement in porous media is proposed. It is also shown that the choice of alcohol and its partitioning in various phases are important criteria for designing surfactant formulation for moderate salinity and temperature conditions. It is shown that the success of the surfactant/polymer flooding is determined by the integrity of the surfactant slug in the porous media.

6.3 Experimental

A commercial petroleum sulfonate, TRS10-80 (Witco Chemical Company) was used as received. This surfactant has an average molecular weight of 418 and is 80% active. KF AA-270, a phosphated ester (BASF Wyandotte Company) was used as received. Alcohols and hydrocarbons used in this study were purchased from Chemical Samples Company with a purity of 99% or better. Sodium carbonate was purchased from Mallinckrodt Company and sodium tripolyphosphate from Fisher Chemical Company. Pusher-1000™ (Dow Chemicals) was used to prepare the polymer solutions. Deionized distilled water was used to prepare the brine. Sandpacks with a dimension of 30 cm length and 2.5 cm

diameter was used as the porous medium for the most part of the study. The sandpacks had a porosity of 38% and permeability of 3-4 Darcy. Rectangular Berea cores with a dimension of 30.5 cm by 2.5 cm by 2.5 cm were also employed in the oil displacement test which had a porosity of 22% and permeability of 0.415 Darcy.

Porous media were conditioned by saturating them with CO_2 to displace air then flooded with brine which was filtered through a 0.22μ filter. The porous medium was then saturated with oil at a high flow rate to irreducible brine content and then flooded with the resident brine to residual oil saturation. A 0.2 PV surfactant slug was then injected which was displaced by polymer solution (about 1.0 PV) and subsequently by drive water. The linear displacement velocity in the water flooding and the subsequent surfactant slug and polymer solution flooding was 1 ft/day. Oil displacement experiments were performed at $80^{O}C$ under a back pressure of 30-40 psi to avoid the development of any gas saturation at $80^{O}C$. The surfactant and alcohol concentration were determined by two phase dye titration method and by the Perkin Elmer 900 gas chromatograph respectively.

6.4 Oil Displacement Studies

In this section, results of oil displacement tests are discussed wherein aqueous surfactant formulations were injected into sandpacks to displace a mixture of nonane and decane (EACN = 9.3) and into Berea cores to displace Ankleshwar crude oil at $80^{O}C$. In all of the oil displacement studies, 20 of PV of aqueous surfactant solution containing 5% TRS10-80, 2% KF AA-270, 3% Alcohol, and electrolytes

were used. All surfactant compositions also contained sacrificial agents, 1% Na_2CO_3 and 0.3% sodium tripolyphosphate. Use of these agents in reducing surfactant adsorption in porous media is well established. Four different alcohols were selected to determine the effect of the structure of the alcohol on effluent surfactant concentration as well as on the oil recovery. Moreover, for a tertiary amyl alcohol containing system, the effect of salinity on oil displacement efficiency and effluent surfactant concentration is also investigated. The phase behavior, viscosity, and alcohol partitioning in various phases were discussed in Chapter V.

6.4.1 Effect of Cosolvent Structure

This section reports on the effect of alcohol structures on tertiary oil recovery by surfactant/polymer flooding. The alcohols used were isopropyl alcohol (IPA), isobutyl alcohol (IBA), secondary butyl alcohol (SBA), and tertiary amyl alcohol (TAA). The optimal salinity of these systems were reported in Table 5.1. The surfactant solutions for oil displacement experiments were prepared in optimal salinity brine for each alcohol. Table 6.1 gives the summary of the surfactant flooding results. The tertiary oil recovery efficiency was 92% when displacing a mixture of nonane and decane with the EACN of 9.3 by a surfactant formulation containing TAA in sandpacks. When the Ankleshwar crude oil was displaced in Berea core by TAA containing surfactant slug, the oil recovery was 79%, significantly less than the oil recovery in sandpacks. This could be explained on the basis of two factors. First, it could be due to lower permeability of Berea core (0.415 darcy) than sandpacks (2 to 3 darcy). Secondly,

Table 6.1 Summary of Flooding* Results: Effect of Alcohol
Structure

Alcohol Used	Residual Oil After Water Flooding (% PV)	Tertiary Oil Recovery Efficiency (%)	Surfactant Recovery (%)	PV at Which Surfactant Concentration Reached a Maximum
SBA+	22	11	57.6	0.50
IPA+	22	14	63.8	0.71
IBA+	15	27	61.3	0.77
TAA+	10	92	78.5	1.10
TAA++	43	79	-	-

+ A mixture of nonane and decane with EACN = 9.3 was displaced in
sandpacks

++ Ankleshwar crude oil was displaced in Berea core

* 0.2 PV of surfactant slug containing 5% (w/v) TRS 10-80, 2% KF
AA-270, 3% alcohol in optimal salinity brine with 1% sodium
carbonate and 0.3% sodium tripolyphosphate was injected in porous
media (sandpack dimensions: 2.5 cm diameter, 30.0 cm length,
permeability of 2-3 darcy; Berea core dimensions: 30.5 cm by 2.5 cm
by 2.5 cm, permeability of 0.415 Darcy). Back pressure of 40 psi
was applied. Flow rate of the injected fluids was 1 ft/day and
the temperature was kept at 80 °C. When displacing the pure alkanes,
1500 ppm Dow Pusher in optimal salinity brine was used after the
surfactant slug. When displacing the crude oil, 2000 ppm Dow Pusher
in optimal salinity brine was used after the surfactant slug.

the loss of surfactant due to adsorption in Berea cores reduces the effectiveness of the surfactant slug in displacing the oil. However, the surfactant slug with other alcohols, namely IPA, IBA, and SBA could not displace more than 30% oil in sandpacks. The difference in the oil recovery when the slug contained different alcohols is explained below in terms of the retention of surfactant in porous media, and the residence time of the surfactant slug in the porous media.

All phases in the produced effluent samples from the oil displacement tests were collected at less than a 0.05 PV interval and they were analyzed for petroleum sulfonate using a two-phase titration technique. The titration technique has significantly less accuracy in systems containing crude oils since the dark-colored crude oil interfered with the visual observations of the endpoint. Hence, determination of surfactant concentration in the effluent was not possible for the crude oil displacement test. Figure 6.2 shows the surfactant concentration in produced fluids as a function of PV injected. The area under each curve gives the amount of surfactant recovered in the effluent. Table 6.1 summarizes the surfactant recovery and the PV at which a maximum in the surfactant concentration occurred for these flooding experiments. The amount of surfactant retention was the least (21.5%) for TAA containing surfactant formulation which gave highest tertiary oil recovery efficiency. However, a significant amount of surfactant was also recovered for the other floods. This suggests the better performing slugs usually are accompanied by lower surfactant retention even though less

EFFECT OF ALCOHOL ON EFFLUENT SURFACTANT CONCENTRATION AT OPTIMAL
SALINITY OF VARIOUS FORMULATIONS

System: TRS 10-80 (5%)+Kleerfac AA-270 (2%)+Na₂CO₃ (1%)+
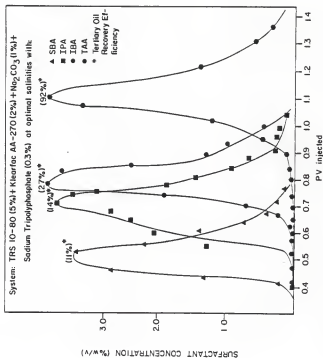Sodium Tripolyphosphate (0.3%) at optimal salinities with:

Figure 6.2   Effect of Alcohol Structure on Effluent Surfactant Concentration
at Optimal Salinity of Various Formulations.

retention does not necessarily mean higher oil recovery (Novosad, 1982; Novosad et al., 1982; Bae et al., 1974). The mechanisms which are viewed as responsible for the mobilization of residual oil (Kraft and Pusch, 1982) during surfactant flooding have been discussed by Chou and Shah (1981) and by Wilhite et al. (1980). The principal mechanism is the solubilization of oil droplets in a water-external, stable, homogeneous middle-phase microemulsion, whose volume depends on the surfactant concentration. A further mechanism which can contribute to the mobilization of residual oil is the inclusion of water into originally immobile residual oil phase, resulting from the transfer of surfactant to the oil phase. The volume increase of the oil phase, which is designated as swelling, gives rise to an increase of the relative permeability to oil and thus to a mobilization of residual oil (Nelson and Pope, 1978).

The drastic difference in oil recovery efficiency when the formulations contained different alcohols cannot be accounted for by the small changes in the viscosity of the middle phase microemulsions containing different alcohols at their respective optimal salinities (Figure 5.19). The highest oil recovery efficiency by TAA containing surfactant formulation suggests that the choice of alcohol is an important parameter for designing formulations for moderate temperature and salinity conditions. As shown in Figure 6.2, for different alcohol the surfactant breakthrough occurred at different pore volumes. When the surfactant formulations contained either IPA, IBA or SBA, the surfactant slug rushed through the porous media much faster than the TAA containing system. Table 6.1 shows the PV at which

the surfactant concentration peaked for different formulations. The residence time available for contacting the residual oil was the highest for the TAA containing system. In Section 5.6, it was shown that the partitioning behavior in equilibrated oil and aqueous phases was different for different alcohols. TAA partitioned significantly more in equilibrated oil than either IPA, SBA, or IBA. On the other hand, TAA did not partition in the equilibrated aqueous phase as much as the other three alcohols. In the present study, the partitioning of TAA in the oil phase seems to correlate with greater oil displacement efficiency.

A proposed explanation for the behavior of the surfactant slug containing IPA, IBA, and SBA in porous media is shown in Figure 6.3. As was discussed in Section 5.6, these alcohols partition significantly more in the aqueous phase than in the oil phase. This leads to the loss of such alcohols in resident brine in porous media, or in other words, there is a chromatographic separation of alcohol and surfactant resulting into formation of stable emulsions by alcohol depleted surfactant slug. These emulsion droplet act as dead pores or block several pore throats resulting in the early breakthrough of surfactant in the effluent. Therefore, the surfactant slug does not come in contact with a significant number of residual oil droplets and is unable to mobilize these drops resulting in a poor oil recovery efficiency. The concept of chromatographic separation of surfactant slug constituents is discussed in Section 6.5.

A proposed explanation for the behavior of the surfactant slug containing TAA is shown in Figure 6.4. The significant partitioning

A PROPOSED EXPLANATION FOR THE BEHAVIOR OF SURFACTANT SLUG CONTAINING IPA, SBA, IBA IN POROUS MEDIA

Mass transfer of alcohol from surfactant slug to resident brine.

Resident Brine   Surfactant Slug
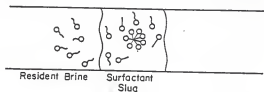
Formation of stable emulsions by alcohol depleted surfactant slug.
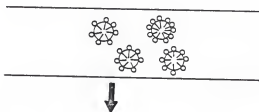
Leading to blockage of several pore throats, resulting in the early breakthrough of surfactant slug.
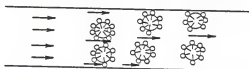
Figure 6.3 A Proposed Explanation For the Behavior of Surfactant Slug Containing IPA, IBA, and SBA in Porous Media.

A PROPOSED EXPLANATION FOR THE BEHAVIOR OF SURFACTANT SLUG CONTAINING TAA IN POROUS MEDIA

Mass transfer of alcohol from surfactant slug to oil ganglia.

Surfactant   Oil Ganglia
Slug
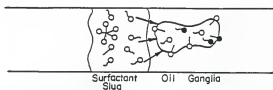
Produces ultra-low IFT and hence promotes mobilization and formatiom of an oil bank.

Surfactant   Oil Bank
Slug

Leading to plug flow condition of the surfactant slug and surfactant breakthrough around IPV of injected fluid.

Surfactant   Oil Bank
Slug
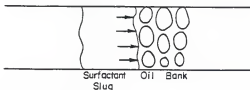
Figure 6.4 A Proposed Explanation for the Behavior of Surfactant Slug Containing TAA in Porous Media.

of TAA in equilibrated oil phase was described in Section 5.6. This partitioning seems to be responsible for the mass transfer of alcohol from surfactant slug to oil ganglia. This produces ultra-low interfacial tension at the oil/brine interface promoting the mobilization and formation of an oil bank. Hence, a condition of plug flow exists for the surfactant slug in porous media. The TAA-containing surfactant slug then comes in contact with most of the residual oil. This is supported by the surfactant breakthrough around 1 PV and oil displacement efficiency of 92% when the residual oil was displaced by a surfactant system with TAA (Table 6.1). An interesting behavior of the addition of alcohol on the surfactant mass transfer from bulk to oil/micellar solution interface in petroleum sulfonate system was reported by Chiang and Shah (1980). It was shown that the presence of alcohol increased the fluidity of the interface and decreased the flattening time and final oil saturation.

6.4.2 Effect of Salinity

For the TAA containing formulation, a series of displacement tests were conducted wherein the salinity of the system was varied around optimal salinity value thereby changing the phase environment, and hence, the phase characteristics of the microemulsion formed in situ. Table 6.2 summarizes the results of these flooding tests. It is seen that the optimal salinity formulation yielded the highest oil recovery efficiency. At salinity higher than optimal salinity, oil recovery was the poorest. The optimal salinity concept involves the formation of a middle phase microemulsion that has ultralow interfacial tensions with both oil and brine and is capable of displacing

Table 6.2 Summary of Flooding* Results: Effect of Salinity

Salinity of Surfactant Slug (% NaCl)	Residual Oil After Water Flooding (% PV)	Tertiary Oil Recovery Efficiency (%)	Surfactant Recovery (%)	PV at Which Surfactant Concentration Reached a Maximum
2.0+	18	31	68.7	0.86
2.5+	16	28	59.0	0.86
3.0+ (optimal salinity)	10	92	78.5	1.10
4.0+	18	10	23.0	0.65
2.8++ (optimal salinity)	43	79	–	–

+ A mixture of nonane and decane with EACN = 9.3 was displaced in sandpacks

++ Ankleshwar crude oil was displaced in Berea core

* 0.2 PV of surfactant slug containing 5% (w/v) TRS 10-80, 2% KF AA-270, 3% TAA in resident brine with 1% sodium carbonate and 0.3% sodium tripolyphosphate was injected in porous media (sandpack dimensions: 2.5 cm diameter, 30.0 cm length, permeability of 2-3 darcy; Berea core dimensions: 30.5 cm by 2.5 cm by 2.5 cm, permeability of 0.415 Darcy). Back pressure of 40 psi was applied. Flow rate of the injected fluids was 1 ft/day and the temperature was kept at 80 °C. When displacing the pure alkanes, 1500 ppm Dow Pusher in resident salinity brine was used after the surfactant slug. When displacing the crude oil, 2000 ppm Dow Pusher in resident brine was used after the surfactant slug.

the residual oil. The validity of this concept depends on the following conditions.

1. The optimal salinity of the surfactant formulation remains nearly constant when the surfactant slug is diluted by oil and brine in the course of flooding.

2. Electrolytes in reservoir brine do not appreciably alter the optimal salinity.

3. There is a sharp minimum of IFT occurring at optimal salinity.

4. The mobility control of the surfactant-polymer flooding is adequately maintained.

5. Surfactant loss is not too severe at the optimal salinity.

The first three conditions are generally recognized as necessary for enhanced oil recovery. The importance of mobility control was discussed by Chou and Shah (1980). The surfactant loss at different salinities is described below.

Surfactant loss in porous media depends upon the salinity of the connate water and that of surfactant slug among other things as described in Chapter I. Figure 6.5 shows the surfactant concentration in effluent as a function of the pore volume of fluids injected at different salinities.. The surfactant breakthrough was the earliest when the injected surfactant slug contained brine of higher than optimal salinity value. The surfactant recovery, or the area under the curve at this salinity was the lowest (Table 6.2). This indicates a significant surfactant retention in porous media because of
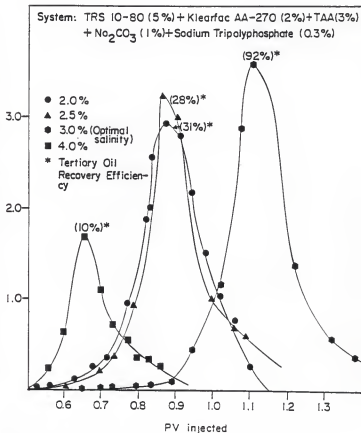
Figure 6.5 Effect of Salinity on Effluent Surfactant Concentration for TAA Containing Surfactant Formulation.

the precipitation of surfactant at higher salinities. This can decrease the stability or prevent the generation of microemulsion _in situ_ and thus can cause unstable, heterogeneous phase to occur. These changes are frequently associated with extremely pronounced differences in the mobility of the phase flowing through the porous medium (Kraft and Pusch, 1982) which results into poor oil recovery. At lower salinities than the optimal salinity, the oil recovery efficiency was higher and the surfactant loss was lower as compared to that above the optimal salinity.

6.5 Chromatographic Separation of Slug Constituents in Porous Media

One potential difficulty in the tertiary oil recovery process by surfactant/polymer flooding, is the chromatographic separation of constituents blended in a surfactant slug. These constituents include isomers of the same surfactant and cosurfactants in electrolyte solution to optimize the oil recovery. If any one of the constituents gets separated from the others as they flow through the oil-bearing formation, the oil recovery efficiency will be impaired. The separation may occur by any one or combination of mechanisms. During the displacement process, a number of fluid phases may coexist at various positions within the formation. Since these phases generally move at different velocities, selective partitioning of one constituent relative to the others can lead to separation (Todd, 1978).

A second possibility is chromatographic separation due to selective adsorption of surfactant constituents onto the reservoir rock

(Harwell et al., 1982). It has been shown the higher equivalent species have a greater tendency to adsorb on the reservoir minerals than the species with lower equivalent weight. Petroleum sulfonates, the surfactants extensively used in tertiary oil recovery, are not isomerically pure and they contain species having a distribution of equivalent weights. The partitioning of species with high equivalent weight on the reservoir rock impairs the integrity of surfactant solution. This may influence the partitioning of alcohol and surfactant in various fluid phases in porous media.

In this section, the separation of surfactant and alcohol in sandpacks as well as Berea cores is investigated. The composition of surfactant slug and the details of flooding experiments are shown in Table 6.3. Dodecane was used as oil in all displacement experiments in this section. Effluent surfactant concentration was measured by a two-phase titration method whereas alcohol concentration was determined using a gas chromatograph. Figure 6.6 shows effluent surfactant and alcohol concentration as well as surfactant to alcohol ratio as a function of pore volumes of fluid injected in sandpacks. The effluent surfactant and alcohol concentration showed maxima as pore volumes of fluid injected in the porous medium. However, the peaks in surfactant and alcohol concentrations occurred at different pore volumes. The surfactant concentration peaked at 1.15 PV while the alcohol concentration at 1.25 PV. This indicates that the surfactant and alcohol constituents did not traverse the porous medium at the same velocity. Surfactant travelled faster than alcohol in sandpacks. However, there was not a significant difference in the

Table 6.3 Specifications of Flow Through Porous Media Experiments

Length of the Sandpack and Berea Core.....30.0 cm

Flow Rate of the Injected Fluids   .....12 cc/hr

Size of the Surfactant Slug   .....20% PV

Composition of the Surfactant Slug   .....1 gm TRS 10-410 +0.7 gm IBA
                                          + 35 cc 1.5% Brine

Composition of the Drive Polymer   .....3000 ppm Dow Pusher-1000
                                          in 1.5% Brine

Optimal Salinity of the Formulation .....1.5 % NaCl

Permeability of Sandpacks   .....2-3 Darcy

Permeability of Berea Cores   .....0.250 Darcy

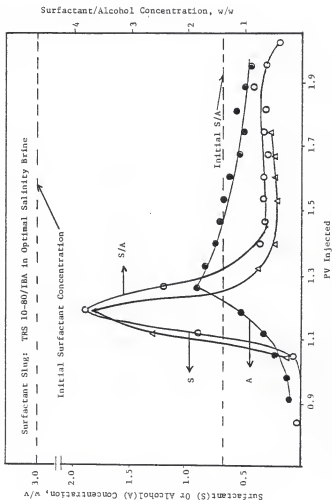Temperature   .....25 °C

Figure 6.6 Surfactant and Alcohol Concentration in the Effluent Fluids in the Case of Sandpacks.

position of maxima for surfactant and alcohol. One of the reasons could be negligible adsorption of surfactant on sand and minimum entrapment of surfactant and alcohol since the formulation was at optimal salinity. Higher salinity would result in the precipitation and hence excessive loss of surfactant in porous media. The surfactant to alcohol ratio in the effluent was higher than that of the injected slug between 1.05 PV and 1.35 PV. After 1.35 PV of the injected fluid, this ratio was significantly lower because of increased alcohol concentration in the effluent. This led to formation of the upper phase microemulsion which was evident from the presence of surfactant in the oil phase in the effluent. It is to be noted that 75% of the total effluent surfactant came out only within 0.35 PV while this was not the case with alcohol.

Figure 6.7 shows the effect of pore volume of fluid injected on effluent surfactant and alcohol concentration in Berea core. The behavior of surfactant and alcohol in the effluent in Berea core was found to be different than that in sandpacks. Even though, the alcohol concentration peaked at the same pore volume (1.25 PV) in Berea core as in sandpack, the maximum in surfactant was delayed in Berea core (1.45 PV). Moreover, the surfactant concentration at the peak was 1.5%, less than the peak surfactant concentration of 2% in sandpack. In Berea core, most of the surfactant and alcohol came out within 0.5 PV. However, surfactant moved much slower than alcohol. This could be due to the adsorption and dispersion of surfactant. This was supported by the higher loss of surfactant in Berea core
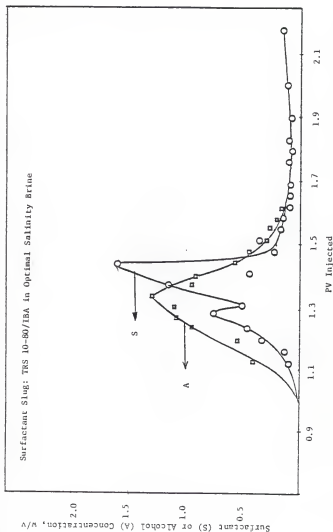
Figure 6.7 Surfactant and Alcohol Concentration in the Effluent Fluids in the Case of Berea Core.

than in sandpack as indicated by a greater area under the surfactant curve for the case of sandpack than that of Berea core.

6.6 Summary

In this chapter the transport of multi-phase, multicomponent systems in porous media was discussed. The effect of salinity and cosolvent structures on oil displacement efficiency for a moderate temperature, $80^{\circ}C$, and moderate salinity, 3.0%, reservoir conditions were investigated experimentally. The concept of chromatographic separation of surfactant slug constituents was examined in sandpacks as well as in Berea core. The following conclusions were drawn from this chapter:

1. For sandpacks at $80^{\circ}C$, the formulations containing TAA, IBA, IPA, and SBA as a cosolvent at corresponding optimal salinity, the tertiary oil recovery efficiency of 92, 27, 14 and 11 respectively. In Berea core, TAA containing formulation displaced 79% crude oil at $80^{\circ}C$.

2. For surfactant formulations containing TAA at 2.0%, 2.5%, 3.0% (optimal salinity), and 4.0% NaCl, the tertiary oil recovery in sandpacks was 31, 28, 92 and 10% respectively.

3. The tertiary oil recovery correlated with surfactant retention, surfactant breakthrough, and alcohol partitioning in the equilibrated phases.

4. It was proposed that since alcohols such as IPA, IBA, and SBA partitioned in brine, the alcohol depleted surfactant slug

formed stable emulsions resulting in the faster breakthrough of the surfactant slug and a lower oil displacement efficiency.

5. It was proposed that since TAA partitioned mainly in the oil phase, there was a mass transfer of alcohol from surfactant slug to oil ganglia. This produced a transient ultra-low interfacial tension between the surfactant slug and oil and mobilized the oil ganglia forming an oil bank. This resulted in a plug flow condition for the surfactant slug and a higher oil displacement efficiency.

6. It was shown that the surfactant and alcohol moved at different velocities in sandpacks and in Berea cores. In sandpacks, it was shown that the surfactant moved faster than alcohol whereas in a Berea core, alcohol moved faster than surfactant. The surfactant loss was more in Berea core than in sandpacks due to the adsorption of surfactant on Berea core.

7.1 Chain Length Compatibility and Interfacial Composition of Microemulsions

It was concluded that there is a chain length compatibility in microemulsions of sodium stearate/pentanol/oil/brine system. When the equation $l_a + l_o = l_s$ is satisfied, there will not be a region of disordered hydrocarbon chains near methyl groups around the microemulsion droplet. The thermal motion of the terminal segment produces a disruptive effect on the packing of surfactant molecules and increases the intermolecular distance between the surfactant molecules at the interface. When dodecane is used in making microemulsions, the relationship $l_a + l_o = l_s$ is approximately satisfied. Therefore, this microemulsion is able to solubilize higher amount of brine due to the cohesive interactions between the hydrocarbon chains.

The optimal salinity of the oil-external microemulsions is defined as the salinity at which the microemulsion solubilizes the maximum amount of brine. It was shown that as the alkyl chain length of oil increases, the optimal salinity increases. The maximum brine solubilization at optimal salinity is explained by the highest molar ratio of alcohol to surfactant at the interface.

The interfacial composition of these microemulsions is determined using a modified three compartment Schulman-Bowcott model. The modified model takes into account the solubility of alcohol in aqueous as well as hydrocarbon phases. For a constant brine/surfactant ratio, it was found that the value of interfacial alcohol to surfactant ratio, $\frac{n_a^i}{n_s}$, is highest for dodecane-containing microemulsions. This is due to the highest molecular packing at the interface resulting from chain length compatibility effect. This modified model assumes that all surfactant molecules are at the interface. It is recommended that the accuracy of this model can be further enhanced by incorporating the partitioning of surfactant in aqueous and hydrocarbon phases.

By the electrical conductivity measurements of the microemulsions, it was shown that at a given brine to oil ratio, the normalized electrical resistance decreases as the alkyl chain length of the oil increases. This behavior is explained on the basis of surface conductance model. This model considers the effective volume conductivity as the sum of parallel bulk and surface conductivity. As the alkyl chain length of oil increases, there is a smaller contribution due to surface resistivity.

7.2 Surface Potential of SDS Micelles Using Fluorescence Methods

The surface potential of SDS micelles is determined using fluorescence spectroscopy. In ionic micelles of SDS, the pH at the micellar surface is different than that in the bulk. A surfactant-type fluorescent dye (4-heptadecyl umbelliferon) is sensitive to

changes at the micellar surface. It was shown that this fluorescent dye orients at the interface.

The pK value of the dye in the micellar solution is compared with that in the bulk water. From the shift in pK, the surface potential of SDS micelle is calculated using the Gouy-Chapman theory and from the shift in pK of the dye, the surface potential of 24 mM SDS micelle was found to be -121 mv. The addition of salt decrease the surface potential of the micelles due to compression of the electrical double layer around the micelle. It is suggested that the effect of the addition of short chain alcohols or multivalent ions on the surface potential of SDS micelle can be investigated using the fluorescence methods.

7.3 Solubilization and Fluorescence Behavior of Microemulsions

There is a critical electrolyte concentration at which the oil-external microemulsions prepared from petroleum sulfonate can solubilize maximum amount of brine. The critical electrolyte concentration corresponds to the optimal salinity of the formulation. As the chain length of oil is increased, the optimal salinity increases. However, the increase in optimal salinity is much greater for water soluble alcohols than for water insoluble alcohols. The maximum brine solubilization capacity of microemulsions decreases as the chain length of oil increases for n-butanol and isobutanol-containing microemulsions. This is explained in terms of partitioning of alcohols in various phases of microemulsions and the interfacial area available for solubilization. There is a preferred chain length of

alcohol, namely, pentanol which can solubilze the highest amount of brine in TRS 10-410/hexadecane/brine system. It was shown that the interfacial alcohol to surfactant ratio is maximum at optimal salinity for this system using the Schulman-Bowcott titrations. Moreover, the amount of alcohol and surfactant at the interface is highest for this system at optimal salinity.

A linear correlation between the fluorescence and solubilization behavior of these microemulsions is presented which is is independent of the type of alcohol or oil used in preparing the microemulsions as well as it is independent of the salinity of the system. The fluorescence behavior of microemulsions is explained on the basis of total amount of surfactant or surface charge density at oil/water interface. It is suggested that the quantitative determination of surface potential may be possible by investigating the effect of pH on the fluorescence behavior of microemulsions in conjunction with the Gouy-Chapman theory.

7.4 EACN Determination and Equilibrium Properties of Microemulsions

The equivalent alkane carbon number (EACN) of a crude oil, namely Ankleshwar crude, is successfully modeled by a mixture of pure alkanes. The EACN of the crude oil is found to be 9.3 and an appropriate mixture of nonane and decane exhibits similar phase behavior as the crude oil. A surfactant system for a water flooded reservoir at 80 °C and having a salinity in the range of 20 -30 gms/liter is formulated by blending a phosphated ester with TRS 10-80 in the weight ratio of 2/5. The addition of KF AA-270 not only

increases the salt tolerance of the petroleum sulfonate system but it also broadens the IFT minimum. The effect of addition of sacrificial agents such as sodium carbonate and sodium tripolyphosphate is to increase the solubilization parameter as well as the optimal salinity of the surfactant formulation. The partitioning of alcohols in equilibrated phases depend upon the structure of the cosolvents. Water-soluble alcohols such as IPA, IBA and SBA partitions mainly in the excess brine in the middle phase. On the other hand, TAA partitions mainly in the excess oil and the middle phase.

7.5 A Mechanism of Oil Displacement Efficiency in Porous Media

From oil displacement tests at 80°C in sandpacks and in Berea core, it was shown that, 0.2 PV of surfactant slug containing TAA, IBA, IPA and SBA at corresponding optimal salinity displaces 92%, 27%, 14%, and 11% oil respectively. In Berea core, TAA-containing surfactant slug displaces 79% crude oil. The same surfactant slug was found to displace 31%, 28%, 92%, and 10% oil at 2.0%, 2.5%, 3.0% (optimal salinity) and 4.0% NaCl respectively.

From the effluent surfactant concentration, it was shown that there is a correlation between the tertiary oil recovery and surfactant breakthrough as well as the surfactant retention in porous media. It is proposed that since alcohols such as IPA, IBA and SBA partition mainly in excess brine in porous media, the alcohol depleted surfactant slug forms a stable emulsions resulting into the faster breakthrough of the surfactant in the effluent and lower oil displacement efficiency. A pressure profile of porous media

experiments is suggested to verify the proposed mechanism. In the case of TAA-containing surfactant slug, there is a partitioning of alcohol in the oil phase. Therefore, there is a mass transfer of alcohol from the surfactant slug to the oil ganglia in porous media. This produces a transient ultralow interfacial tension between the residual oil and the surfactant solution which mobilizes the oil. This results in a plug flow condition for the surfactant slug as indicated by the effluent surfactant concentrstion profile.

REFERENCES

Abrams, A., Soc. Pet. Eng. J., 15, 437 (1975).

Adamson, A.W., J. Colloid Int. Sci., 29, 261 (1969).

Ahmad, S.I., Shinoda, K., and Friberg, S., J. Colloid Int. Sci., 47, 32 (1974)

Alexander, A.E., Adv. Colloid Sci., 3, 67 (1950).

Almgren, M., Photochem. Photobiol. 15, 297 (1972).

Almgren, M., Griesen, P., and Thomas, J.K., J. Am. Chem. Soc. 101, 279 (1979).

Anacker, E.W., J. Phys. Chem., 62, 41 (1958).

Aodia, M., and Rodgers, M.A., J. Am. Chem. Soc., 101, 6777 (1979).

Arkin, L., and Singleterry, C.R., J. Am. Chem. Soc., 70, 3965 (1948).

Atherton, N.M., and Strack, S.J., Farad. Trans. II, 68, 374, (1972).

Atkinson, H., U.S. Patent 1,651,311 (1927).

Bae, J.H., and Petrick, C.B., paper presented at the SPE Improved Oil Recovery Symposium, Tulsa, OK, Mar. (1976).

Bae, J.H., and Petrick, C.B., Soc. Pet. Eng. J., 17, 353 (1977).

Bae, J.H., and Petrick, C.B., Soc. Pet. Eng. J., 21, 573 (1981).

Bae, J.H., Petrick, C.B., and Ehrlich, R., presented at the SPE Improved Oil Recovery Symposium, Tulsa, OK, April (1974).

Bansal, V.K., Chan, K.S., McCallough, R., and Shah, D.O., J.Can. Pet. Tech., 17, 1 (1978).

Bansal, V.K., Chinnaswamy, K., Ramachandran, C., and Shah, D.O.,

J. Colloid Int. Sci., 72, 524 (1979).

Bansal, V.K., and Shah, D.O., J. Am. Oil Chem. Soc., 55, 376 (1978a).

Bansal, V.K., and Shah, D.O., J. Colloid Int. Sci., 65, 451 (1978b).

Bansal, V.K., Shah, D.O., and O'Connell, J.P., J. Colloid Int. Sci., 75, 462 (1980).

Barakat, H.Z., and Clark, J. Heat Transfer, 88, 421, (1966).

Baviere, M., presented at the 51st Annual Fall Technical Conference and Exhibition of the SPE of AIME, New Orleans, LA, Oct, (1976).

Baviere, M., Schechter, R.S. and Wade, W.H., J. Colloid Int. Sci., 81, 266 (1981).

Bellocq, A.M., and Fourche, G., J. Colloid Int. Sci., 78, 275 (1980).

Bennion, B.C., and Eyring, E.M., J. Colloid Int. Sci., 32, 286 (1970).

Bernard, G.G., J. Pet. Tech., 27, 179 (1975).

Biais, J., Bothorel, P., Clin, B., and Lalanne, P., J. Colloid Int. Sci., 80, 136 (1981).

Birdi, K.S., Singh, H.N., and Dalsager, S.O., J. Phy. Chem., 83, 2733 (1979).

Bockstade, V., Martens, J., Put, J., Derderen, J., Boens, N., and Schrijver, F., Chem. Phy. Lett., 58, 211 (1978).

Boneau, P.F., and Clampitt, R.L., J. Pet. Tech., 29, 501 (1977).

Boussaha, A., and Ache, H., J. Colloid Int. Sci., 78, 258 (1980).

Bowcott J.E., and Schulman, J.H., Z. Electochem. 59, 283 (1955).

Brand, L., and Gohlke, J.R., Ann. Rev. Biochem., 41, 843 (1972).

Brinkman, R., J. Chem. Phy. 20, 571 (1952).

Cameron, A., and Crouch, R.F., Nature (London), 198, 475 (1963).

Cayias, J.L., Schechter, R.S., and Wade, W.H., Soc. Pet. Eng. J., 16, 351 (1976).

Chan, K.S., Ph.D. Dissertation, University of Florida (1978).

Chan, K.S., and Shah, D.O., paper presented at the SPE Symposium on Oilfield and Geothermal Chemistry Meeting, Houston, TX (1979).

Chan, K.S., and Shah, D.O., J. Dispersion Sci. and Tech. 1, 55 (1980).

Chen, M., Gratzel, M., and Thomas, J.K., Chem. Phy. Lett., 24, 65 (1974).

Chiang, M.Y., and Shah, D.O., paper presented at the SPE Oilfield and Geothermal Chemistry Meeting, Stanford, CA, May (1980).

Chiang, M.Y., Chan, K.S., and Shah, D.O., J. Can. Pet. Tech. 17, 1 (1978).

Chou, S.I., Ph.D. Dissertation, University of Florida (1980).

Chou, S.I., and Shah, D.O., J. Cand. Pet. Tech., 20, 459 (1981).

Clausse, M., Hail, J., Peyrelase J., and Boned, C., J. Colloid Int. Sci., 87, 584 (1982).

Clausse, M., Sheppard, R.J., Boned, C., and Essex, C.G. in "Colloid Interface Science," M. Kerker, ed., Academic Press, New York (1976).

Clifford, J., and Pethica, B.A., Trans. Farad. Soc. 61, 182 (1965).

Coats, K.H., and Smith, B.D., Soc. Pet. Eng. J., 4, 73 (1964).

Cook, C.E., and Schulman, J.H. in "Surface Chemistry," Munksgaard, Copenhagen (1965).

Corrin, M.L., and Harkins, W.D., J. Am. Chem. Soc., 69, 679 (1949).

Craft, B.C., and Hawkins, M.F., "Applied Petroleum Reservoir Engineering," Prentice-Hall, Inc., Englewood Cliffs, N.J. (1959).

Damaszewki, L., and Mackay, R.A., J. Colloid Int. Sci., 97, 166 (1984).

Dauben, D.L., and Froning, H.R., J. Pet. Tech., 23, 614 (1971).

Davies, J.T., and Rideal, E.K., "Interfacial Phenomena," Academic Press, New York (1967).

Dawson, R., and Lantz, R.B., Soc. Pet. Eng. J., 12, 448 (1972).

Dean, J.A., ed., "Langes Handbook of Chemistry," McGraw-Hill, New York (1973).

Debye, P., Ann. New York Acad. Sci., 51, 575 (1949).

Debye, P. and Anacker, E.W. J. Phy. Chem., 55, 644 (1951).

Desai, N.N., Ph.D. Dissertation, University of Florida (1983).

Dorich, M.J., Mann, J.A. and Kawamoto, A., J. Colloid Int. Sci. 41, 145 (1972).

Edelman, G.M. and McClure, W.O., Accounts Chem. Res. 1, 65 (1968).

Eicke, H.F., J. Colloid Int. Sci. 52, 65 (1975).

Eicke, H.F., in "Micellization, Solubilization and Microemulsions," K. Mittal, ed., Vol. 2, Plenum Press, New York (1977).

Eicke, H.F., paper presented at the 3rd International Conference on Surface and Colloid Science, Stockholm, Sweden, Aug. (1979).

Eicke, H.F., Top. Current Chem. 87, 86 (1980).

Eicke, H.F., and Christen, H., J. Colloid Int. Sci., 48, 281 (1974).

Eicke, H.F., and Rehak, J., Helv. Chim Acta, 59, 2883 (1976).

Eicke, H.F., and Sheperd, J.C.W., Helv. Chim Acta, 53, 1951 (1977).

Eicke, H.F., and Zinsli, P.E., J. Colloid Int. Sci., 65, 131 (1978).

Ekwall, P., in "4th International Conference on Surface Active Substances," J.TH.G. Overbeek, ed., Gordon and Breach, New York (1964).

Ekwall, P., J. Colloid Int. Sci., 29, 16 (1969).

Ekwall, P., Danielson, I., and Stenius, P. in "Phys. Chem. Series one, Vol. 7; Surface Colloids and Chemistry," M. Kerker., ed., Butterworths, London (1972).

Emerson, M.W., and Holtzer, A., J. Phy. Chem., 71, 1898 (1967).

Erickson, J.C., and Gilberg, G., Acta Chem. Scand., 20, 2019 (1966).

Ewing, G.W. "Instrumental Methods of Chemical Analysis," McGraw-Hill, New York (1975).

Fayers, F. J., and Perrine, R.L., Petroleum Trans. AIME, 216, 277 (1959).

Fendler, E.J., Chang, S.A., Fendler, J.H., Medsy, R.T., El Soud,

O.A., and Woods, V.A. in "Reaction Kinetics in Micelles," E. Cordes, ed., Plenum Press, New York, pp 127 (1973).

Fendler, E.J., Day, C.L., and Fendler, J.H., J. Phy. Chem., 76,1460 (1972).

Fendler, J.H., J. Phy. Chem., 76, 1460 (1972).

Fendler, J.H., and Fendler, E.J. "Catalysis in Micellar and Macromolecular Systems," Academic Press, New York (1975).

Fernandez, M.S., and Fromhertz, P., J. Phy. Chem., 81, 1754 (1977).

Fleming, P.D., and Vinatieri, J.E., J. Chem. Phys. 66, 31147 (1977).

Forest, B.J., and Reeves, L.W., Chem. Rev., 81, 1 (1981).

Fort, T. Jr., J. Phy. Chem., 66, 1136 (1962).

Foster, W.R., J. Pet. Tech., 25, 205 (1973).

Franks, F. ed., "Water: A Comprehensive Treatise," Vol. IV, Plenum Press, New York (1975).

Friberg, S., J. Am. Oil Chem. Soc., 48, 578 (1971).

Friberg, S., in "Microemulsions: Theory and Practice," L.M. Prince, ed., Academic Press, New York (1977).

Friberg, S., and Buraczenka, I., Progr. Colloid Poly. Sci. 63, 1 (1978).

Friberg, S., Lapczynska, I., and Gillberg, J., J. Colloid Int. Sci., 56, 15 (1976).

Friedman, F., and Ramirez, W. F., Chem. Eng. Sci., 32, 687 (1977). (1977).

Funasaki, N., J. Colloid Int. Sci., 60, 54 (1977a).

Funasaki, N., J. Colloid Int. Sci., 62, 189 (1977b).

Funasaki, N., J. Colloid Int. Sci., 62, 336 (1977c).

Gale, W.W., and Sandvik, E.L., Soc. Pet. Eng. J., 13, 191 (1973).

Gale, W.W., Saunder, R.K., and Ashcraft, T.L. Jr., U.S. Patent, 3,977,471 (1976).

Gerbacia, W., and Rosano, H.L., J. Colloid Int. Sci., 44, 242 (1973).

Gilberg, G., Lehtinen, H., and Friberg, S., J. Colloid Int. Sci., 33, 40 (1970).

Glinsmann, G.R., paper presented at the 54th SPE-AIME Meeting, Las Vegas, NV, Sept. (1979).

Glover, C.J., Puerto, M.C., Maerker, J.M., and Sandvik, E.L. Soc. Pet. Eng. J., 19, 183 (1979).

Goddard, E.D., Advanc. in Colloid and Int. Sci. 4, 45 (1974).

Gogarty, W.B., J. Pet. Tech., 28, 93 (1976).

Gogarty, W.B., paper presented at SPE Improved Oil Recovery Symposium, Tulsa, OK, April (1978).

Gogarty, W.B., J. Pet. Tech., 35, 1581 (1983).

Gogarty, W.B., Meabon, H.P., and Milton, H.W., J. Pet. Tech., 22, 14 (1970).

Gogarty, W.B., and Tosch, W.C., J. Pet. Tech., 20, 1407 (1968).

Goldberg, R.H., paper presented at the SPE-AIME 52nd Annual Meeting, Denver, CO, Oct. (1977).

Gratzel, M., and Thomas, J.K., J. Am. Chem. Soc., 95, 6885 (1973).

Gratzel, M., and Thomas, J.K. in "Modern Fluorescence Spectroscopy," Wehry, E.L., ed., Plenum Press, New York (1976).

Gupta, S.P., and Greenkorn, R.A., Water Resource Res., 9,1357 (1973).

Gupta, S.P., and Trushenski, S.P., Soc. Pet. Eng. J., 19, 116 (1979).

Hanna, H.S., and Somasundaran, P., in "Improved Oil Recovery by Surfactant and Polymer Flooding," D.O. Shah and R.S. Schechter, eds. Academic Press, New York (1977).

Hartley, G.S., "Aqueous Solution of Paraffin Chain Salts," Herrmann, Paris (1936).

Hartley, G.S., in "Progress in Chemistry of Fats and other Lipids," Pergamon Press, London (1955).

Hartley, G.S., in "Micellization, Solubilization and Microemulsions," K.L. Mittal, ed., Plenum Press, New York (1977).

Harwell, J.H., Helfferich, F.G., and Schechter, R.S., A.I.Ch.E.J. 28, 448 (1982).

Hatfield, J.C., Davis, H.T., and Scriven, L.E., paper presented at A.I.Ch.E. 8th National Meeting, New Orleans, June (1978).

Hauser, M., and Klein, U., Z. Phy. Chem., 78, 32 (1972).

Hayes, M.E., Bourrel, M., El-Emary, M.M., Schechter, R.S., and Wade, W.H., Soc. Pet. Eng. J., 19, 107 (1974).

Healy, R.N., and Reed, R.L., Soc. Pet. Eng. J., 14, 491 (1974).

Healy, R.N., and Reed, R.L., Soc. Pet. Eng. J., 16, 147 (1976).

Healy, R.N., Reed, R.L., and Carpenter, C.W., Soc. Pet. Eng. J., 15, 87 (1975).

Helfferich, F.G., Soc. Pet. Eng. J., 21, 51 (1981).

Helfferich, F.G., and Klein, G., "Multicomponent Chromatography," Marcel Dekker, Inc., New York (1970).

Herman, U., and Schelly, Z.A., J. Am. Chem. Soc., 101, 2665 (1979).

Hill, H.J., and Lake, L.W., Soc. Pet. Eng. J., 18, 445 (1978).

Hill, H.J., Reisberg, J., and Stegmeir, G.L., J. Pet. Tech., 25, 186 (1973).

Hirasaki, G.J., Soc. Pet. Eng. J., 21, 191 (1981).

Hirasaki, G.J., van Domselaar, H.R., and Nelson, R.C., paper presented at the SPE Improved Oil Recovery Symposium, Tulsa, OK, April (1980).

Holm, L.W., J. Pet. Tech., 23, (1971).

Holm, H.W., and Josendal, V.A., Oil and Gas J., 70, 158 (1972).

Horowitz, P., J. Colloid Int. Sci., 61, 197 (1977).

Hsieh, W.C., Ph.D. Dissertation, University of Florida (1976).

Hsieh, W.C., and Shah, D.O., paper presented at the SPE-AIME Symposium on Oilfield and Geothermal Chemistry Meeting, La Jolla, CA, June (1977).

Huh, C., J. Colloid Int. Sci., 71, 408 (1979).

Hurd, B.G., paper presented at SPE Improved Oil Recovery Symposium Tulsa, OK, Mar. (1976).

Improved Oil Recovery, Exxon Background Series, (1982).

Infelta, P., Chem. Phy. Lett., 61, 88 (1979).

Infelta, P., and Gratzel, M., J. Chem. Phy., 70, 179 (1979).

IUPAC Manual of Symbols and Terminology, App. II, Part I,
   Intl. Union of Applied Chemistry, 31, No. 4, 612 (1972).

Kaurmann, W., Adv. Protein Chem., 14, 1 (1959).

Keh, E., and Valeur, B., J. Colloid Int. Sci., 79, 465 (1981).

Kim, J., Kim, C., Song, P., and Lee, K., J. Colloid Int. Sci., 80,
   294 (1981).

Kitahara, A., Katsuta, M., Haibara, S., and Kon-No, K., paper presented
   at the 3rd International Conference on Surface and Colloid
   Science, Stockholm, Sweden, Aug. (1979).

Kitahara, A., Watanabe, K., Kon-No, K., and Ishikawa, T.,
   J. Colloid Int. Sci., 29, 15 (1969).

Klein, A., and Haar, W., Chem. Phys. Lett., 58, 531 (1978).

Kon-No, K., and Kitahara, A., J. Colloid Int. Sci., 35, 409 (1971a).

Kon-No, K., and Kitahara, A., J. Colloid Int. Sci., 35, 636 (1971b).

Kon-No, K., and Kitahara, A., J. Colloid Int. Sci., 37, 499 (1971c).

Kraft, H.R., and Pusch, G., paper presented at SPE/DOE Improved
   Oil Recovery Symposium, Tulsa, OK, April (1982).

Krecheck, G.C., in "Water: A Comprhensive Treatise," Vol.IV,
   F. Franks, ed., Plenum Press, New York (1975).

Kremesec, V.J., and Treiber, L.E., J. Pet. Tech., 30, 52 (1978).

Kubota, Y., Kodama, M., and Miura, M. Bull. Chem. Soc. Jap.,
   46, 100 (1973).

Kumar, C., and Balasubramanian, D., J. Colloid Int. Sci., 74, 64 (1980).

Lagues, M., Ober, R., and Taupin, C.J., J. Phy. Lett. Fr.,
   39, 487 (1975).

Lake, L.W., and Helfferich, F., Soc. Pet. Eng. J., 18, 435 (1978).

Lang, J., and Eyring, E.M., J. Poly. Sci., A-2, 89, (1972).

Langmuir, I., Phy. Rev., 6, 79 (1915).

Langnes, A., Robertson, J.O. Jr., and Chillinger, G.V. "Secondary Recovery and Carbonate Reservoirs," American Elseveir Publishing Co., New York (1972).

Lantz, R.B., Soc. Pet. Eng. J., 11, 315 (1971).

Lapidus, L., and Amundson, N.R., J. Phys. Chem., 56, 984,(1952).

Larson, R.G., Soc. Pet. Eng. J., 19, 411 (1979).

Larson, R.G., and Hirasaki, G.J., Soc. Pet. Eng. J., 18, 42 (1978).

Lawson, J.B., paper presented at SPE Improved Oil Recovery Symposium Tulsa, OK, April (1978).

Levine, S., and Robinson, K., J. Phy. Chem., 76, 876 (1972).

Levy, G.C., Komoroski, R.A., and Halskod, J.A., J. Am. Chem. Soc., 95, 4871 (1973).

Lindblom, G., Lindman, B., and Mandell, L., J. Colloid Int. Sci., 34, 262 (1970).

Lindman, B., and Wennerstrom, H., Top. Current Chem. 87, 3 (1980).

Mackay, R.A., Jacobson, K., and Tourian, J., J. Colloid Int. Sci., 76, 515 (1980).

Maddox, J. Jr., Tale, J.F., and Shupe, R.D., U.S. Patent 3,916,996 (1975).

Malmberg, E.N., and Smith, L., in "Improved Oil Recovery by Surfactant and Polymer Flooding," D.O. Shah and R.S. Schechter, eds., Academic Press, New York (1977).

Mast, R.C., and Haynes, L.V., J. Colloid Int. Sci., 53, 35 (1975).

Matsumoto, S., and Sherman, P., J. Colloid Int. Sci., 30, 524 (1969).

McBain, J.W., Nature, 145, 702 (1940).

Melrose, J.C., and Brandner, C.F., J. Pet. Tech., 26, 54 (1974).

Miller, C.A., Hwan, R.A., Bentom, W.J., and Tourian, J., J. Colloid Int. Sci., 61, 554 (1977).

Montal, M., and Gitler, C., Bioenergetics, 4, 363 (1973).

Motomura, K., and Baret, J.F., J. Colloid Int. Sci., 91, 391 (1983).

Mukerjee, P., J. Phy. Chem., 76, 2054 (1969).

Mukerjee, P., Adv. Colloid and Int. Sci., 1, 241 (1976).

Mukerjee, P., and Banerjee, K., J. Phy. Chem., 68, 3567 (1964).

Mukerjee, P., Cardinal, J.R., and Desai, N.R. in "Micellization Solubilizations and Microemulsions," K.L. Mittal, ed., Plenum Press, New York (1977).

Muller, N., and Platko, F.E., J. Phy. Chem., 75, 547 (1971).

Nagarajan, R., and Ruckenstein, E., J. Colloid Int. Sci., 60, 221 (1977).

Nelson, R.C., paper presented at SPE Improved Oil Recovery Symposium, Tulsa, OK, April (1980).

Nelson, R.C., and Pope, G.A., Soc. Pet. Eng. J., 18, 325 (1978).

Nemethy, G., Ange. Chem., 6, 195 (1967).

Novosad, J., Soc. Pet. Eng. J., 22, 962 (1982).

Novosad, J., Maini, B., and Batycky, J., J. Am. Oil Chem. Soc., 59, 833 (1982).

Noronha, J., Ph.D. Dissertation, University of Florida (1980).

Noronha, J., and Shah, D.O., A.I.Ch.E. Symposium Series, 78, No.212, 42 (1982).

Oakes, J., J. Chem. Soc. Farad. Trans.II 69, 1321 (1973).

O'Connell, J.P., and Brugman, R.J. in "Improved Oil Recovery by Surfactant and Polymer Flooding," D.O. Shah and R.S. Schechter, eds., Academic Press, New York (1977).

O'Conski, C.T., J. Phy. Chem., 64, 605 (1968).

Overbeek, J.Th.G., Disc. Farad. Soc., 65, 7 (1978).

Paul, G.W., and Froning, H.R., J. Pet. Tech., 25, 957 (1973).

Perkins, T.K., and Johnston, O.C., Soc. Pet. Eng. J., 3, 70 (1966).

Pithapurwala, Y.K., and Shah, D.O., Chem. Eng. Comm., In Press (1984a).

Pithapurwala, Y.K., and Shah, D.O., J. Am. Oil Chem. Soc., In Press (1984b).

Pope, G.A., Soc. Pet. Eng. J., 20, 191 (1980).

Pope, G.A., and Nelson, R.C., Soc. Pet. Eng. J., 18, 339 (1978).

Prince, L.M., J. Colloid Int. Sci., 23, 165 (1967).

Prince, L.M., J. Colloid Int. Sci., 29, 216 (1969).

Prince, L.M., "Microemulsions, Theory and Practice," Academic Press, New York (1977).

Puerto, M.C., and Gale, W.W., Soc. Pet. Eng. J., 17, 193 (1977).

Puerto, M.C., and Reed, R.L., paper presented at SPE/DOE Improved Oil Recovery Symposium, Tulsa, OK, April (1982).

Radda, G.K., Curr. Top. Bioenerg., 4, 81 (1971).

Ramirez, W.F., and Riley, K.F., Chem. Eng. Comm., 25, 363 (1984).

Rance, D.G., and F.B., J. Colloid Int. Sci., 60, 207 (1977).

Rathmell, J.J., Smith, F.W., Salter, S.J., and Fink, T.R., paper presented at SPE Improved Oil Recovery Symposium, Tulsa, OK, April (1978).

Ray, A., J. Am. Chem. Soc., 91, 6511 (1969).

Reed, R.L., and Healy, R.N., in "Improved Oil Recovery by Surfactant and Polymer Flooding," D.O. Shah and R.S. Schechter, eds., Academic Press, New York (1977).

Rehbinder, P.A., Proc. 2nd Intl. Congr. Surface Activity, London, 1, 476 (1957).

Rehfeld, S.J., J. Colloid Int. Sci., 34, 518 (1970a).

Rehfeld, S.J., J. Phy. Chem., 74, 117 (9170b).

Reiss, H., J. Colloid Int. Sci., 53, 61 (9175).

Reiss-Husson, F., and Luzzati, V., J. Colloid Int. Sci., 32, 286 (1970).

Roscoe, R., Brit. J. Appl. Phy. 3, 267 (1952).

Rubalcava, B., DeMunoz, D.M., and Gitler, C., Biochemistry, 8, 2742 (1969).

Ruckenstein, E. in "Micellization, Solubilization and Microemulsions," K.L. Mittal, ed., Plenum Press, New York (1976).

Ruckenstein, E., and Chi, J.C., J. Chem. Soc. Fard. Trans. II, 11, 1960 (1975).

Ruckenstein, E., and Krishnan, R., J. Colloid Int. Sci., 71, 321 (1979).

Ruckenstein, E., snd Krishnan, R., J. Colloid Int. Sci., 76, 188 (1980).

Ruckenstein, E., and Nagarajan, R., J. Phy. Chem., 79, 2622, (1975).

Ruckenstein, E., and Nagarajan, R., J. Colloid Int. Sci., 57, 388 (1976).

Saito, H., and Shinoda, K., J. Colloid Int. Sci., 32, 647 (1970).

Salager, J.L., Bourrel, M., Morgan, J.C., Schechter, R.S., and Wade, W.H., Soc. Pet. Eng. J., 16, 147 (1976).

Salager, J.L., Vasquez, E., Morgan, J.C., Schechter, R.S., and Wade, W.H., Soc. Pet. Eng. J., 19, 107 (1979).

Salter, S.J., paper presented at the Fall SPE Meeting, Denver, CO, Oct. (1977).

Satter, A.S., Shum, Y.M., Adams, T., and Davis, A., Soc. Pet. Eng. J., 20, 129 (1980).

Schick, M.J., and Fowkes, F.M., J. Phy. Chem., 61, 1062 (1957).

Schulman, J.H., and Friend, J.A., J. Colloid Int. Sci., 3, 497 (1949).

Schulman, J.H., and Riley, D.P., J. Colloid Int. Sci., 3, 313 (1948).

Scriven, L.E., Nature, 236, 123 (1976).

Scriven, L.E. in "Micellization, Solubilization and Microemulsions," K.L. Mittal, ed., Plenum Press, Vol. 2, New York (1977).

Shah, D.O., Chem. Eng. Education, 11, 14 (1977).

Shah, D.O., paper presented at the Second European Symposium on EOR, Bournemouth, England, Sept. (1981a).

Shah, D.O., ed., "Surface Phenomena in Enhanced Oil Recovery," Plenum Press, New York (1981b).

Shah, D.O., Bansal, V.K., Chan, K.S., and Hsieh, W.C. in "Improved Oil Recovery by Surfactant and Polymer Flooding," D.O Shah and R.S. Schechter, eds., Academic Press, New York (1977).

Shah, D.O., and Hamlin, R.M. Jr., Science, 171, 483 (1971).

Shah, D.O., and Shiao, S.Y., Adv. Chem. Ser., 144, 153 (1975).

Shah, D.O., and Schechter, R.S., eds., "Improved Oil Recovery by Surfactant and Polymer Flooding," Academic Press, New York (1977).

Shah, D.O., Tamjeedi, A., Falco, J.W., and Walker, R.D. Jr., A.I.Ch.E.J., 18, 1116 (1972).

Shah, D.O., Walker, R.D., Hsieh, W.C., Shah, N.J., Dwivedi, S., Nelander, J., Pepinsky, K., and Deamer, D.W., paper presented at the SPE Improved Oil Recovery Symposium, Tulsa, OK, April (1976).

Shankar, P.K., Bae, J.H., and Enick, R.M., paper presented at the SPE Symposium on Oilfield and Geothermal Chemistry, Dalla, TX Jan. (1982).

Sharma, A.K., Pithapurwala, Y.K., and Shah, D.O., paper presented at the SPE Symposium on Oilfield and Geothermal Chemistry, Denver, CO, June (1983).

Shiao, S.Y., Ph.D. Dissertation, University of Florida (1976).

Shinitzky, M., Dianaux, A., Gitler, C., and Weber, G., Biochemistry, 36, 592 (1971).

Shinoda, K. ed., "Solvent Properties of Surfactant Solutions," Marcel Dekker, New York (1967a).

Shinoda, K., J. Colloid Int. Sci., 24, 4 (1967b).

Shinoda, K., and Friberg, S, Adv. Colloid Int. Sci., 4, 281 (1975).

Shinoda, K., and Kuneida, H., J. Colloid Int. Sci., 42, 381 (1973).

Shinoda, K., and Saito, H., J. Colloid Int. Sci., 26, 70 (1968).

Siano, D.B., J. Colloid Int. Sci., 93, 1 (1983).

Singleterry, C.R., and Weinberger, L., J. Am. Chem. Soc.,73, 4574 (1951).

Stegmeir, G.L. in "Improved Oil Recovery by Surfactant and Polymer Flooding," D.O. Shah and R.S. Schechter, eds., Academic Press, New York (1977).

Stigter, D., and Mysels, K.J., J. Phy. Chem., 59, 45 (1955).

Stockenius, W., Schulman, J.H., and Prince, L.M., Kolloid-Z., 169, 170 (1960).

Talmon, Y., and Prager, S., J. Chem. Phy. 69, 517 (1978).

Tanford, C. "The Hydrophobic Effect; Formationa of Micelles, and Biological Membranes," John Wiley and Sons, New York (1973).

Tanford, C. in "Micellization, Solubilization and Microemulsions," K.L. Mittal, ed., Plenum Press, Vol 1, New York (1977).

Tham, M.K., and Lorenz, P.B., paper presented at First European Symposium on EOR, Bournemouth, England, Sept. (1981).

Thomas, J.K., Acc. Chem. Res., 10, 133 (1977).

Thurston, G.B., Salager, J.L., and Schechter, R.S., J. Colloid Int. Sci., 70, 517 (1979).

Tiessie, J., J. Colloid Int. Sci., 70, 90 (1979).

Todd, M.R., Dietrich, J.K., and Larson, R.G., paper presented at the SPE Symposium on Improved Oil Recovery, Tulsa, OK, April (1978).

Trushenski, S.P., Dauben, D.L., and Parrish, D.R., Soc. Pet. Eng. J., 14, 633 (1974).

Trushenski, S.P. in "Improved Oil Recovery by Surfactant and and Polymer Flooding," D.O. Shah and R.S. Schechter, eds., Academic Press, New York (1977).

Turner, D.C., and Brand, L., Biochemistry, 7, 3381 (1968).

Van Quy, N., and Labrid, J., Soc. Pet. Eng. J., 23, 461 (1983).

Vinatieri, J.E., and Fleming, P.D., Soc. Pet. Eng. J., 19, 289 (1979).

Wade, W.H., Morgan, J.C., Jacobson, J., Salager, J.L., and Schechter, R.S., Soc. Pet. Eng. J., 18, 242 (1978).

Waggoner, A.S., Griffith, O.H., and Christensen, C.R., Proc. Nat. Acad. Sci. U.S., 57, 1198 (1967).

Wallace, S.C., and Thomas, J.K., Chem. Phy. Lett., 23, 359 (1974).

Weber, G., Adv. Protein Chem., 8, 415 (1953).

Weber, G., and Laurence, D.J.R., Proc. Biochem. Soc., 56, 31 (1954).

Weber, G. and Shinitzky, M., Proc. Nat. Acad. Sci. U.S., 65, 823 (1970).

Wennerstrom, H., and Lindman, B., Phy. Rev., 52, 1 (1979).

Widmayer, R.H., Satter, A., Frazier, G.D., and Graves, R.H., J. Pet. Tech., 29, 933 (1977).

Wilhite, G.P., Green, D.W., Okoye, D.M., and Looney, M.D., Soc. Pet. Eng. J., 20, 459 (1980).

Williams, E., Sears, B., Allerhand, A., and Cordes, E.H., J. Am. Chem. Soc., 95, 4871 (1973).

Winsor, P.A., Trans. Farad. Soc., 44, 376 (1948).

Winsor, P.A., Trans. Farad. Soc., 46, 762 (1950).

Winsor, P.A., in "Solvent Properties of Amphiphilic Compounds," Butterworths, London (1954).

Winsor, P.A., Chem. Rev., 68, 1 (1968).

Winsor, P.A., in "Liquid Crystals and Plastic Crystals," G.W. Gray and P.A. Winsor, eds., Ellis Horwood, Ltd., Vol. 1, Chichester (1974).

Zettlemoyer, A.C., Ann. Rev. Phys. Chem., 9, 439 (1958).

BIOGRAPHICAL SKETCH

Yusuf Pithapurwala was born on December 8, 1953, to Mr. and Mrs. K.T. Pithapurwala in Dahod, Gujarat, India. He did his schooling at Mohammediya and Panjataniya High School, Dahod, graduating in May, 1970. He joined the Maharaja Sayajirao University, Baroda, from which he was graduated in July, 1976, with a B.E. in chemical engineering. He was admitted to the graduate program at Polytechnic Institute of New York, Brooklyn, and obtained his M.S. in chemical engineering in June, 1978. He then entered the doctoral program in chemical engineering at the University of Florida.

I certify that I have read this study and that in my opinion it conforms to acceptable standards of scholarly presentation and is fully adequate, in scope and quality, as a dissertation for the degree of Doctor of Philosophy.

Dinesh O. Shah, Chairman
Professor of Chemical Engineering

I certify that I have read this study and that in my opinion it conforms to acceptable standards of scholarly presentation and is fully adequate, in scope and quality, as a dissertation for the degree of Doctor of Philosophy.
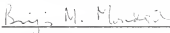
Raymond W. Fahien
Professor of Chemical Engineering

I certify that I have read this study and that in my opinion it conforms to acceptable standards of scholarly presentation and is fully adequate, in scope and quality, as a dissertation for the degree of Doctor of Philosophy.

Dale W. Kirmse
Associate Professor of Chemical Engineering

I certify that I have read this study and that in my opinion it conforms to acceptable standards of scholarly presentation and is fully adequate, in scope and quality, as a dissertation for the degree of Doctor of Philosophy.

Brij M. Moudgil
Associate Professor of Materials
Science and Engineering

I certify that I have read this study and that in my opinion it conforms to acceptable standards of scholarly presentation and is fully adequate, in scope and quality, as a dissertation for the degree of Doctor of Philosophy.

Federico A. Vilallonga
Professor of Pharmacy

This dissertation was submitted to the Graduate Faculty of the College of Engineering and to the Graduate School, and was accepted as partial fulfillment of the requirements for the degree of Doctor of Philosophy.

August, 1984

Dean, College of Engineering

Dean for Graduate Studies
and Research